



THE UNIVERSITY of EDINBURGH

Edinburgh Research Explorer

The Impact of Stellar Multiplicity on Planetary Systems, I.

Citation for published version:

Kraus, AL, Ireland, MJ, Huber, D, Mann, AW & Dupuy, TJ 2016, 'The Impact of Stellar Multiplicity on Planetary Systems, I. The Ruinous Influence of Close Binary Companions', *Astronomical Journal*, vol. 152, no. 1. <https://doi.org/10.3847/0004-6256/152/1/8>

Digital Object Identifier (DOI):

[10.3847/0004-6256/152/1/8](https://doi.org/10.3847/0004-6256/152/1/8)

Link:

[Link to publication record in Edinburgh Research Explorer](#)

Document Version:

Peer reviewed version

Published In:

Astronomical Journal

General rights

Copyright for the publications made accessible via the Edinburgh Research Explorer is retained by the author(s) and / or other copyright owners and it is a condition of accessing these publications that users recognise and abide by the legal requirements associated with these rights.

Take down policy

The University of Edinburgh has made every reasonable effort to ensure that Edinburgh Research Explorer content complies with UK legislation. If you believe that the public display of this file breaches copyright please contact openaccess@ed.ac.uk providing details, and we will remove access to the work immediately and investigate your claim.



THE IMPACT OF STELLAR MULTIPLICITY ON PLANETARY SYSTEMS, I.: THE RUINOUS INFLUENCE OF CLOSE BINARY COMPANIONS

ADAM L. KRAUS¹, MICHAEL J. IRELAND², DANIEL HUBER^{3,4,5} ANDREW W. MANN¹, TRENT J. DUPUY¹

Draft version October 14, 2018

ABSTRACT

The dynamical influence of binary companions is expected to profoundly influence planetary systems. However, the difficulty of identifying planets in binary systems has left the magnitude of this effect uncertain; despite numerous theoretical hurdles to their formation and survival, at least some binary systems clearly host planets. We present high-resolution imaging of 382 Kepler Objects of Interest (KOIs) obtained using adaptive-optics imaging and nonredundant aperture-mask interferometry (NRM) on the Keck-II telescope. Among the full sample of 506 candidate binary companions to KOIs, we super-resolve some binary systems to projected separations of < 5 AU, showing that planets might form in these dynamically active environments. However, the full distribution of projected separations for our planet-host sample more broadly reveals a deep paucity of binary companions at solar-system scales. For a field binary population, we should have found 58 binary companions with projected separation $\rho < 50$ AU and mass ratio $q > 0.4$; we instead only found 23 companions (a 4.6σ deficit), many of which must be wider pairs that are only close in projection. When the binary population is parametrized with a semimajor axis cutoff a_{cut} and a suppression factor inside that cutoff S_{bin} , we find with correlated uncertainties that inside $a_{cut} = 47^{+59}_{-23}$ AU, the planet occurrence rate in binary systems is only $S_{bin} = 0.34^{+0.14}_{-0.15}$ times that of wider binaries or single stars. Our results demonstrate that a fifth of all solar-type stars in the Milky Way are disallowed from hosting planetary systems due to the influence of a binary companion.

Subject headings:

1. INTRODUCTION

Radial velocity surveys and ground-based transit searches have discovered nearly 1000 confirmed planets around other stars (Wright et al. 2011) and thousands of additional candidates (Borucki et al. 2010; Batalha et al. 2012; Burke et al. 2014), revolutionizing the demography of planetary systems (e.g., Fischer & Valenti 2005; Johnson et al. 2010; Bowler et al. 2010). The emerging consensus is that planetary systems are ubiquitous (Dressing & Charbonneau 2013; Petigura et al. 2013; Foreman-Mackey et al. 2014; Muirhead et al. 2015), occurring with a frequency near unity across a wide range of stellar masses. However, most previous planet searches have only targeted single stars and very wide binaries since close companions complicate the observations and analysis. The majority of all solar-type stars form with at least one binary companion (Duquennoy & Mayor 1991; Raghavan et al. 2010; Kraus et al. 2008, 2011), so the impact of stellar binarity on planet occurrence could represent one of the largest remaining systematic uncertainties in the Kepler era.

Binary companions should have a profound dynamical influence on the planet formation process, truncating disks (Artymowicz & Lubow 1994; Jang-Condell

et al. 2008; Andrews et al. 2010; Jang-Condell 2015), dynamically stirring planetesimals (Quintana et al. 2007; Haghighipour & Raymond 2007; Rafikov & Silsbee 2015a; Silsbee & Rafikov 2015), and enhancing both accretion (Artymowicz & Lubow 1994; Jensen et al. 2007) and photoevaporation (Alexander 2012). These processes suggest that disks in binary systems could be short-lived and that such systems would represent hostile sites for planets to grow. Furthermore, even if planets can be formed, then secular evolution of the orbits and even stellar evolution can drive systems through unstable states that destroy them on Myr to Gyr timescales (Holman & Wiegert 1999; Haghighipour 2006; Kratter & Perets 2012; Kaib et al. 2013), though dynamical interactions also have been suggested as a channel for producing the many giant planets discovered well inside the snow line (Kozai 1962; Fabrycky & Tremaine 2007; Winn et al. 2010; Naoz et al. 2012; but also Ngo et al. 2015).

In spite of the dynamical barriers, ground-based exoplanet surveys show that some binary systems do host planets. A handful of giant planets have been identified in nearby short-period binary systems (Hatzes et al. 2003; Correia et al. 2008; Kane et al. 2015), though it has been suggested that they might result from small-N dynamical interactions rather than in-situ formation (e.g. Pfahl & Muterspaugh 2006). Circumbinary gas giants are now being reported by Kepler (Doyle et al. 2011), perhaps as frequently as for single stars (Welsh et al. 2012), and orbit monitoring for planet-hosting binary KOIs is also uncovering a population of small planets in close binaries (e.g., Kepler-444; Dupuy et al. 2016). Numerous wide binary companions to planet hosts have been identified as well (Mugrauer et al. 2005; Daemgen et al. 2009; Muterspaugh et al. 2010; Bergfors et al.

¹ Department of Astronomy, The University of Texas at Austin, Austin, TX 78712, USA

² Australia National University, Australia

³ Sydney Institute for Astronomy (SIfA), School of Physics, University of Sydney, NSW 2006, Australia

⁴ SETI Institute, 189 Bernardo Avenue, Mountain View, CA 94043, USA

⁵ Stellar Astrophysics Centre, Department of Physics and Astronomy, Aarhus University, Ny Munkegade 120, DK-8000 Aarhus C, Denmark

2012), and it appears that wide binary systems are common exoplanet hosts (Eggenberger et al. 2007; Desidera & Barbieri 2007; Duchêne 2010). However, the observational biases against exoplanet discovery in the presence of a companion star mean that the frequency, properties, and provenance of planets in close binary systems are still largely unconstrained by data; some ground-based RV surveys have been launched and have yet to report any detections (e.g., Eggenberger 2010; Desidera et al. 2010), but the final statistics have not been reported yet. These inputs will be crucial as theory investigates the circumstances under which planets apparently can form in binary systems (e.g., Jang-Condell et al. 2008; Rafikov 2013; Jang-Condell 2015; Rafikov & Silsbee 2015b).

This question has long been considered from a planet formation perspective, where the occurrence and properties of protoplanetary disks can be compared for binary systems versus single stars (Ghez et al. 1997; White & Ghez 2001; Cieza et al. 2009; Duchêne 2010) to demonstrate a striking depletion of protoplanetary disks among close binary systems. This trend emerged most clearly from a combination of a binary census of the Taurus-Auriga star-forming region with a disk census from Spitzer (Kraus et al. 2011, 2012), which showed that at the age of ~ 2 Myr, 80% of single stars and 90% of wide binaries host a protoplanetary disk, whereas only 35% of close (< 40 AU) binaries host disks. An analysis of younger regions shows that this depletion occurs within < 1 Myr (Cheetham et al. 2015). The detailed properties of protoplanetary disks reveal an even more striking trend. Harris et al. (2012) showed that even when binaries host protoplanetary disks, then disk masses are depleted by a factor of ~ 5 for 30–300 AU binaries and by a factor of ~ 25 for < 30 AU binaries; the only exception is a small number of circumbinary disks which are quite massive. However, detailed spectroscopic studies of many of the same protoplanetary disks (Pascucci et al. 2008; Skemer et al. 2011) demonstrate that the surviving disks do undergo the same evolutionary processes of grain growth and dust settling. Studies of intermediate-age debris disk hosts also reveal that debris exists in binary systems (Trilling et al. 2007; Rodriguez et al. 2015), albeit suppressed by a factor of ~ 3 for 1–50 AU systems when compared to tighter or wider systems.

The recent explosion in exoplanet discoveries from the Kepler mission (Borucki et al. 2010) offers a new opportunity to characterize the influence of stellar multiplicity on planet occurrence. The coarse spatial resolution and nearly blind target selection of Kepler with respect to stellar multiplicity have rendered the Kepler Objects of Interest (KOIs; Batalha et al. 2012) largely unbiased to stellar multiplicity, offering the first planet sample for which the presence of close binaries is uncorrelated with planet discovery. Numerous high-resolution imaging surveys have targeted Kepler planet hosts (Adams et al. 2012, 2013; Lillo-Box et al. 2012, 2014; Law et al. 2013; Dressing et al. 2014; Wang et al. 2014b), discovering a large number of wide ($\gtrsim 100$ AU) binary companions and vetting many of the KOIs to eliminate blends and other sources of false positives. The sum of those observations seem to suggest that the wide binary population is in line with that seen for the full stellar population (Horch et al. 2014; Deacon et al. 2016), but since KOIs are distant (in all but a handful of cases, $d \gtrsim 100$ pc), then conven-

tional AO imaging can not access binary companions on solar-system scales ($\rho \sim 5\text{--}20$ AU). RV monitoring has indicated at $\sim 2\sigma$ that the close ($\lesssim 20$ AU) binary occurrence rate might be suppressed among the set of KOIs with multiple observations (e.g., Wang et al. 2015a), but with uncertain selection effects resulting from the choice of which targets merit RV followup.

In this paper, we report nonredundant aperture-mask interferometry and adaptive optics imaging of 382 KOIs at higher spatial resolution, capable of detecting binary companions down to Solar System scales (inner working angles of 2–5 AU). We find a striking paucity of close companions to planet host stars, which supports theoretical predictions that these binary systems (which are known to represent $\sim 25\%$ of all Sun-like stars) must be extremely hostile sites for extrasolar planets to form and/or survive. In Section 2, we describe our selection of a volume-limited sample of Kepler planet hosts, and in Section 3, we describe our observations and data analysis. In Section 4, we describe the binary population unveiled by our survey and update the properties of the planet hosts and planetary systems in light of the flux contributions of the previously-unidentified binary companions. Finally, in Section 5, we discuss the properties of the binary population among planet host stars, and infer the impact of those binary companions on the formation and survival of extrasolar planetary systems.

2. THE SAMPLE

The Kepler target list (Batalha et al. 2010) consists of 2×10^5 stars which are optically bright ($K_p \lesssim 16$) and comprises 10^5 G dwarfs (explicitly selected to be suitable for detecting Earth analogs), 2×10^4 F dwarfs, 2×10^4 K dwarfs, 3×10^3 M dwarfs, 10^3 OBA dwarfs, and at least 1.5×10^4 giants of all types (e.g. Hekker et al. 2011; Mann et al. 2012; Stello et al. 2013). The Kepler targets were selected from the Kepler Input Catalog, which was constructed using broadband ($grizJHK_s$) and intermediate-band (D51) photometry to infer T_{eff} , $\log(g)$, [Fe/H], and A_V for 1.3×10^7 sources in the Kepler field. As of 2013-07-31, the Kepler survey had yielded 4914 Kepler Objects of Interest (KOIs) that included 3548 candidate or confirmed planets transiting 2664 host stars.⁶ For this work, we use the KOI list from that epoch as an input sample.

Most of our targets represent a volume-based subsample of KOIs, selected from the July 2013 list using spectrophotometric distances. We initially estimated the effective temperature T_{eff} and the bolometric flux m_{bol} based on two methods. First, we used SED fitting of photometry from 2MASS (Skrutskie et al. 2006), SDSS (Ahn et al. 2012), and USNO-B1.0 (Monet et al. 2003), as described in Kraus & Hillenbrand (2007) and Kraus et al. (2014), to estimate both parameters. Second, we directly adopted the KIC T_{eff} , and then combined a relation between K_p and $g'r'$ in the Kepler documentation⁷ with the Kraus & Hillenbrand (2007) relation between $g/r/T_{eff}$ and m_{bol} to derive a relation between K_p and m_{bol} . In both cases, we then used the Kraus & Hillenbrand (2007) relation between T_{eff} and M_{bol} to compute the photometric distance modulus, $DM = m_{bol} - M_{bol}(T_{eff})$, and then prioritized targets in order of ascending distance.

⁶ <http://exoplanetarchive.ipac.caltech.edu/>

⁷ <http://keplergo.arc.nasa.gov/CalibrationZeropoint.shtml>

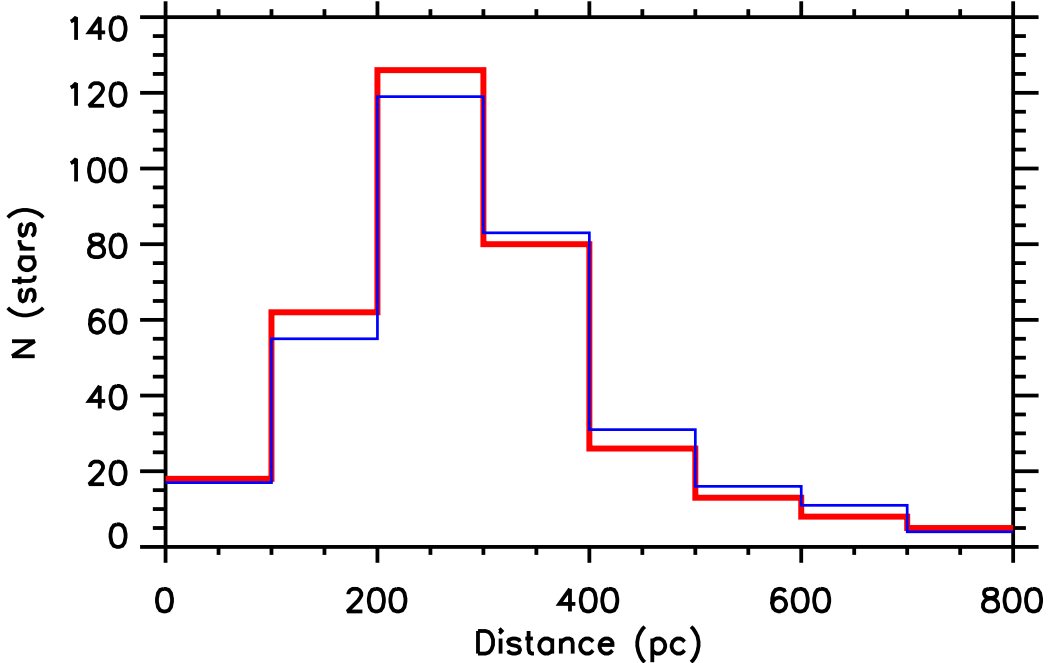


FIG. 1.— Distance distribution for our observed sample, where red shows the initial distance estimates and blue shows distances corrected for flux contributions from binaries (Malmquist bias). To maintain clarity for the majority of the sample, the extended tail of 19 targets with $d > 800$ pc (and extending to >2000 pc, for some giants) are not shown. If the population were distributed uniformly in space, there should be 2.4 times as many targets at $200 < d < 300$ pc as at $d < 200$, indicating that the flux-limited sample of KOIs is incomplete beyond 200 pc. However, by weighting binaries with a $1/V_{max}$ weight, we can still control for the Malmquist bias introduced by the $K_p \sim 16$ limit of Kepler and by the enhanced planet detectability seen for bright stars with high-SNR Kepler data.

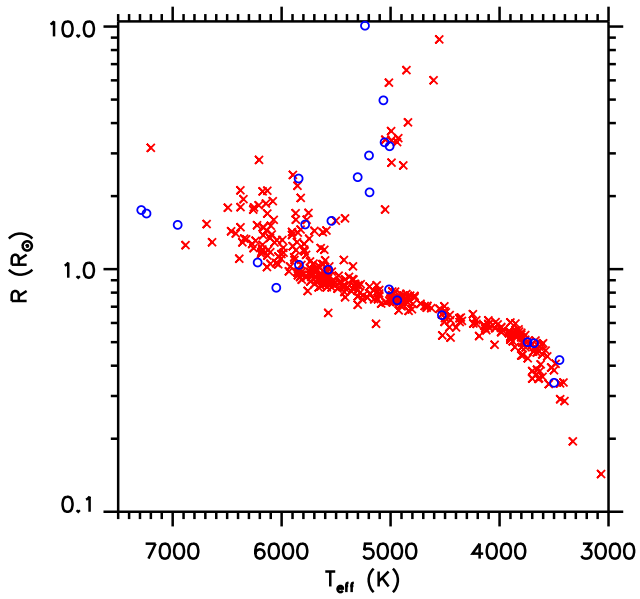


FIG. 2.— HR diagram (radius versus temperature) for our observed sample. Candidate and confirmed planet hosts are shown with red crosses, while false positives that we omit from our statistical analysis are shown with blue open circles. The vast majority of targets are main sequence stars. Our observations of giants are less likely to detect low-mass companions because the large distance imposes a penalty on both sensitivity and resolution. However, our detection limits account for the distance in turning observational limits (in magnitudes and arcseconds) into physical limits (in mass ratios and AU), so we retain the giants in order to maintain a uniform treatment of all stars.

After the majority of these observations had occurred, we adopted updated distances based on the latest version of the Kepler stellar properties catalog (Q1-17; DR24⁸), initially described by Huber et al. (2014). To derive self-consistent stellar properties and distances, we followed the method by Serenelli et al. (2013) to calculate posterior distribution functions for each model parameter by marginalizing isochrones from the Dartmouth Stellar Evolution Program (Dotter et al. 2008) conditioned on literature values for atmospheric properties (T_{eff} , $\log(g)$, and $[Fe/H]$). Distance posteriors were calculated using absolute K-band magnitudes from the isochrone grid and the reddening map by Amôres & Lépine (2005), assuming the KOI is a single star with the given stellar parameters. All reported stellar properties are based on the posterior mode, and uncertainties are calculated based on the closest 1σ interval around the mode.

Input values and uncertainties for T_{eff} , $\log(g)$, and $[Fe/H]$ were taken from the Kepler stellar properties catalog except for 13 M dwarfs for which we adopted new temperatures and metallicities based on medium resolution spectra obtained with the SNIFS spectrograph following the method given in Mann et al. (2013), and Kepler-444 for which we adopted the Hipparcos distance and input parameters by Campante et al. (2015). In total, 74 stars (19%) in our sample have input parameters from asteroseismology, 235 stars (62%) from spectroscopy, and 73 stars (19%) from broadband colors. By construction, our stellar properties are in close agreement with Huber et al. (2014), except for 21 K stars

⁸ http://exoplanetarchive.ipac.caltech.edu/docs/Kepler_stellar_docs.html

with poorly constrained photometric $\log(g)$ values which are classified as evolved ($\sim 2 - 4R_{\odot}$) subgiants in Huber et al. (2014), but have main-sequence radii ($\sim 1R_{\odot}$) in our work. This difference is due to the fact that the Huber et al. (2014) estimates are based on maximum likelihood values while probabilistically, given the large uncertainty of 0.4 dex in $\log(g)$, smaller radii are favored due to longer main-sequence lifetimes compared to the subgiant branch. Within the uncertainties, however, all classifications are consistent within 3σ .

The revised distances derived using the above procedure were used to rerank our list. Future observations will prioritize the closest KOIs from this list, and we hereafter use these updated distances (modified for the flux contributions of binary companions if necessary) to convert angular separations into physical separations. Since binaries are overrepresented in a flux-limited sample, our model comparisons will build in Malmquist bias with a V/V_{max} weighting (e.g., Schmidt 1968) such that binaries with a flux addition from a companion are predicted with greater frequency set by the fractionally larger volume within which they occur. We also report observations for 23 stars that were subsequently identified as likely false positives (e.g., Slawson et al. 2011; Mann et al. 2012; Huber et al. 2013) after we observed them, since high-resolution imaging is useful for further confirming their non-planetary nature, but do not use them in the statistical analysis.

We list all of the observed KOIs and their stellar parameters in Table 1, divided into the likely planet hosts (359 KOIs that have been confirmed or remain as candidates) and the false positives (23 stars that have been rejected). Where available, we list Kepler numbers for the hosts of confirmed planets and the reference by which the false positives have been rejected. Many of the false positives are labeled as such on the Kepler Community Follow-On Project (CFOP) website⁹, so we attribute those labels to specific community members when their identities are known. In Figure 1, we present a distance histogram for the statistical sample. In Figure 2, we present an HR diagram for the sample using the stellar parameters reported by Huber et al. (2014) and our inferred distances. The final sample of 382 stars consists of 3 A stars, 52 F stars, 137 G stars, 134 K stars, and 56 M stars, based on the T_{eff} -SpT relation of Kraus & Hillenbrand (2007). The distribution of AFG stars is roughly consistent with the present-day mass function of the solar neighborhood (e.g., Reid et al. 2002), but there is a distinct paucity of K and especially M stars due to the emphasis on solar analogs in the Kepler target list.

3. OBSERVATIONS AND DATA ANALYSIS

3.1. High-Resolution Imaging and Nonredundant Mask Interferometry Observations

The technique of non-redundant aperture masking (NRM) has been well established as a means of achieving the full diffraction limit of a single telescope (Nakajima et al. 1989; Tuthill et al. 2000, 2006; Ireland 2013), beyond what can be achieved with standard AO imaging. The core innovation of aperture masking is to resample the telescope's single aperture into a sparse interferometric array; this allows for data analysis using interfero-

metric techniques (such as closure-phase analysis) that calibrate out the phase errors that limit traditional astronomical imaging by inducing speckle noise. As we described in Kraus et al. (2008, 2011), aperture-masking observations can yield contrasts as deep as $\Delta K \sim 6$ at λ/D and $\Delta K \sim 4$ at $1/3 \lambda/D$ with observations of ~ 5 –15 minutes, and we have used the technique to identify dozens of binary companions that fall inside the detection limits of traditional imaging surveys. More detailed discussions of the benefits and limitations of aperture masking, as well as typical observing strategies, can be found in Kraus et al. (2008) and in Readhead et al. (1988); Nakajima et al. (1989); Tuthill et al. (2000, 2006); Lloyd et al. (2006); Martinache et al. (2007); Ireland et al. (2008).

We observed our targets with the Keck-II telescope and either natural guide star (NGS) or laser guide star (LGS) AO in vertical angle mode. Our observations were taken over the space of 22 half or full nights between 2012 May and 2014 August. All observations were conducted with the facility adaptive optics imager NIRC2, which also has a 9-hole aperture mask installed in a cold filter wheel near the pupil stop. All observations used the smallest pixel scale (9.952 ± 0.002 mas/pix; Yelda et al. 2010) and we corrected for geometric distortion using their NIRC2 distortion solution. Each observing sequence consisted of four steps:

1. AO acquisition, requiring 1 minute for NGSAO or 4 minutes for LGSAO.
2. Shallow imaging, requiring 1 minute to obtain 1–2 integrations of 10–20 seconds with few Fowler samples. These observations were intended for initial target acquisition and to reconnoiter for obvious binarity, as well as offering sensitivity to some additional companions between the inner working angle of the coronagraph ($\rho \sim 400$ mas) and the typical angle inside of which NRM supercedes imaging ($\rho \sim 150$ mas).
3. Deep imaging, requiring 2 minutes to obtain 2 integrations of 20 seconds with many Fowler samples. These observations were intended to search for faint companions at wide projected separations ($\rho > 0.5''$). Targets brighter than $K_{2M} \sim 10.6$ were placed behind the 600 mas coronagraphic spot to avoid saturation of the primary, since many Fowler samples can only be conducted with long integrations. Fainter targets were observed without the coronagraph because there was insufficient flux for the primary to be detected through the coronagraph (impeding the measurement of precise astrometry for candidate companions).
4. Nonredundant mask interferometry, requiring 3–4 minutes to obtain 6–8 integrations of 20s with the 9H mask in place. We chose the number of observations to match target brightness and observing conditions, with the goal of achieving a contrast of $\Delta K' > 3$ at λ/D even for the faintest targets and well above median seeing. The median contrast limit at the diffraction limit was $\Delta K' \sim 4.3$, while for bright targets in good conditions, the contrast limit typically was $\Delta K' \sim 5$.

⁹ <https://exofop.ipac.caltech.edu/cfop.php>

The observing sequence was fully scripted, requiring ~ 7 minutes for NGSAO observations and ~ 10 minutes for LGSAO observations. A typical interferometric measurement requires the observation of one or more source-calibrator pairs. However, our sample included numerous targets with similar positions and brightnesses, so we instead observed groups of science targets and intercalibrated between them, omitting binary systems from the calibration as they were identified. The actual number of observations obtained at each step can vary somewhat, due to ongoing optimization of our observing strategy, the rejection of bad frames (i.e., when the AO system lost lock), and some cases where we exited the script to obtain additional frames in compensation for obviously bad data (such as from bad seeing, windshake, or intermittent clouds).

We summarize the salient details of our imaging observations in the same tables as our detection limits (Table 2 and Table 4), as described below.

3.2. Imaging Analysis for Isolated Primaries

Each science frame was linearized using the IDL task `linearize_nirc2.pro`¹⁰, and then dark-subtracted and flat-fielded using the most contemporaneous darks and flats from each run. We then identified dead pixels from an analysis of K' superflats (constructed from at least 20 frames in one night) from 41 separate nights, spanning 2006–2013, identifying and interpolating over any pixel with a response of $<30\%$ in at least half of all superflats. Similarly, we identified hot pixels from an analysis of long-integration superdarks (constructed from at least 30 frames in one night, with 1 coadd of $t_{int} = 20$ sec, taken with 16 or more Fowler samples) from 38 separate nights, identifying any pixel as hot if it had ≥ 10 counts in at least half of the superdarks. Finally, we corrected cosmic rays and transient hot pixels by identifying all pixels with fluxes $> 10\sigma$ above the median of the 8 adjacent pixels or 16 once-removed pixels, replacing them with that median value.

For each science frame, we used two different methods of PSF subtraction. The first method of PSF subtraction, intended to find faint sources at wide separations (in the background- or readnoise-limited regime), was to subtract an azimuthal median PSF model. This PSF model was constructed from a five-pixel boxcar median, calculated in concentric rings around the science target and interpolated to the exact distance for every pixel. This method leaves all high-frequency structure (i.e., speckles and diffraction spikes) from the primary star PSF, so it is not ideal for identifying close ($\rho \lesssim 1''$) companions. However, it has the virtue of adding negligible noise at large separations (as would occur by subtracting empirical PSF templates), and hence allowing for the most robust identification of wide candidate companions. Many of our observations had modest Strehl (15–30%), with much of the flux in a broad seeing-limited halo, so the subtraction of this smooth halo uncovered faint sources that otherwise would have been missed.

The second method of PSF subtraction, intended to find sources within the primary star’s PSF halo, uses empirical PSFs of other targets (observed within the same run) to more closely match the primary star PSF for

subtraction. Our observations are short and do not show substantial sky rotation, so for each science frame, we begin with an initial library of all science frames for other targets that were taken in the same filter and coronagraph (or lack thereof) and that have not been identified as binary systems. We then rescale each potential template frame to the science frame in question and measure the χ^2 of the residuals in an annulus of $\rho = 150$ –300 mas (for non-coronagraphic data) or $\rho = 450$ –750 mas (for coronagraphic data). Since our imaging observations are not deep, the vast majority of structure in the PSF is represented by the diffraction spikes and by a few well-established, long-term superspeckles, and hence the number of free parameters in this fit is small. We therefore only use a single frame as a PSF template and globally optimize the fit, since otherwise the flux from any companions rapidly becomes a dominant source of residuals and therefore is fit and subtracted as well.

Using the coadded stacks of all median-subtracted and all template-subtracted frames on a science target, we identified candidate companions by measuring the flux through 80 mas (diameter) apertures centered on every pixel of the image. We then measured the standard deviation of the fluxes among all apertures in a sliding 5-pixel annulus around the primary star, identifying any aperture with a $> +6\sigma$ outlier as the location of a potential astrophysical source. We set the corresponding detection limit for that projected separation to the contrast associated with that $+6\sigma$ flux value (as measured in comparison to an identical aperture centered on the primary star). To reconcile the possible detections in the median-subtracted and template-subtracted images, we only accepted a potential astrophysical source if it was identified in both sets of residuals, or if it was identified in one set and fell below the detection limits for the other set. Hence, faint potential sources at wide projected separations typically would be included if they were in the median-subtracted image and not the template-subtracted image (but not vice versa), because the median-subtracted image had deeper limits. At small projected separations, the converse was true, because template-subtracted images had deeper limits. This process still passed through residual cosmic rays that had not escaped our early correction steps, as well as some faint artifacts along diffraction spikes and near the largest superspeckles, so we then visually inspected each remaining candidate to determine if it was a cosmic ray or corresponded to PSF features that could be seen in contemporaneous observations of other science targets.

Once a potential source was accepted as a bona fide astrophysical object (and hence a candidate companion), we measured aperture photometry for the candidate companion (in both the median-subtracted or template-subtracted images) and the science target (in the processed, unsubtracted images) in order to determine the relative astrometry and photometry of the candidate. By default, this aperture photometry used an aperture with diameter of 80 mas and a sky annulus with inner and outer radii of 100–150 mas. We visually inspected each companion to determine which PSF-subtraction technique produced a cleaner detection, and adopted that measurement for all subsequent analysis.

3.3. Imaging Analysis for Close Pairs

¹⁰ <http://www.astro.subsys.edu/metchev/ao.html>

We found that our default imaging pipeline failed in cases where a candidate companion was bright enough to have a substantial PSF halo and that halo impinged significantly on the primary star, as it was no longer valid to fit the flux distribution with a single PSF template. We therefore also used an alternate pipeline for the production of PSF-subtracted images of multiple sources, which iteratively uses the best-fit PSF template to fit for the parameters of the binary or triple (projected separation, PA, and contrast of each other source with respect to the brightest object), and then creates double-star or triple-star templates of all empirical PSFs and tests them to find which empirical PSF is best. This process then iterated until the same template is used to find the same binary or trinary parameters, at which point the multi-PSF template is subtracted and the template-subtracted image is fed to subsequent pipeline steps for identification of further candidate companions. The PSF-fit values for projected separation, PA, and contrast are adopted in place of the aperture photometry described above.

3.4. NRM Analysis

The data analysis follows almost the same prescription as in Kraus et al. (2008, 2011), so we discuss here only a general background to the technique and differences from Kraus et al. (2008). The data analysis takes three broad steps: basic image analysis (flat-fielding, bad pixel removal, dark subtraction), extraction and calibration of squared visibility and closure phase, and binary model fitting. Unless fitting to close, near-equal binaries, we fit only to closure phase, as this is the quantity most robust to changes in the AO point-spread function (PSF).

In previous papers we used Monte-Carlo simulations based on carefully modeled data covariance matrices in order to compute detection limits. In this work, the empirical closure-phase covariance matrix was not always easy to estimate, because the number of contemporaneous point sources observed with any target was heterogeneous with such a large data set. Instead, we chose a more conventional approach of scaling the uncertainties so that the best fit binary model to closure-phase had a reduced chi-squared of 1.0. Any companion solutions that had a significance of more than 6σ were called detections, and non-detections were assigned a detection-limit equal to this 6σ threshold; the detection limit reported is then the azimuthal average of this threshold. This limit was similar to (but in most cases a little more conservative than) the Monte-Carlo technique used in previous papers. As visibility amplitude is very useful for the closest binary solutions in breaking a contrast/separation degeneracy, we included visibility amplitude in our fits whenever the best fit solution using amplitudes had $\rho < 40$ mas and $\Delta K' < 1$ mag, and where the inclusion of visibility amplitudes did not reduce the significance below the 6σ cutoff (as could happen in the case of poorly calibrated visibility amplitudes).

3.5. Candidate Companion Stellar Properties

Candidate companion properties were estimated in the same procedure as described in Section 2 for the primary. For each primary model of fixed age and metallicity, we used the observed flux ratio $\Delta K'$ to interpolate stellar properties to the absolute K magnitude of the secondary,

and assigned the interpolated models the posterior probability of the corresponding primary model (thereby assuming the same age, metallicity and distance for both stars). Stellar properties were then derived by marginalizing the posterior probabilities and calculating the mode of the posterior distribution function for each stellar parameter. Uncertainties in $\Delta K'$ were taken into account by repeating the procedure for the $\pm 1\sigma$ limits in $\Delta K'$ and adding the resulting difference in quadrature to the estimate obtained with the observed $\Delta K'$ value.

In addition to secondary temperature, radius and mass, we additionally directly computed the mass ratio so that the correlated errors between secondary and primary mass (which results from the uncertain distance, age, and metallicity) partially cancel. Finally, we also use absolute Kepler bandpass magnitudes provided in the Dartmouth grid to estimate the flux ratio in the Kepler bandpass (ΔK_p), which will be useful in removing flux dilution of transits and fitting updated planetary radii.

For all candidate companions, we estimate the projected separation (in AU) from the projected angular separation using the distances calculated in Section 2, after accounting for the excess flux due to the candidate companion(s). The original 2MASS photometry was conducted with an aperture of radius $4''$, so we only include companions closer than that limit. The updated distances are reported in a separate column of Table 1.

4. RESULTS

4.1. Candidate Companions to Kepler KOIs

Our NRM observations were used to identify 26 candidate companions among the 346 KOIs observed with this technique, revealing candidates at projected separations as low as 16 mas ($1/3 \lambda/D$). We summarize the detection limits and the details of the observations in Table 2, and list the candidate companions and their observed properties in Table 3. The median target had contrast limits of $\Delta K' = 4.3$ mag at $\rho = 40$ mas ($0.8 \lambda/D$) and $\Delta K' = 3.0$ mag at $\rho = 20$ mas ($0.4 \lambda/D$). The nominal limit at $\rho = 40$ mas also applies for all larger separations, though for most targets this limit was superceded by imaging at $\rho \sim 100$ –150 mas.

Our imaging observations have identified 486 candidate companions among the full sample of 382 KOIs. We summarize the detection limits and the details of the observations in Table 4, and list the 427 candidate companions measured with aperture photometry in Table 5. In Table 6, we list the 43 close pairs and 7 close triples for which we used our multi-PSF fitting algorithm, as well as the observed properties of the candidate companion(s) with respect to the brightest star in the system. The median target had contrast limits of $\Delta K' = 5.5$ mag at $\rho = 150$ mas ($3 \lambda/D$), typically superceding the masking limits at $\rho \gtrsim 100$ mas. At wide separations, the median limit (corresponding to the fainter majority of stars that were not observed with the coronagraph) were $\Delta K' = 8.0$ mag at $\rho > 1''$. For coronagraphic data, we achieved contrast limits as deep as $\Delta K' > 12$ mag at wide separations ($\gtrsim 2''$, in the sky- and readnoise-limited regime).

We summarize the full set of detections and detection limits for the 359 planet hosts (excluding false positives) in terms of $\Delta K'$ (in mag) versus separation (in mas) in Figure 3, and correspondingly in terms of K'_{sec} (in mag)

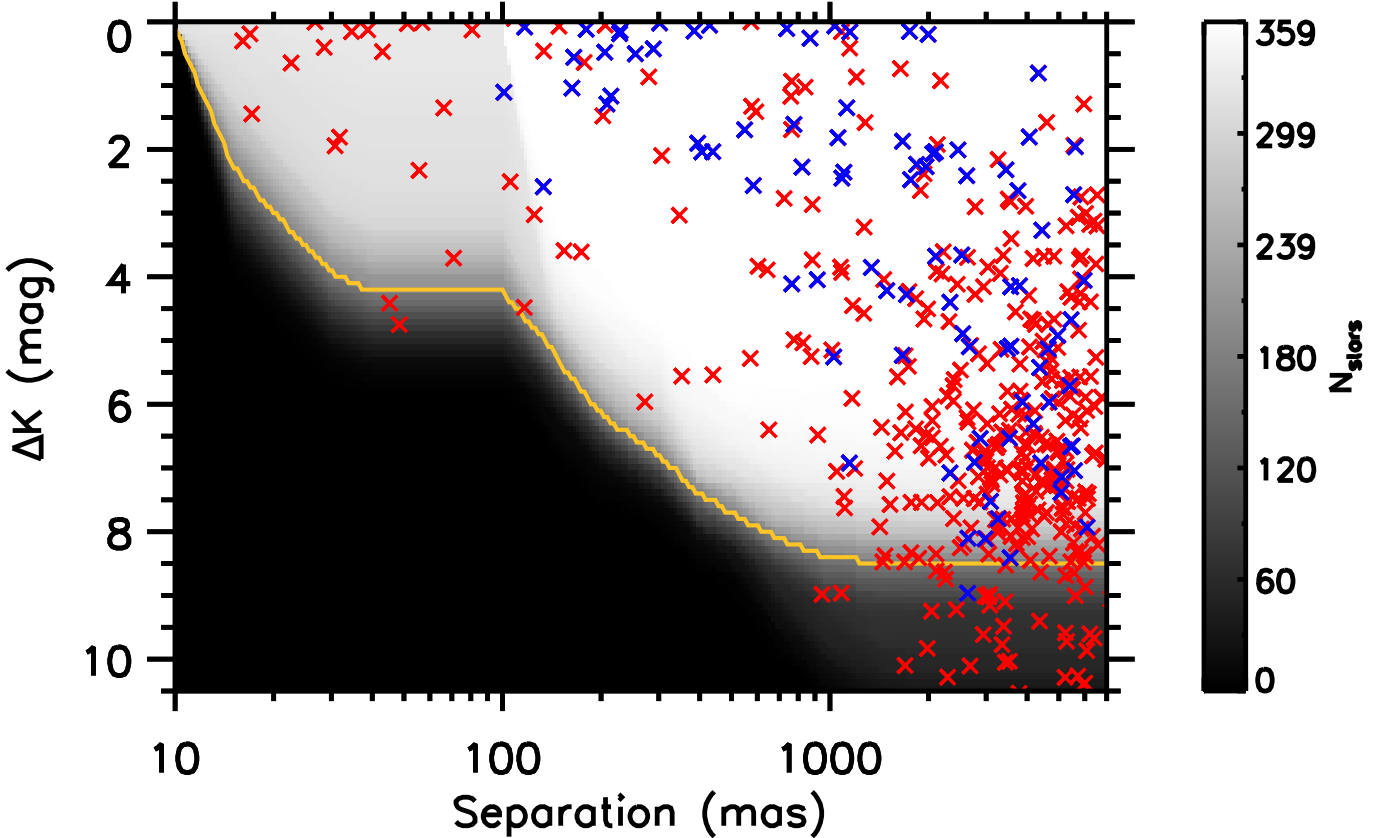


FIG. 3.— Detections and detection limits for our survey, in terms of contrast $\Delta K'$ in magnitudes and angular separation ρ in milliarcseconds. The detections are shown with red crosses for newly detected sources and blue crosses for previously identified sources, while the detection limits are shown in a shaded background trending from black (no observations sensitive to that combination of contrast and separation) to white (all 359 planet hosts that are sensitive to that combination). The orange solid line shows the median limit for the survey. There were no known binaries among this volume-limited sample with $\rho < 0.1''$, the regime uniquely probed by NRM (upper left) that represents the potential for discovering binary companions on solar system scales.

versus separation (in mas) in Figure 4. Of our detections, 5 were detected with both masking and imaging, while 27 were detected in both coronagraphic and non-coronagraphic imaging. In case of duplication, we use the companion properties from masking over those of imaging (since they typically are more precise) and those of imaging over those of coronagraphy (since the coronagraph introduces additional astrometric and photometric uncertainties). We report the redundant detections that are not used in our analysis at the bottom of each table.

We similarly show the detections and detection limits for the 359 planet hosts in terms of mass ratio q (M_s/M_p) versus separation (in AU) in Figure 5, and in terms of M_{sec} (M_\odot) versus separation (in AU) in Figure 6. Figure 5 demonstrates the exceptional resolution offered by NRM observations. Contrasts of $\Delta K' \sim 4$ and $\Delta K' \sim 6$ correspond to approximate mass ratios of $q \sim 0.2$ and $q \sim 0.1$ respectively; given that the mass ratio distribution of binary companions is approximately flat in the solar regime, then $\sim 80\%$ and $\sim 90\%$ of bound companions should fall above these limits. As we discuss further in Section 4.2, it indeed appears that almost all objects with higher contrast are unassociated objects seen in chance alignment. In this work, we avoid the most contaminated portions of parameter space and correct the remainder on a statistical basis; future papers in this

series will present second-epoch and multi-color imaging to conclusively distinguish bound companions from interlopers.

4.2. Probability of Chance Alignments

Given the low galactic latitude of the Kepler field, particularly at its southeast corner, then significant background star contamination is to be expected. We have estimated this contamination in our sample using star count models that we first described in Kraus & Hillenbrand (2012), which are based on those of Bahcall & Soneira (1980) with an update to operate in the K' filter. This formalism considers the Milky Way in terms of three components (thin disk, thick disk, and halo), and then integrates the 3D density distribution, convolved with the field present-day luminosity function, along each sightline to estimate the number of unassociated Milky Way stars per unit area.

These models are sensitive to galactic structure at low galactic latitudes, but this typically takes the form of a multiplicative factor for the number of sources as a function of magnitude. We compared our model to source counts available in 2MASS, and found that the predicted counts were a factor of ~ 2 too low, so we have scaled our source count estimates to compensate. Our predictions are similar to those from the TRILEGAL survey (Girardi

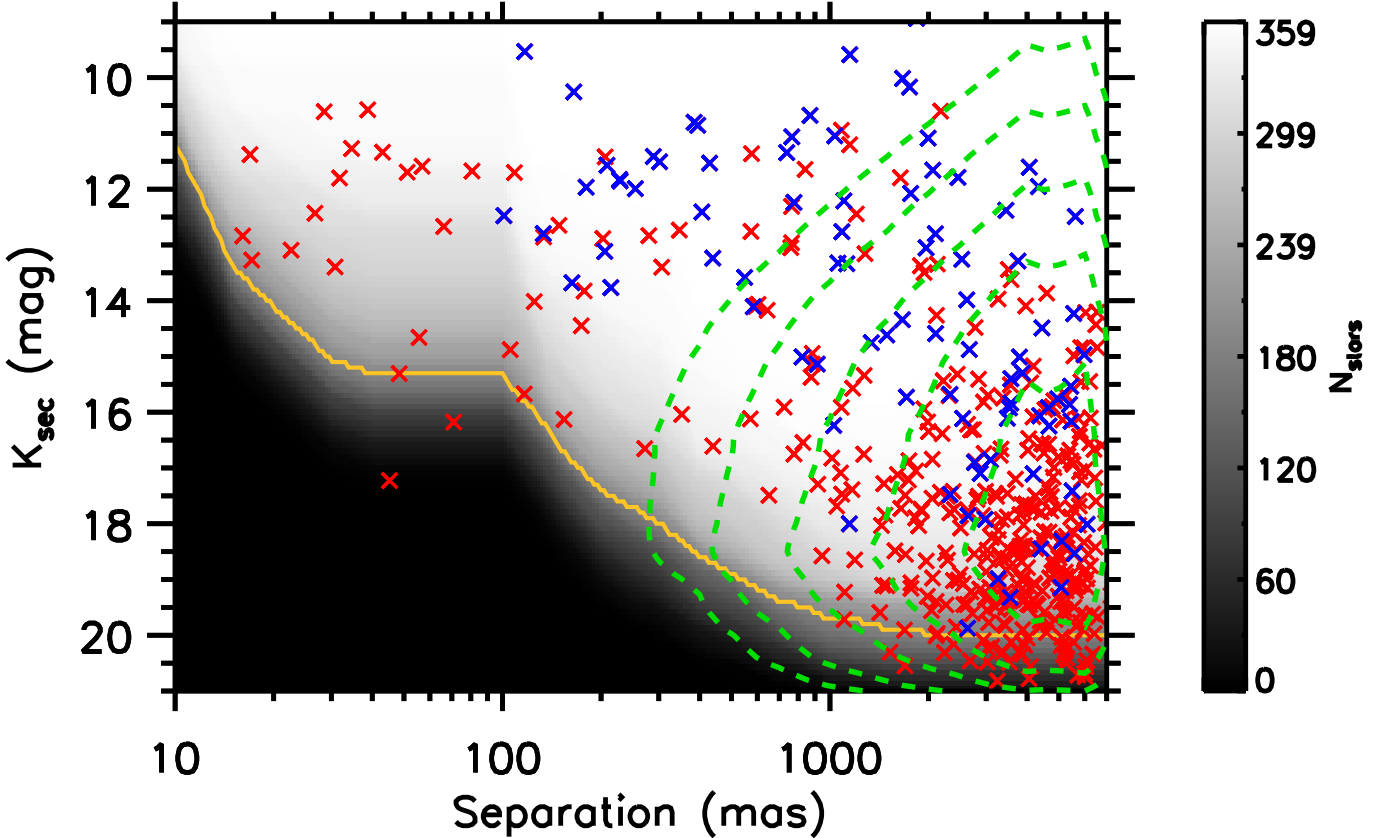


FIG. 4.— Detections and detection limits for our survey, in terms of companion apparent magnitude K' in magnitudes and angular separation ρ in milliarcseconds. The detections are shown with red crosses for newly detected sources and blue crosses for previously identified sources, while the detection limits are shown in a shaded background trending from black (no observations sensitive to that combination of contrast and separation) to white (all 359 planet hosts that are sensitive to that combination). The orange solid line shows the median limit for the survey. The green dashed lines show the expected contours of the field contaminant distribution, drawn such that 1, 3, 10, 30, and 100 background stars would fall outside of the concentric contours.

et al. 2005), which also requires a similar rescaling factor.

When these densities are summed for the entire target list, we find that at projected separations of $\rho < 3''$, there should be 7.1 contaminants with $K' \leq 16$ and 25.4 contaminants with $K' \leq 19$. In Figure 4, we show the expected contamination rate with green dashed contours drawn such that 1, 3, 10, 30, or 100 background stars would fall outside (i.e., leftward and above) the contour. The conclusion is that nearly all candidate companions with $K' > 16$ are likely to be background interlopers, but nearly all brighter companions are likely to be bound companions. Given the typical brightness and distance of our observed targets, contamination should be negligible for $\rho < 1500$ AU and $q > 0.4$.

4.3. Comparison to Past Surveys

We have recovered a total of 93 candidate companions that were previously reported by imaging surveys in the literature, in addition to the 413 candidates that are newly reported here. There were no candidate companions that should have fallen above our detection limits and on the NIRC2 detector that we did not recover. We mark the overlapping targets in Tables 5 and 6. The vast majority of these recoveries can be attributed to three survey programs: 46 reported by Adams et al. (2012, 2013) and Dressing et al. (2014), 16 reported by

Lillo-Box et al. (2012, 2014), and 23 reported by Law et al. (2013). Most of these recovered candidates are among the brighter and wider candidates of our sample, since past surveys were typically conducted with smaller-aperture telescopes that did not achieve the full resolution possible with NRM or the full depth possible with a 10m telescope. Every candidate companion that we detected within $\rho < 100$ mas is a new detection.

For cases with significant overlap of well-resolved companions, we can compare our angular separations to those of past surveys, testing the relative platescale calibrations of NIRC2 (e.g., Yelda et al. 2010) and the other cameras. We found that for 42 candidate companions observed by Adams et al. (2012, 2013) and Dressing et al. (2014) that have projected separations of $\rho > 0.5''$, our projected separations are systematically $+3.1 \pm 0.4\%$ larger, suggesting that the relative platescales should be scaled by that amount before conducting direct comparisons. Similarly, for 16 overlapping candidates observed by Lillo-Box et al. (2012, 2014) with $\rho > 0.5''$, we find our projected separations are of $+0.54 \pm 0.42\%$ larger, and for 19 overlapping candidates observed by Law et al. (2013) with $\rho > 0.25''$, we find our projected separations are $-1.2 \pm 0.5\%$ smaller.

After applying these platescale offsets, we find that the RMS scatter in the difference of the projected sepa-

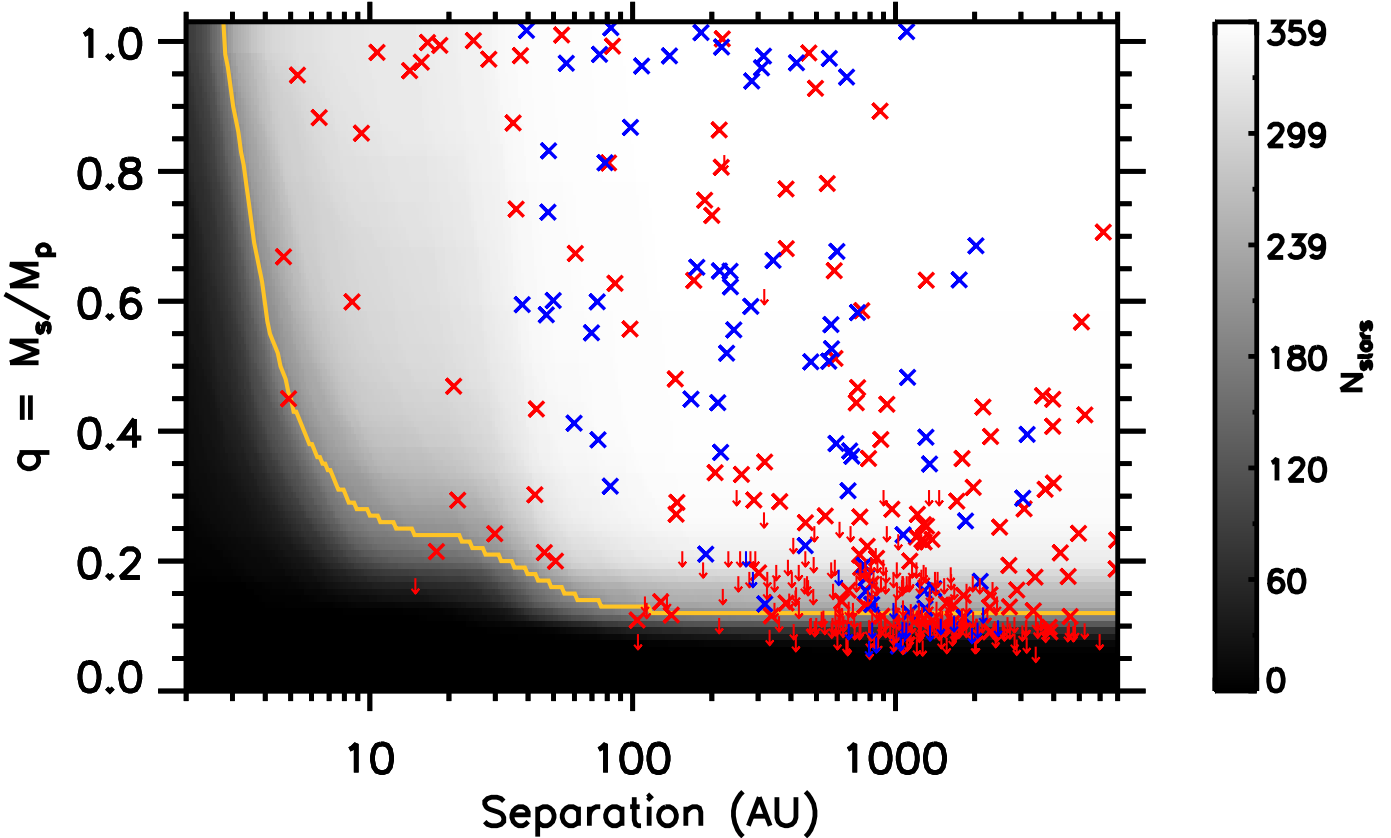


FIG. 5.— Detections and detection limits for our survey, in terms of binary mass ratio $q = m_s/m_p$ (if it were a bound companion) and physical projected separation ρ in AU. The detections are shown with red crosses for newly detected sources and blue crosses for previously identified sources, while the detection limits are shown in a shaded background trending from black (no observations sensitive to that combination of contrast and separation) to white (all 359 planet hosts that are sensitive to that combination). The orange solid line shows the median limit for the survey. None of our sample members had a previously known companion with projected physical separation $\rho < 40$ AU, demonstrating the need for NRM to probe the deep paucity of binary companions on solar-system scales.

rations is $\sigma_\rho = 60$ mas, $\sigma_\rho = 50$ mas, and $\sigma_\rho = 27$ mas, respectively. This scatter is broadly consistent with the proper motion of these KOIs and the difference in observational epoch, and hence might be additional evidence that wider candidates are significantly contaminated by background stars (e.g., Section 4.2).

The position angles also can be similarly tested against each other. We find that the PAs reported by Adams et al. (2012, 2013) and Dressing et al. (2014) are best fit to our own with a rotation of $+0.8 \pm 0.4$ degrees, with an RMS scatter of 2.8 degrees. The offset for Lillo-Box et al. (2012, 2014) is -0.44 ± 0.15 degrees, with an RMS of 0.59 degrees, while the offset for Law et al. (2013) is -1.6 ± 0.4 degrees, with an RMS of 1.6 degrees.

The contrast measurements of Lillo-Box et al. (2012, 2014) and Law et al. (2013) can't be directly tested since the measurements were conducted in the optical. However, we find that our contrast measurements agree with the K_s or K' measurements of Adams et al. (2012, 2013) and Dressing et al. (2014) with an offset of $+0.09 \pm 0.03$ mag, with an RMS scatter of 0.20 mag on the difference. Most of the largest outliers were near the detection limits, and hence the measurements are broadly consistent within the mutual uncertainties.

A small number of other candidates were also reported by other observing programs, albeit not in sufficient num-

bers to directly compare our results to theirs. The optical speckle imaging programs of Howell et al. (2011); Horch et al. (2012); Everett et al. (2015) reported 9 candidate companions in common with our program. Wang et al. (2014b) reported 12 candidate companions in common with our survey based on analysis of a wide range of observations downloaded from the Kepler Community Follow-Up Observing Project (CFOP), but given the heterogeneous data sources, no single calibration applies to the full dataset. Finally, Gilliland et al. (2015) reported HST imaging observation with three overlapping candidates, including all components in the close triple KOI-2626.

Our sample partially overlaps with the set of KOIs that have multi-epoch RV observations that could also identify binary companions (e.g., Wang et al. 2015b). That team identified KOI-0005 to have a parabolic linear trend (Wang et al. 2014b) that they later attributed to a substellar companion (Wang et al. 2015a). Our survey confirms that there is another component in the system, but it is actually an equal-brightness companion at $\rho \sim 15.7$ AU. The observed RV trend for KOI-0005 most likely tracks the flux-weighted velocity centroid of the spectrally-unresolved pair, an effect that should be common in flux-limited samples that are subject to Malmquist bias. Their RV monitoring observations (with

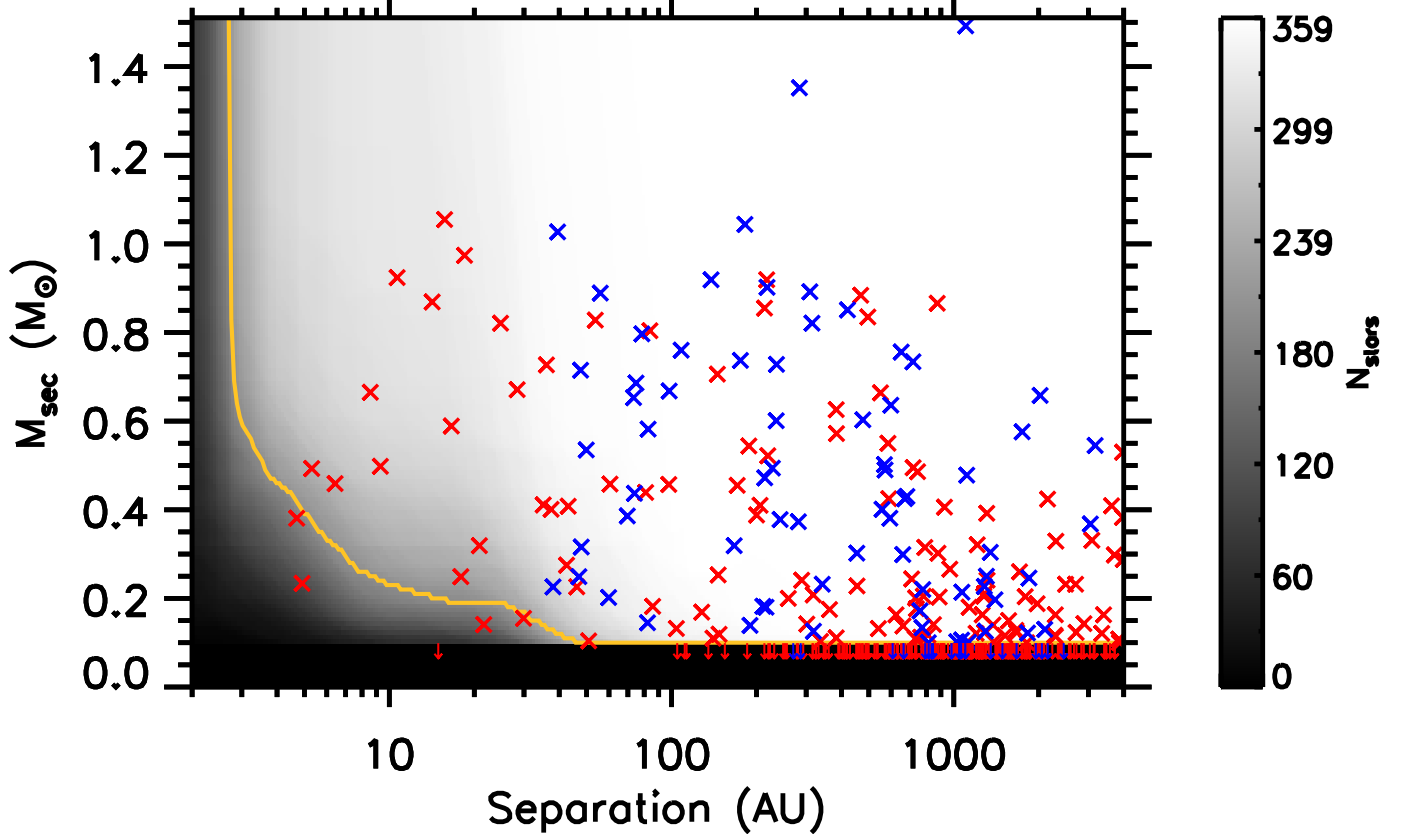


FIG. 6.— Detections and detection limits for our survey, in terms of candidate companion mass M in M_{\odot} (if it were a bound binary companion) and physical projected separation ρ in AU. The detections are shown with red crosses for newly detected sources and blue crosses for previously identified sources, while the detection limits are shown in a shaded background trending from black (no observations sensitive to that combination of contrast and separation) to white (all 359 planet hosts that are sensitive to that combination). The orange solid line shows the median limit for the survey.

5 epochs spanning one observing season) did not detect the equal-brightness companion to KOI-0289 ($\rho \sim 10.7$ AU), likely because RV changes in the flux-weighted centroid velocity are again heavily diluted. Conversely, we did not detect any companions to the system KOI-0069, for which they identified an RV trend of 12.2 ± 0.2 m s $^{-1}$ yr $^{-1}$. The source of the trend is likely either a substellar companion or a short-period equal-brightness companion with flux dilution. We therefore conclude that while both approaches can find close-in companions, the effects of flux dilution and Malmquist bias likely need to be factored into future analyses of RV data, as adding KOI-0005 and KOI-0069 to the previous analyses would significantly increase the inferred close-in companion fraction.

Finally, a number of candidate binaries were also identified by Kolbl et al. (2015) based on spectral decomposition of Keck/HIRES optical echelle spectra. Twelve of their candidate binaries were observed in the course of our survey so far. Seven of these targets (KOI-0005, 0652, 1361, 1613, 2059, 2311, and 2813) do indeed have candidate companions within $\lesssim 1''$, though in general their predicted temperatures and contrasts do not match ours. This disagreement also has been noted by Teske et al. (2015), and could be a systematic differences in spectral information content as a function of temperature (e.g., Gullikson et al. 2016). The other five candidate

binaries (KOI-0969, 2867, 3506, 3528, and 3782) do not have any imaged candidate companions that could be counterparts in our own observations, even down to projected separations of $\rho = 20\text{--}30$ mas. Far less than half of our sample has a similar-brightness companion within $\rho \lesssim 1''$, suggesting that their method is indeed able to identify some binaries. Furthermore, several of the unrecovered companions are to KOIs that are likely false positives, suggesting that these could be short-period spectroscopic binaries where Kolbl et al. detected the same (stellar) companion that is producing the transit signal (and that we could not detect). Multi-epoch RV analysis would be needed to confirm if this is the case.

5. THE BINARY POPULATION AMONG KEPLER PLANET HOSTS

Binary companions should raise many dynamical barriers to the formation and survival of planetary systems, including the tidal opening of wide disk gaps, dynamical stirring of planetesimal populations, accelerated disk clearing, and ejection of planets due to long-term secular evolution of their orbits. However, our discovery of so many binary companions suggests that planet formation is possible for some binary systems, at least within restricted ranges of parameter space. The most influential feature should be the semimajor axis of the binary; wide binaries exert a weaker force on close-in planetary

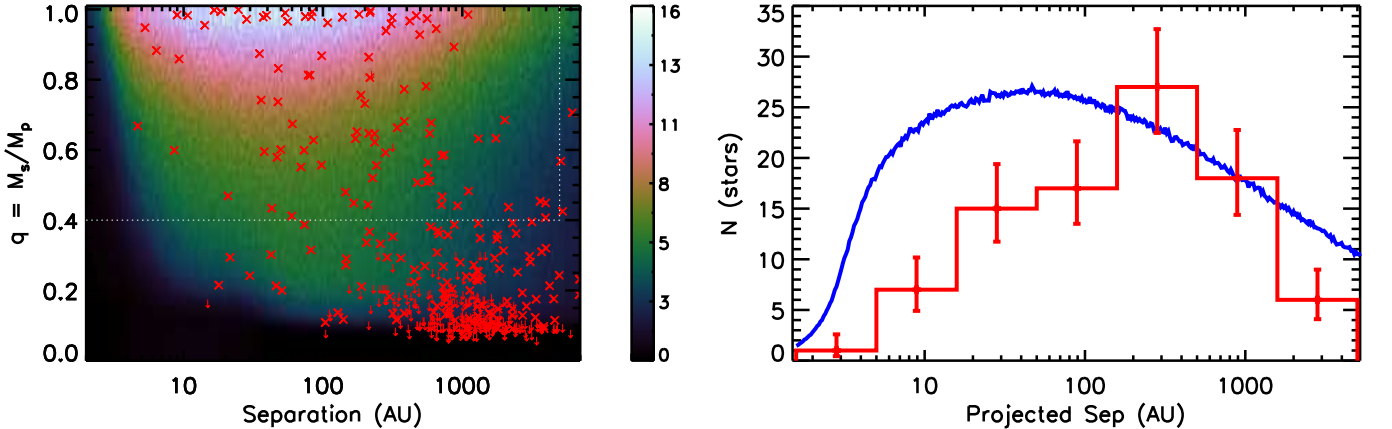


FIG. 7.— Left: Candidate companions (red crosses) among our sample, plotted on top of the expected density of binary companions in the observed parameter space $N(\rho, q)$ if binary companions were drawn out of the distribution reported by Raghavan et al. (2010), simulated with a random orbital phase, and then subjected to Malmquist bias and our observational detection limits. There is a clear deficit of candidates at small projected separation (denoting a paucity of short-period binaries) and an excess of faint, wide candidates (denoting the regime where background star contamination dominates). The uncontaminated space where we conduct statistical tests ($q > 0.4$, $a < 5000$ AU) is outlined with a white dotted line. Right: The marginalized distribution of projected separations, $N(\rho)$, for all companions with $q > 0.4$ (which omits nearly all background stars). The red histogram shows our observed sample, while the blue curve shows the predicted population if binary companions were drawn out of the distribution reported by Raghavan et al. (2010). As in the left panel, the deficit of close binaries is clearly evident; the distributions differ with $\chi^2 = 74.14$ or $\chi^2_\nu = 10.6$ with 7 degrees of freedom (since this is a pure comparison with no fit parameters). We observe 23 companions with $\rho < 50$ AU, while the distributions of Raghavan et al. (2010) predict 58.0 ± 7.6 such companions; we therefore see a 4.6σ deficit in this regime, and many of these detections likely are wide-orbiting companions that we see close only in projection. This deficit demonstrates that close binaries host planets at a lower occurrence rate than single stars or wider binary systems.

systems. The scale at which this transition occurs provides a strong constraint on the sum of the processes that impede planet formation and survival.

Our survey is only conducted at a single epoch, and most of our binary systems have orbital periods that are too long to measure, so we only know the instantaneous projected angular separation to each the binary companions in our sample. Due to projection effects, detection limits, and Malmquist bias, the distribution of projected separations can not be directly compared to the semimajor axis distribution of the full field population. We therefore have used a Monte Carlo routine to forward-model the binary frequency and the predicted distributions of semimajor axis, eccentricity, mass ratio, and geometric viewing angles into our observed parameter spaces. We base this model on the log-normal semimajor axis distribution and the linear-flat mass ratio and eccentricity distributions reported by Raghavan et al. (2010) for solar-type stars. These distributions appear to be valid for $0.5 < M < 1.5M_\odot$ stars, encompassing 90% of our sample. The small number of targets with $M < 0.5M_\odot$ might have fewer companions at $\gtrsim 500$ AU (e.g., Reid et al. 2001; Burgasser et al. 2003), but the companion frequency per dex of semimajor axis is remarkably constant in the $\lesssim 500$ AU regime across the mass range our entire sample (Duchêne & Kraus 2013).

In our forward-modeling Monte Carlo, we randomly draw binary parameters (a , e , and q), and then generate a random viewing angle in order to calculate the projected separation ρ for that simulated binary. Finally, we multiply that detection by the binary frequency of $F = 56\%$, the fraction of our sample with detection limits sensitive to that combination of ρ and q , and the fractional excess volume from which binaries of that mass ratio were se-

lected ($V_{bin}(q)/V_{single}$), and add the result to a 2D histogram of the number of binary companions that were expected in our sample, $N(\rho, q)$. We repeat this process to create 10^7 binaries, which we find is more than sufficient to minimize numerical errors in the resulting distributions. To more directly compare the projected separations, we end by marginalizing this distribution over the range of q where background stars are not a significant contributor ($0.4 < q < 1.0$) to produce a 1D histogram of the number of binary companions expected in our sample, $N(\rho)$.

In Figure 7 (left), we show the 2D histogram of $N(\rho, q)$ that would be predicted for our KOI sample if the binary companions are drawn from the field binary population of Raghavan et al. (2010), as well as the projected separations and mass ratios of our observed binary companions. The forward-model of Raghavan's binary population clearly captures the excess of equal-mass binaries due to Malmquist bias, as well as the overall variations in binary counts at 100–1000 AU. However, the predicted number of binary companions at $\rho \lesssim 50$ AU is clearly higher than the number we observe. In Figure 7 (right), we show the corresponding histogram of $N(\rho)$ (for $q > 0.4$) that we observe and the companion separation distribution that the Raghavan binary population would produce. This figure emphasizes the deep paucity of binary companions at small projected separations; while the Raghavan model would predict 58 binary companions with $\rho = 1.5$ –50 AU, we only observe 23 such companions. The goodness of fit for the right-hand panel is $\chi^2 = 74.1$ with 7 degrees of freedom (since there are no fit parameters), or $\chi^2_\nu = 10.6$.

However, we would expect a few close companions just from projection effects for wide edge-on or eccen-

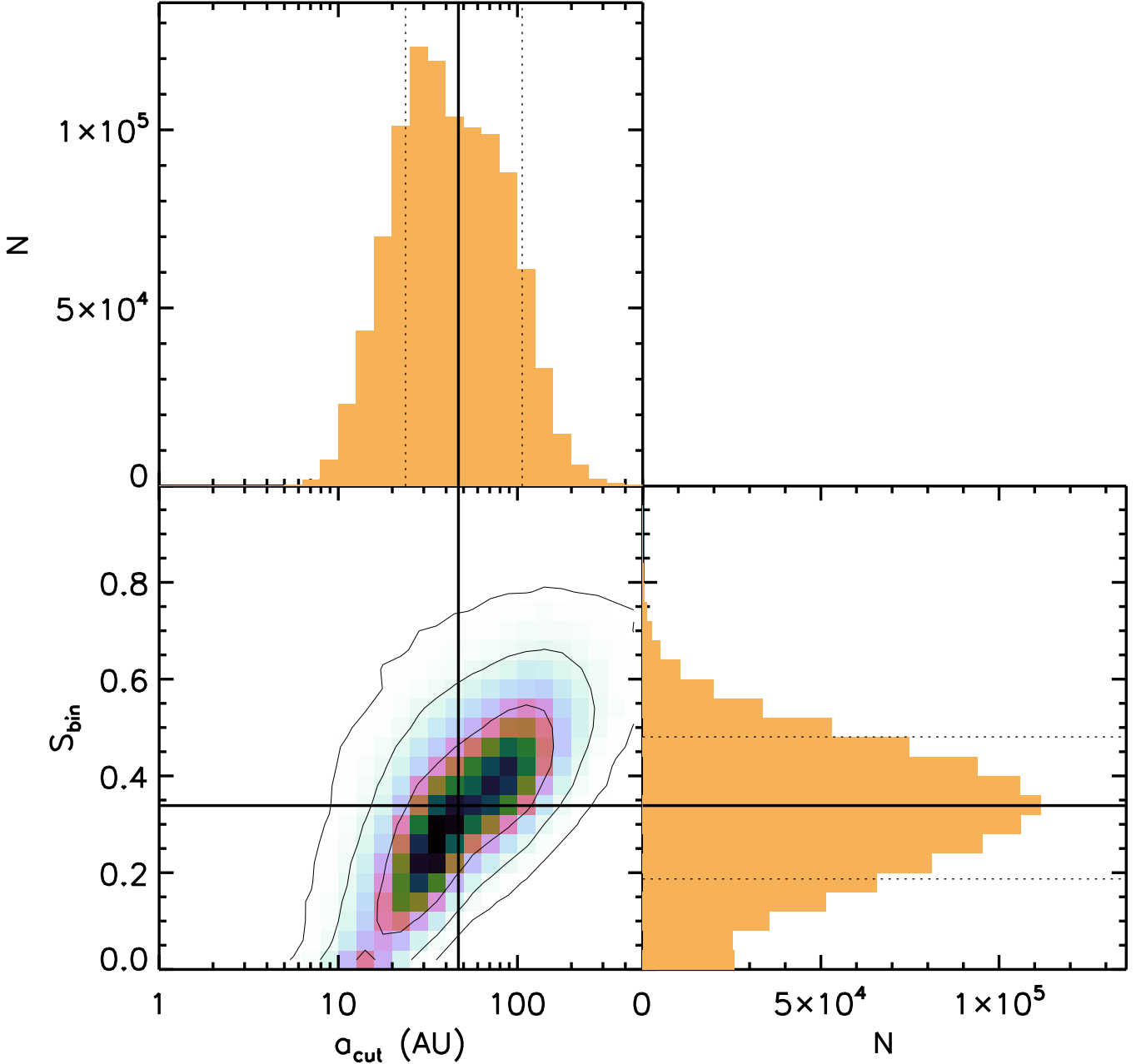


FIG. 8.—Joint confidence interval for the model parameters a_{cut} and S_{bin} , shown with contours at 1σ , 2σ , and 3σ , as well as marginalized 1D histograms for the posterior of each parameter. We show the median value for each parameter, as well as the central 68% credible interval, using solid and dashed lines respectively. The joint constraint on the two parameters is correlated, such that a larger value of a_{cut} (suppressing planet occurrence in wider binaries) allows for a higher value of S_{bin} (weakening the suppression). However, values of $a_{cut} \lesssim 10$ AU or $S_{bin} \gtrsim 0.65$ are disallowed at 2σ for any value of the other parameter. The null hypothesis ($a_{cut} = 0$ AU or $S_{bin} = 1.0$) is ruled out at 4.6σ confidence.

tric systems, even if there were no binary companions with small semimajor axes. To quantify this paucity, we have constructed a model whereby the binary population to planet hosts is similar to the Raghavan et al. (2010) distribution, except with a cutoff in semimajor axis a_{cut} inside which the binary occurrence rate is multiplied by a suppressive factor S_{bin} . Again, since binary companions are unlikely to be strongly affected by much less mas-

sive planets, then this model actually corresponds to the suppression rate of planet occurrence in the (known) binary population with $a < a_{cut}$. We then reran the Monte Carlo for a range of possible values for a_{cut} and S_{bin} and computed the χ^2 goodness of fit with respect to the observed projected separation distribution. The posterior was computed using an Metropolis-Hastings MCMC that explored the joint parameter space of the two parameters

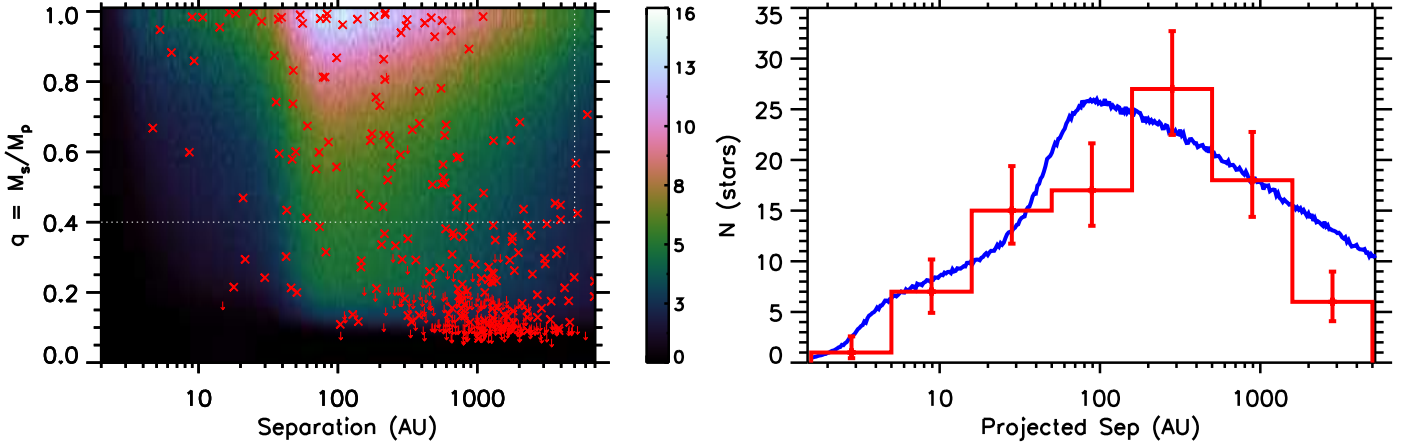


FIG. 9.— As in Figure 7, but for our best-fitting model that suppresses binary occurrence inside $a_{cut} = 47$ AU by a factor of $S_{bin} = 0.34$. The distributions differ with $\chi^2 = 6.03$ or $\chi^2_\nu = 1.21$. Given that $\chi^2_\nu \sim 1$, it appears that the current data can not support more complicated models (such as with multiple cutoffs or a gradual transition). These results demonstrate the ruinous impact of close binary companions on planetary systems; these binary systems must exist, they simply don't have planets and therefore are almost totally absent from the KOI sample.

using 5 walkers producing chains of $N = 2 \times 10^5$ samples. We used a log-flat prior on a_{cut} (matching the broadly logarithmic nature of the binary semimajor axis distribution; Raghavan et al. 2010) and a Beta prior on S_{bin} (since it is a binomial parameter; Jeffreys 1939).

In Figure 8, we show the joint posterior on a_{cut} and S_{bin} and the corresponding marginalized posteriors for each parameter. There is clearly a degeneracy between the allowed values of a_{cut} and S_{bin} , such that a less severe suppression factor is allowed if the cut is at large semimajor axis. However, the null hypothesis ($a_{cut} = 0$ AU or $S_{bin} = 1.0$) is ruled out at 4.6σ or $>99.99\%$ confidence, demonstrating that despite the degeneracy between the range and severity of the effect, the occurrence rate of short-period binaries is clearly suppressed. The median values and 68% credible intervals for each marginalized parameter distribution are $a_{cut} = 47^{+59}_{-23}$ AU and $S_{bin} = 34^{+14}_{-15}\%$.

In Figure 9, we show the corresponding best-fit models of $N(\rho, q)$ and $N(\rho)$ for our observed population of binary companions to planet hosts, using the median values of a_{cut} and S_{bin} from the marginalized distributions shown in Figure 8. The resulting goodness of fit is $\chi^2 = 6.03$ for 5 degrees of freedom ($\chi^2_\nu = 1.21$). Even this simple toy model produces an excellent fit to the data, arguing against the use of a more sophisticated model without a significantly larger dataset.

6. IMPLICATIONS FOR PLANET FORMATION AND SURVIVAL

The sharp suppression factor in our two-parameter model emphasizes the ruinous impact of close binary companions on planetary systems. There are no allowed values of S_{bin} that are consistent at 2σ with $a_{cut} \lesssim 10$ AU or $S_{bin} \gtrsim 0.65$, and those limits are only approached for extreme values of the other parameter (low S_{bin} or high a_{cut} , respectively). Clearly it is rare for planetary systems to form when a binary companion is present on a solar-system scale, as is consistent with the theoretical hurdles discussed in Section 1. The low planet occurrence rate has strong implications for the planet searches in the

solar neighborhood; many of the nearest Sun-like stars (such as α Cen, 61 Cyg, and 40 Eri) have binary companions at relevant semimajor axes. Those targets must be weighed carefully when designing intensive surveys to identify the nearest Earth-like planets, and controversial discoveries like Alpha Cen Bb (Dumusque et al. 2012; Hatzes 2013) must be considered with this strong prior against planet existence in mind.

The trend that we see is consistent with previous studies of RV and ground-based transit discoveries, which found that the planet population in wide binary systems ($a \gtrsim 100$ AU) is consistent with that seen for single stars (Bonavita & Desidera 2007; Mugrauer & Neuhauser 2009), but also that there might be a paucity of systems with $\rho \lesssim 100$ AU (Roell et al. 2012) or equivalently that the typical orbital radii are wider for planet host stars (Bergfors et al. 2012). Surveys of the KOIs at lower spatial resolution largely echo the former point (Horch et al. 2014), but due to the large distance to these stars, most high-resolution imaging surveys have not probed solar-system scales for KOIs. Wang et al. (2014b,a) have used RV trends (or the lack thereof) to probe the binary occurrence rate for KOIs on smaller spatial scales, estimating with $1-2\sigma$ significance that binary occurrence could be suppressed even to $a \sim 1500$ AU, but with a larger suppression factor at <100 AU.

The paucity of planets in close binary systems parallels results seen in star-forming regions (Cieza et al. 2009; Duchêne 2010; Kraus et al. 2012). The fast clearing of protoplanetary disks in these systems, when paired with the sharp suppression of planet occurrence, clearly indicates that planet formation is strongly inhibited by the dynamical influence of the companion. However, the disk-clearing effect only extends to $\rho \sim 50$ AU, whereas the disk occurrence rate is nearly 100% for all wider systems. Also, some close binary systems (such as CoKu Tau/4; Ireland & Kraus 2008) clearly still host disks and therefore might plausibly produce planets. Jang-Condell (2015) has used dynamical models of known planet-hosting binaries to show that in cases where a disk (otherwise equivalent to that around a single star)

is simply truncated by the binary companion, then its mass reservoir is indeed still sufficient to form the planets that were observed. It therefore remains plausible that the suppression of planet occurrence results from some combination of dynamical heating of the planetesimals (e.g., Quintana et al. 2007; Haghighipour & Raymond 2007; Rafikov & Silsbee 2015a, fast disk dissipation (out to $a \sim 50$ AU; Alexander 2012; Kraus et al. 2012) and the lower disk mass reservoir available for planet formation (out to 500 AU), as reported by Harris et al. (2012).

Finally, the question remains whether planet formation is totally suppressed over some range of semimajor axes. Our current results only restrict the population to a degenerate single-parameter family of values for a_{cut} and S_{bin} , and values of $S_{bin} = 0$ would be allowed if $a_{cut} \sim 10\text{--}20$ AU. Some theoretical models of planet formation make strong claims against the feasibility of planet formation in close binaries (e.g., Kley & Nelson 2008; Zsom et al. 2011), suggesting that the handful of systems could form via processes like small-N dynamical capture (e.g., Martí & Beaugé 2012). However, close binary systems are now known to host RV-discovered gas giants (e.g., γ Cep and HD 196885; Hatzes et al. 2003; Correia et al. 2008), multi-planet systems of transiting rocky planets (e.g., Kepler-444; Dupuy et al. 2016), and transiting circumbinary gas giants (Doyle et al. 2011, Welsh et al. 2012). The regime within which planet occurrence rates can be zero is therefore shrinking. Future orbit monitoring for close KOI binaries (e.g., Dupuy et al. 2016), when combined with the known orbits for systems like γ Cep and HD 196885, will break the degeneracy between a_{cut} and S_{bin} by constraining a for each binary and not simply the instantaneous projected separation ρ . These measurements also will cast further light on the reason that some planets survive in these dynamically harsh environments, whether as random unlikely events or because some binary configurations (such as low orbital eccentricity or mutual inclination) are less likely to inhibit planet formation.

7. SUMMARY

We have reported the discovery of 506 candidate companions to 382 Kepler Objects of Interest, probing down to solar-system scales ($\rho = 1.5\text{--}50$ AU) using nonredundant aperture-mask interferometry and deep adaptive optics imaging with Keck-II/NIRC2. We super-resolve some binary systems to projected separations as tight as $\rho = 2\text{--}3$ AU, showing that planets might form in these dynamically active environments. However, the full distribution of projected separations for our planet-host sample more broadly reveals a deep paucity of binary

companions at solar-system scales. For a field binary population, we should have found 58 binary companions with projected separation $\rho < 50$ AU and mass ratio $q > 0.4$; we instead only found 23 companions (a 4.6σ deficit), many of which must be wider pairs that are only close in projection. When the binary population is parametrized with a semimajor axis cutoff a_{cut} and a suppression factor inside that cutoff S_{bin} , we find that inside $a_{cut} = 47$ AU, the planet occurrence rate in binary systems is only $S_{bin} = 0.34$ times that of wider binaries or single stars. In contrast, the occurrence rate of wider binary companions to planet-host stars is similar to that of the full field population, suggesting that no suppression occurs outside solar-system scales. Given the mean semimajor axis ($\bar{a} = 50$ AU) and the frequency ($F = 56\%$) of solar-type binaries, our results demonstrate that a fifth of all solar-type stars in the Milky Way are disallowed from hosting planetary systems due to the influence of a binary companion.

The authors thank Joshua Carter, Dan Fabrycky, Andrew Youdin, Jason Wright, Kaitlin Kratter, Sean Andrews, Phil Muirhead, Roman Rafikov, and Hannah Jang-Condell for interesting and helpful discussions over the course of this research program. We also thank the referee for providing a helpful critique of the work.

This work was supported by NASA Keck PI Data Awards to A. Kraus and T. Dupuy, administered by the NASA Exoplanet Science Institute, and by NASA XRP grant 14-XRP14-2-0106 to A. Kraus. A. Mann was supposed by a Harlan J. Smith postdoctoral fellowship. D. Huber acknowledges support by the Australian Research Council's Discovery Projects funding scheme (project number DE140101364) and support by the National Aeronautics and Space Administration under Grant NNX14AB92G issued through the Kepler Participating Scientist Program.

Data presented herein were obtained at the W. M. Keck Observatory from telescope time allocated to the National Aeronautics and Space Administration through the agency's scientific partnership with the California Institute of Technology and the University of California. The Observatory was made possible by the generous financial support of the W. M. Keck Foundation. The authors wish to recognize and acknowledge the very significant cultural role and reverence that the summit of Mauna Kea has always had within the indigenous Hawaiian community. We are most fortunate to have the opportunity to conduct observations from this mountain.

REFERENCES

- Adams, E. R., Ciardi, D. R., Dupree, A. K., Gautier, III, T. N., Kulesa, C., & McCarthy, D. 2012, AJ, 144, 42
- Adams, E. R., Dupree, A. K., Kulesa, C., & McCarthy, D. 2013, AJ, 146, 9
- Ahn, C. P., et al. 2012, ApJS, 203, 21
- Alexander, R. 2012, ApJ, 757, L29
- Amôres, E. B., & Lépine, J. R. D. 2005, AJ, 130, 659
- Andrews, S. M., Czekala, I., Wilner, D. J., Espaillat, C., Dullemond, C. P., & Hughes, A. M. 2010, ApJ, 710, 462
- Artymowicz, P., & Lubow, S. H. 1994, ApJ, 421, 651
- Bahcall, J. N., & Soneira, R. M. 1980, ApJS, 44, 73
- Batalha, N. M., et al. 2010, ApJ, 713, L109
- . 2012, ArXiv e-prints
- Bergfors, C., et al. 2012, MNRAS, 12
- Bonavita, M., & Desidera, S. 2007, A&A, 468, 721
- Borucki, W. J., et al. 2010, Science, 327, 977
- Bowler, B. P., et al. 2010, ApJ, 709, 396
- Burgasser, A. J., Kirkpatrick, J. D., Reid, I. N., Brown, M. E., Miskay, C. L., & Gizis, J. E. 2003, ApJ, 586, 512
- Burke, C. J., et al. 2014, ApJS, 210, 19
- Campante, T. L., et al. 2015, ApJ, 799, 170
- Cheetham, A. C., Kraus, A. L., Ireland, M. J., Cieza, L., Rizzuto, A. C., & Tuthill, P. G. 2015, ApJ, 813, 83
- Cieza, L. A., et al. 2009, ApJ, 696, L84
- Correia, A. C. M., et al. 2008, A&A, 479, 271

- Daemgen, S., Hormuth, F., Brandner, W., Bergfors, C., Janson, M., Hippler, S., & Henning, T. 2009, *A&A*, 498, 567
- Deacon, N. R., et al. 2016, *MNRAS*, 455, 4212
- Desidera, S., & Barbieri, M. 2007, *A&A*, 462, 345
- Dotter, A., Chaboyer, B., Jevremović, D., Kostov, V., Baron, E., & Ferguson, J. W. 2008, *ApJS*, 178, 89
- Doyle, L. R., et al. 2011, *Science*, 333, 1602
- Dressing, C. D., Adams, E. R., Dupree, A. K., Kulesa, C., & McCarthy, D. 2014, *AJ*, 148, 78
- Dressing, C. D., & Charbonneau, D. 2013, ArXiv e-prints
- Duchêne, G. 2010, *ApJ*, 709, L114
- Duchêne, G., & Kraus, A. 2013, *ARA&A*, 51, 269
- Dumusque, X., et al. 2012, *Nature*, 491, 207
- Duquennoy, A., & Mayor, M. 1991, *A&A*, 248, 485
- Eggenberger, A., Udry, S., Chauvin, G., Beuzit, J., Lagrange, A., Ségransan, D., & Mayor, M. 2007, *A&A*, 474, 273
- Everett, M. E., Barclay, T., Ciardi, D. R., Horch, E. P., Howell, S. B., Crepp, J. R., & Silva, D. R. 2015, *AJ*, 149, 55
- Fabrycky, D., & Tremaine, S. 2007, *ApJ*, 669, 1298
- Fischer, D. A., & Valenti, J. 2005, *ApJ*, 622, 1102
- Foreman-Mackey, D., Hogg, D. W., & Morton, T. D. 2014, *ApJ*, 795, 64
- Ghez, A. M., White, R. J., & Simon, M. 1997, *ApJ*, 490, 353
- Gilliland, R. L., Cartier, K. M. S., Adams, E. R., Ciardi, D. R., Kalas, P., & Wright, J. T. 2015, *AJ*, 149, 24
- Girardi, L., Groenewegen, M. A. T., Hatziminaoglou, E., & da Costa, L. 2005, *A&A*, 436, 895
- Haghighipour, N. 2006, *ApJ*, 644, 543
- Haghighipour, N., & Raymond, S. N. 2007, *ApJ*, 666, 436
- Harris, R. J., Andrews, S. M., Wilner, D. J., & Kraus, A. L. 2012, *ApJ*, 751, 115
- Hatzes, A. P. 2013, *ApJ*, 770, 133
- Hatzes, A. P., Cochran, W. D., Endl, M., McArthur, B., Paulson, D. B., Walker, G. A. H., Campbell, B., & Yang, S. 2003, *ApJ*, 599, 1383
- Hekker, S., et al. 2011, *MNRAS*, 414, 2594
- Holman, M. J., & Wiegert, P. A. 1999, *AJ*, 117, 621
- Horch, E. P., Howell, S. B., Everett, M. E., & Ciardi, D. R. 2012, *AJ*, 144, 165
- . 2014, *ApJ*, 795, 60
- Howell, S. B., Everett, M. E., Sherry, W., Horch, E., & Ciardi, D. R. 2011, *AJ*, 142, 19
- Huber, D., et al. 2013, ArXiv e-prints
- . 2014, *ApJS*, 211, 2
- Ireland, M. J. 2013, ArXiv e-prints
- Ireland, M. J., Kraus, A., Martinache, F., Lloyd, J. P., & Tuthill, P. G. 2008, *ApJ*, 678, 463
- Ireland, M. J., & Kraus, A. L. 2008, *ApJ*, 678, L59
- Jang-Condell, H. 2015, *ApJ*, 799, 147
- Jang-Condell, H., Mugrauer, M., & Schmidt, T. 2008, *ApJ*, 683, L191
- Jensen, E. L. N., Dhital, S., Stassun, K. G., Patience, J., Herbst, W., Walter, F. M., Simon, M., & Basri, G. 2007, *AJ*, 134, 241
- Johnson, J. A., Aller, K. M., Howard, A. W., & Crepp, J. R. 2010, *PASP*, 122, 905
- Kaib, N. A., Raymond, S. N., & Duncan, M. 2013, *Nature*, 493, 381
- Kane, S. R., et al. 2015, *ApJ*, 815, 32
- Kolbl, R., Marcy, G. W., Isaacson, H., & Howard, A. W. 2015, *AJ*, 149, 18
- Kozai, Y. 1962, *AJ*, 67, 591
- Kratter, K. M., & Perets, H. B. 2012, *ApJ*, 753, 91
- Kraus, A. L., & Hillenbrand, L. A. 2007, *AJ*, 134, 2340
- . 2012, *ApJ*, 757, 141
- Kraus, A. L., Ireland, M. J., Hillenbrand, L. A., & Martinache, F. 2012, *ApJ*, 745, 19
- Kraus, A. L., Ireland, M. J., Martinache, F., & Hillenbrand, L. A. 2011, *ApJ*, 731, 8
- Kraus, A. L., Ireland, M. J., Martinache, F., & Lloyd, J. P. 2008, *ApJ*, 679, 762
- Kraus, A. L., Shkolnik, E. L., Allers, K. N., & Liu, M. C. 2014, *AJ*, 147, 146
- Law, N. M., et al. 2013, ArXiv e-prints
- Lillo-Box, J., Barrado, D., & Bouy, H. 2012, *A&A*, 546, A10
- . 2014, *A&A*, 566, A103
- Lloyd, J. P., Martinache, F., Ireland, M. J., Monnier, J. D., Pravdo, S. H., Shaklan, S. B., & Tuthill, P. G. 2006, *ApJ*, 650, L131
- Mann, A. W., Gaidos, E., & Ansdel, M. 2013, *ApJ*, 779, 188
- Mann, A. W., Gaidos, E., Lépine, S., & Hilton, E. J. 2012, *ApJ*, 753, 90
- Martinache, F., Lloyd, J. P., Ireland, M. J., Yamada, R. S., & Tuthill, P. G. 2007, *ApJ*, 661, 496
- Monet, D. G., et al. 2003, *AJ*, 125, 984
- Mugrauer, M., & Neuhauser, R. 2009, *A&A*, 494, 373
- Mugrauer, M., Neuhauser, R., Seifahrt, A., Mazeh, T., & Guenther, E. 2005, *A&A*, 440, 1051
- Muirhead, P. S., et al. 2015, *ApJ*, 801, 18
- Muterspaugh, M. W., et al. 2010, *AJ*, 140, 1657
- Nakajima, T., Kulkarni, S. R., Gorham, P. W., Ghez, A. M., Neugebauer, G., Oke, J. B., Prince, T. A., & Readhead, A. C. S. 1989, *AJ*, 97, 1510
- Naoz, S., Farr, W. M., & Rasio, F. A. 2012, *ApJ*, 754, L36
- Ngo, H., et al. 2015, *ApJ*, 800, 138
- Pascucci, I., Apai, D., Hardegree-Ullman, E. E., Kim, J. S., Meyer, M. R., & Bouwman, J. 2008, *ApJ*, 673, 477
- Petigura, E. A., Howard, A. W., & Marcy, G. W. 2013, *Proceedings of the National Academy of Science*, 110, 19273
- Quintana, E. V., Adams, F. C., Lissauer, J. J., & Chambers, J. E. 2007, *ApJ*, 660, 807
- Rafikov, R. R. 2013, *ApJ*, 765, L8
- Rafikov, R. R., & Silsbee, K. 2015a, *ApJ*, 798, 69
- . 2015b, *ApJ*, 798, 70
- Raghavan, D., et al. 2010, *ApJS*, 190, 1
- Readhead, A. C. S., Nakajima, T. S., Pearson, T. J., Neugebauer, G., Oke, J. B., & Sargent, W. L. W. 1988, *AJ*, 95, 1278
- Reid, I. N., Gizis, J. E., & Hawley, S. L. 2002, *AJ*, 124, 2721
- Reid, I. N., Gizis, J. E., Kirkpatrick, J. D., & Koerner, D. W. 2001, *AJ*, 121, 489
- Roell, T., Neuhauser, R., Seifahrt, A., & Mugrauer, M. 2012, *A&A*, 542, A92
- Serenelli, A. M., Bergemann, M., Ruchti, G., & Casagrande, L. 2013, *MNRAS*, 429, 3645
- Silsbee, K., & Rafikov, R. R. 2015, *ApJ*, 798, 71
- Skemer, A. J., Close, L. M., Greene, T. P., Hinz, P. M., Hoffmann, W. F., & Males, J. R. 2011, *ApJ*, 740, 43
- Skrutskie, M. F., et al. 2006, *AJ*, 131, 1163
- Slawson, R. W., et al. 2011, *AJ*, 142, 160
- Stello, D., et al. 2013, *ApJ*, 765, L41
- Tuthill, P., et al. 2006, in Presented at the Society of Photo-Optical Instrumentation Engineers (SPIE) Conference, Vol. 6272, Society of Photo-Optical Instrumentation Engineers (SPIE) Conference Series
- Tuthill, P. G., Monnier, J. D., Danchi, W. C., Wishnow, E. H., & Haniff, C. A. 2000, *PASP*, 112, 555
- Wang, J., Fischer, D. A., Xie, J.-W., & Ciardi, D. R. 2014a, *ApJ*, 791, 111
- Wang, J., Xie, J.-W., Barclay, T., & Fischer, D. A. 2014b, *ApJ*, 783, 4
- Welsh, W. F., et al. 2012, *Nature*, 481, 475
- White, R. J., & Ghez, A. M. 2001, *ApJ*, 556, 265
- Winn, J. N., Fabrycky, D., Albrecht, S., & Johnson, J. A. 2010, *ApJ*, 718, L145
- Wright, J. T., et al. 2011, *PASP*, 123, 412
- Yelda, S., Lu, J. R., Ghez, A. M., Clarkson, W., Anderson, J., Do, T., & Matthews, K. 2010, *ApJ*, 725, 331

TABLE 1
 KEPLER OBJECTS OF INTEREST

Name	RA	DEC	m_{K_p} (mag)	m_{K_s} (mag)	T_{eff} (K)	M_{prim} (M_\odot)	Distance (pc) ^a (Uncorr.)	Distance (pc) ^a (Corr.)	Ref
<i>Candidate or Confirmed Planet Hosts</i>									
KOI-0001	19 07 14.033	+49 18 59.04	11.34	9.85	5850± 117	0.950 ^{+0.065} _{-0.065}	195.6 ^{+9.7} _{-11.6}	206.4	(Kepler-1; TRES-2)
KOI-0002	19 28 59.348	+47 58 10.28	10.46	9.33	6350± 127	1.472 ^{+0.071} _{-0.086}	330.8 ^{+16.0} _{-19.1}	331.6	(Kepler-2; HAT-P-7)
KOI-0003	19 50 50.244	+48 04 51.07	9.17	7.01	4780± 95	0.810 ^{+0.031} _{-0.036}	38.3 ^{+1.5} _{-1.8}	38.3	(Kepler-3; HAT-P-11)
KOI-0005	19 18 57.532	+44 38 50.71	11.66	10.21	5753± 115	1.095 ^{+0.105} _{-0.075}	411.8 ^{+29.4} _{-29.4}	550.3	
KOI-0012	19 49 48.896	+41 00 39.56	11.35	10.23	6638± 180	1.227 ^{+0.206} _{-0.147}	336.4 ^{+119.6} _{-42.7}	341.4	(Kepler-448)
KOI-0013	19 07 53.086	+46 52 06.09	9.96	9.43	9071± 317	1.642 ^{+0.133} _{-0.133}	356.7 ^{+75.4} _{-47.1}	487.2	(Kepler-13)
KOI-0041	19 25 32.637	+41 59 24.97	11.20	9.77	5825± 116	1.042 ^{+0.103} _{-0.074}	285.2 ^{+20.9} _{-17.4}	285.2	(Kepler-100)
KOI-0042	18 52 36.167	+45 08 23.40	9.36	8.14	6325± 126	1.176 ^{+0.084} _{-0.084}	130.2 ^{+7.9} _{-7.9}	141.3	(Kepler-410)
KOI-0063	19 16 54.280	+49 32 53.52	11.58	10.00	5576± 112	0.934 ^{+0.057} _{-0.057}	194.0 ^{+23.1} _{-12.8}	194.0	(Kepler-63)
KOI-0069	19 25 40.393	+38 40 20.49	9.93	8.37	5669± 113	0.881 ^{+0.062} _{-0.062}	93.2 ^{+4.6} _{-5.6}	93.2	(Kepler-93)
KOI-0070	19 10 47.520	+42 20 19.38	12.50	10.87	5466± 109	0.895 ^{+0.055} _{-0.055}	278.8 ^{+36.9} _{-18.4}	281.9	(Kepler-20)
KOI-0072	19 02 43.052	+50 14 28.68	10.96	9.50	5627± 112	0.863 ^{+0.062} _{-0.034}	180.0 ^{+8.8} _{-8.8}	180.2	(Kepler-10)
KOI-0075	19 25 59.334	+42 43 42.53	10.77	9.39	5896± 117	1.257 ^{+0.088} _{-0.088}	395.8 ^{+31.8} _{-19.8}	396.2	
KOI-0082	18 45 55.854	+47 12 28.91	11.49	9.35	4903± 98	0.792 ^{+0.041} _{-0.041}	113.0 ^{+6.6} _{-6.6}	113.0	(Kepler-102)
KOI-0084	19 21 40.994	+37 51 06.48	11.90	10.32	5541± 110	0.869 ^{+0.054} _{-0.054}	206.5 ^{+22.9} _{-14.3}	206.5	(Kepler-19)
KOI-0085	19 14 45.286	+41 09 04.25	11.02	9.81	6169± 123	1.207 ^{+0.062} _{-0.112}	283.2 ^{+14.6} _{-17.6}	283.3	(Kepler-65)
KOI-0087	19 16 52.200	+47 53 04.06	11.66	10.15	5642± 112	0.843 ^{+0.060} _{-0.050}	209.2 ^{+12.4} _{-10.4}	209.2	(Kepler-22)
KOI-0089	19 59 17.080	+43 48 51.37	11.64	10.85	6688± 134	1.250 ^{+0.131} _{-0.109}	519.1 ^{+127.3} _{-63.7}	519.1	
KOI-0092	18 53 29.956	+43 47 17.59	11.67	10.30	5921± 118	0.998 ^{+0.074} _{-0.061}	260.3 ^{+32.9} _{-21.5}	260.3	
KOI-0094	19 49 19.937	+41 53 28.04	12.20	10.93	6176± 124	1.117 ^{+0.113} _{-0.075}	417.9 ^{+97.3} _{-44.2}	417.9	(Kepler-89)
KOI-0098	19 10 50.120	+47 19 58.98	12.13	10.99	6378± 127	1.443 ^{+0.085} _{-0.153}	758.8 ^{+37.5} _{-60.1}	982.9	(Kepler-14)
KOI-0099	19 41 44.238	+44 31 52.03	12.96	10.98	5086± 102	0.750 ^{+0.047} _{-0.040}	232.4 ^{+13.6} _{-13.6}	233.4	
KOI-0103	19 26 44.004	+37 45 05.73	12.59	11.05	5651± 113	0.927 ^{+0.057} _{-0.057}	310.6 ^{+42.0} _{-21.0}	310.7	
KOI-0104	18 44 46.736	+47 29 49.67	12.90	10.59	4781± 96	0.807 ^{+0.031} _{-0.031}	201.2 ^{+9.9} _{-9.9}	201.2	(Kepler-94)
KOI-0105	19 55 44.890	+44 51 28.48	12.87	11.21	5660± 113	0.823 ^{+0.058} _{-0.048}	321.7 ^{+53.2} _{-26.6}	327.3	
KOI-0112	19 42 35.691	+48 29 44.02	12.77	11.37	5837± 117	0.978 ^{+0.060} _{-0.072}	404.3 ^{+67.9} _{-33.9}	471.6	
KOI-0116	20 03 27.356	+44 20 15.18	12.88	11.43	5858± 117	0.960 ^{+0.060} _{-0.072}	413.3 ^{+62.8} _{-34.9}	413.5	(Kepler-106)
KOI-0117	19 48 06.782	+48 12 31.00	12.49	11.06	5851± 117	1.203 ^{+0.039} _{-0.128}	500.9 ^{+25.8} _{-30.9}	500.9	(Kepler-107)
KOI-0118	19 09 27.070	+38 38 58.56	12.38	10.90	5747± 114	1.004 ^{+0.084} _{-0.070}	437.7 ^{+28.5} _{-23.5}	443.9	
KOI-0119	19 38 14.202	+46 03 44.38	12.65	10.98	5854± 117	1.473 ^{+0.055} _{-0.183}	765.1 ^{+37.8} _{-56.6}	1066.1	(Kepler-108)
KOI-0122	18 57 55.788	+44 23 52.95	12.35	10.80	5699± 113	1.085 ^{+0.116} _{-0.073}	437.3 ^{+32.8} _{-23.4}	437.3	(Kepler-95)
KOI-0137	19 52 19.065	+44 44 46.75	13.55	11.76	5345± 106	0.915 ^{+0.042} _{-0.035}	483.1 ^{+40.2} _{-33.5}	483.1	(Kepler-18)
KOI-0141	19 12 09.192	+50 39 05.80	13.69	11.99	5340± 107	0.948 ^{+0.039} _{-0.047}	468.3 ^{+51.8} _{-25.9}	531.6	
KOI-0144	19 46 05.830	+39 14 59.14	13.70	11.46	4958± 99	0.844 ^{+0.028} _{-0.042}	310.8 ^{+18.5} _{-15.4}	311.1	
KOI-0148	19 56 33.413	+40 56 56.47	13.04	11.22	5194± 104	0.870 ^{+0.046} _{-0.046}	301.8 ^{+28.6} _{-16.4}	303.5	(Kepler-48)
KOI-0152	20 02 04.109	+44 22 53.69	13.91	12.61	6189± 124	1.107 ^{+0.109} _{-0.081}	911.5 ^{+197.8} _{-98.9}	914.2	(Kepler-79)
KOI-0153	19 11 59.495	+50 56 39.58	13.46	11.26	4725± 94	0.748 ^{+0.038} _{-0.027}	247.7 ^{+12.1} _{-14.6}	247.7	(Kepler-113)
KOI-0156	19 36 29.143	+48 20 58.28	13.74	11.37	3983± 80	0.560 ^{+0.041} _{-0.066}	167.3 ^{+13.4} _{-16.1}	167.3	(Kepler-114)
KOI-0157	19 48 27.627	+41 54 32.91	13.71	12.18	5663± 113	0.921 ^{+0.055} _{-0.028}	610.5 ^{+43.2} _{-19.6}	615.4	(Kepler-11)
KOI-0161	19 08 12.414	+40 12 41.59	13.34	11.24	4984± 100	0.855 ^{+0.035} _{-0.042}	282.6 ^{+19.6} _{-14.0}	284.0	
KOI-0174	19 47 17.497	+48 06 27.19	13.78	11.54	4804± 96	0.711 ^{+0.037} _{-0.037}	273.3 ^{+15.9} _{-15.9}	285.9	
KOI-0177	19 52 42.532	+42 14 13.35	13.18	11.64	5711± 114	0.948 ^{+0.073} _{-0.061}	445.7 ^{+7.8} _{-35.4}	606.0	
KOI-0197	19 23 19.951	+38 11 03.66	14.02	11.96	4945± 99	0.781 ^{+0.039} _{-0.039}	365.7 ^{+21.7} _{-21.7}	365.7	
KOI-0205	19 41 59.202	+42 32 16.41	14.52	12.66	5216± 148	0.807 ^{+0.078} _{-0.078}	532.0 ^{+76.1} _{-54.3}	532.5	
KOI-0214	19 54 29.971	+48 34 38.82	14.26	12.47	5528± 173	0.913 ^{+0.092} _{-0.092}	587.1 ^{+157.5} _{-72.7}	598.9	(Kepler-424)
KOI-0216	19 56 51.160	+41 25 29.39	14.71	12.71	5274± 165	0.903 ^{+0.068} _{-0.082}	614.7 ^{+134.8} _{-56.2}	620.3	(Kepler-118)
KOI-0227	18 57 24.485	+41 31 09.12	14.27	11.49	4093± 82	0.578 ^{+0.035} _{-0.035}	194.1 ^{+13.6} _{-16.4}	273.7	
KOI-0232	19 24 26.850	+39 56 56.79	14.25	12.83	6050± 121	0.994 ^{+0.076} _{-0.064}	866.0 ^{+177.6} _{-80.7}	866.0	(Kepler-122)
KOI-0242	19 22 32.761	+38 42 27.60	14.75	13.05	5640± 170	0.960 ^{+0.106} _{-0.089}	823.6 ^{+233.4} _{-89.8}	823.6	
KOI-0244	19 06 33.215	+39 29 16.37	10.73	9.49	6270± 125	1.140 ^{+0.084} _{-0.084}	232.8 ^{+14.6} _{-14.6}	232.8	(Kepler-25)
KOI-0245	18 56 14.290	+44 31 05.57	9.70	7.94	5417± 108	0.807 ^{+0.048} _{-0.058}	63.0 ^{+3.1} _{-3.1}	63.0	(Kepler-37)
KOI-0246	19 24 07.756	+49 02 24.98	10.00	8.59	5793± 115	1.027 ^{+0.093} _{-0.077}	137.8 ^{+8.8} _{-7.0}	137.8	(Kepler-68)
KOI-0247	18 59 59.663	+50 08 48.44	14.22	11.12	3852± 80	0.575 ^{+0.029} _{-0.041}	148.7 ^{+13.3} _{-13.3}	148.7	
KOI-0249	18 59 41.243	+45 58 20.64	14.49	11.15	3548± 80	0.357 ^{+0.061} _{-0.073}	79.0 ^{+14.7} _{-14.7}	79.0	
KOI-0251	19 53 01.948	+47 36 17.78	14.75	11.68	3770± 80	0.533 ^{+0.033} _{-0.052}	168.5 ^{+17.4} _{-20.9}	170.3	(Kepler-125)
KOI-0252	19 21 36.357	+48 49 21.32	15.61	12.55	3858± 80	0.543 ^{+0.040} _{-0.040}	265.1 ^{+27.2} _{-27.2}	265.1	
KOI-0253	19 02 17.842	+49 57 44.17	15.25	12.29	3900± 80	0.622 ^{+0.026} _{-0.031}	285.1 ^{+17.5} _{-21.0}	285.1	

TABLE 1
KEPLER OBJECTS OF INTEREST

KOI-0254	19 31 29.495	+41 03 51.37	15.98	12.89	3820 ± 80	$0.566^{+0.029}_{-0.041}$	$322.3^{+31.3}_{-21.3}$	323.1	(Kepler-45)
KOI-0255	19 11 25.950	+42 32 33.46	15.11	12.08	3900 ± 80	$0.528^{+0.030}_{-0.038}$	$212.5^{+19.4}_{-23.2}$	216.1	
KOI-0257	18 58 32.446	+40 43 11.39	10.87	9.62	6184 ± 123	$1.178^{+0.048}_{-0.086}$	$223.4^{+11.4}_{-11.4}$	223.4	
KOI-0260	19 17 23.357	+44 12 30.64	10.50	9.34	6239 ± 124	$1.061^{+0.107}_{-0.067}$	$221.2^{+13.6}_{-13.6}$	221.2	(Kepler-126)
KOI-0261	19 48 16.707	+40 31 30.47	10.30	8.87	5690 ± 114	$0.964^{+0.061}_{-0.061}$	$122.1^{+20.2}_{-9.0}$	122.1	(Kepler-96)
KOI-0262	19 12 24.207	+50 02 01.38	10.42	9.20	6225 ± 124	$1.257^{+0.065}_{-0.144}$	$238.8^{+17.7}_{-12.6}$	238.8	(Kepler-50)
KOI-0268	19 02 54.910	+38 30 25.10	10.56	9.60	6343 ± 126	$1.193^{+0.073}_{-0.102}$	$253.4^{+15.9}_{-13.2}$	270.1	
KOI-0269	19 09 22.976	+43 22 42.21	10.93	9.75	6463 ± 129	$1.282^{+0.074}_{-0.095}$	$299.8^{+15.0}_{-21.0}$	299.9	
KOI-0270	19 34 55.877	+41 54 02.98	11.41	9.70	5588 ± 111	$0.926^{+0.067}_{-0.037}$	$267.9^{+15.0}_{-10.7}$	338.9	(Kepler-449)
KOI-0271	19 00 45.600	+46 01 40.66	11.48	10.23	6106 ± 122	$1.228^{+0.060}_{-0.070}$	$345.4^{+13.8}_{-22.1}$	345.4	(Kepler-127)
KOI-0273	19 09 54.844	+38 13 43.82	11.46	9.97	5739 ± 114	$1.075^{+0.044}_{-0.062}$	$230.2^{+11.9}_{-11.9}$	230.2	
KOI-0274	18 49 58.132	+43 58 48.75	11.39	10.11	6072 ± 121	$1.095^{+0.144}_{-0.072}$	$374.0^{+28.5}_{-20.3}$	374.6	(Kepler-128)
KOI-0275	19 01 14.700	+47 50 54.83	11.70	10.25	5770 ± 115	$1.271^{+0.165}_{-0.037}$	$391.8^{+29.2}_{-24.3}$	391.8	(Kepler-129)
KOI-0276	19 18 39.456	+48 42 22.36	11.85	10.48	5982 ± 119	$1.024^{+0.091}_{-0.065}$	$318.6^{+19.8}_{-16.5}$	318.6	
KOI-0280	19 06 45.469	+39 12 42.88	11.07	9.78	6134 ± 122	$0.984^{+0.079}_{-0.056}$	$207.5^{+12.1}_{-9.7}$	207.5	
KOI-0281	19 10 37.200	+39 14 39.44	11.95	10.45	5622 ± 112	$0.871^{+0.051}_{-0.031}$	$372.8^{+17.5}_{-14.6}$	372.8	
KOI-0282	19 13 48.157	+40 14 43.18	11.53	10.49	5884 ± 117	$0.925^{+0.067}_{-0.067}$	$307.6^{+18.5}_{-15.4}$	307.6	(Kepler-130)
KOI-0283	19 14 07.398	+40 56 32.28	11.52	10.08	5685 ± 114	$0.983^{+0.062}_{-0.062}$	$221.5^{+31.1}_{-17.1}$	221.5	(Kepler-131)
KOI-0284	18 52 56.594	+41 20 34.94	11.82	10.42	5933 ± 119	$0.937^{+0.066}_{-0.066}$	$266.0^{+52.9}_{-26.4}$	355.7	(Kepler-132)
KOI-0285	19 16 20.654	+41 33 46.65	11.56	10.40	5871 ± 117	$1.153^{+0.158}_{-0.079}$	$444.3^{+28.3}_{-28.3}$	449.2	(Kepler-92)
KOI-0288	19 34 51.951	+46 13 35.95	11.02	9.70	6174 ± 123	$1.476^{+0.068}_{-0.135}$	$406.7^{+23.9}_{-28.7}$	419.0	
KOI-0289	18 51 46.956	+47 34 29.66	12.75	11.19	5868 ± 117	$0.945^{+0.091}_{-0.065}$	$463.7^{+108.7}_{-72.4}$	629.3	
KOI-0291	19 49 06.716	+48 19 13.20	12.85	11.32	5608 ± 112	$0.981^{+0.084}_{-0.060}$	$480.0^{+107.6}_{-67.3}$	544.9	(Kepler-133)
KOI-0298	19 21 58.623	+52 03 19.87	12.71	10.89	5253 ± 105	$0.800^{+0.052}_{-0.043}$	$241.0^{+20.4}_{-14.6}$	326.5	
KOI-0299	19 02 38.796	+37 57 52.20	12.90	11.25	5539 ± 111	$0.958^{+0.058}_{-0.058}$	$371.8^{+70.9}_{-32.2}$	372.0	(Kepler-98)
KOI-0303	19 34 42.078	+41 17 43.30	12.19	10.63	5637 ± 113	$0.890^{+0.065}_{-0.054}$	$263.6^{+46.0}_{-23.0}$	263.6	
KOI-0305	19 49 24.961	+41 18 00.18	12.97	10.76	4782 ± 96	$0.789^{+0.033}_{-0.040}$	$211.0^{+10.4}_{-12.4}$	211.0	(Kepler-99)
KOI-0306	19 57 16.692	+41 23 04.70	12.63	10.76	5323 ± 106	$0.890^{+0.046}_{-0.055}$	$251.9^{+20.3}_{-14.5}$	270.6	
KOI-0313	18 48 32.527	+43 02 20.76	12.99	11.16	5187 ± 104	$0.820^{+0.042}_{-0.051}$	$271.2^{+23.9}_{-13.3}$	271.2	(Kepler-137)
KOI-0314	19 21 31.560	+43 17 34.76	12.93	9.51	3871 ± 80	$0.547^{+0.034}_{-0.041}$	$67.8^{+6.1}_{-7.4}$	67.8	(Kepler-138)
KOI-0315	19 49 05.251	+43 19 59.91	12.97	10.81	4899 ± 98	$0.717^{+0.045}_{-0.038}$	$197.3^{+13.7}_{-9.8}$	197.3	
KOI-0316	18 49 34.065	+43 53 21.66	12.70	11.17	5619 ± 112	$1.024^{+0.063}_{-0.063}$	$382.9^{+78.5}_{-31.4}$	382.9	(Kepler-139)
KOI-0321	19 27 23.533	+44 58 05.59	12.52	10.97	5676 ± 114	$1.008^{+0.063}_{-0.053}$	$338.1^{+47.2}_{-26.2}$	338.1	(Kepler-406)
KOI-0323	18 56 14.670	+45 30 24.66	12.47	10.83	5427 ± 109	$0.877^{+0.045}_{-0.054}$	$256.3^{+27.8}_{-13.9}$	256.3	
KOI-0338	19 51 53.013	+47 43 54.06	13.45	11.39	4910 ± 98	$0.821^{+0.034}_{-0.041}$	$295.2^{+17.5}_{-14.6}$	295.2	(Kepler-141)
KOI-0345	19 06 05.955	+48 41 00.96	13.34	11.18	4869 ± 97	$0.752^{+0.037}_{-0.037}$	$246.0^{+14.7}_{-12.3}$	246.0	
KOI-0346	19 54 38.621	+48 36 22.93	13.52	11.55	5104 ± 102	$0.813^{+0.041}_{-0.041}$	$324.6^{+22.3}_{-14.9}$	325.5	
KOI-0348	19 34 44.575	+48 49 30.51	13.93	11.68	4687 ± 94	$0.729^{+0.036}_{-0.036}$	$296.4^{+17.6}_{-14.7}$	296.4	
KOI-0356	19 50 56.733	+49 38 13.74	13.81	11.89	5301 ± 155	$0.730^{+0.125}_{-0.054}$	$354.2^{+84.2}_{-35.1}$	389.7	
KOI-0365	19 49 56.858	+49 37 24.42	11.19	9.65	5555 ± 111	$0.878^{+0.053}_{-0.055}$	$155.9^{+19.1}_{-10.6}$	155.9	
KOI-0366	19 26 39.404	+38 37 09.32	11.71	10.63	6207 ± 124	$1.764^{+0.112}_{-0.224}$	$846.0^{+147.7}_{-147.7}$	846.8	
KOI-0367	18 57 53.320	+39 54 42.52	11.10	9.64	5736 ± 115	$0.982^{+0.062}_{-0.062}$	$180.0^{+28.4}_{-14.2}$	180.0	
KOI-0370	19 25 33.061	+44 31 44.80	11.93	10.63	6144 ± 122	$1.360^{+0.064}_{-0.160}$	$549.0^{+32.6}_{-39.1}$	549.0	(Kepler-145)
KOI-0372	19 56 29.385	+41 52 00.34	12.39	10.91	5815 ± 116	$0.941^{+0.059}_{-0.059}$	$309.1^{+43.1}_{-23.9}$	309.3	
KOI-0387	19 08 52.493	+38 51 45.08	13.58	11.09	4528 ± 90	$0.662^{+0.033}_{-0.033}$	$204.4^{+10.3}_{-12.4}$	207.3	
KOI-0421	19 59 37.419	+45 26 22.84	14.99	13.07	5349 ± 161	$0.872^{+0.087}_{-0.087}$	$703.9^{+158.7}_{-79.4}$	707.1	
KOI-0435	19 19 07.324	+49 53 47.51	14.53	12.99	5690 ± 114	$0.916^{+0.056}_{-0.056}$	$773.3^{+130.3}_{-60.2}$	773.3	(Kepler-154)
KOI-0438	19 13 58.997	+51 04 54.98	14.26	11.81	3985 ± 80	$0.551^{+0.033}_{-0.033}$	$203.9^{+17.4}_{-20.9}$	217.3	(Kepler-155)
KOI-0463	20 00 49.460	+45 01 05.30	14.71	11.45	3605 ± 80	$0.382^{+0.054}_{-0.076}$	$96.0^{+17.4}_{-17.4}$	96.0	
KOI-0464	19 34 59.304	+45 06 25.99	14.36	12.59	5587 ± 171	$0.950^{+0.101}_{-0.084}$	$657.7^{+191.4}_{-68.4}$	657.7	
KOI-0478	19 52 25.371	+48 24 04.14	14.27	10.96	3825 ± 80	$0.580^{+0.029}_{-0.035}$	$138.8^{+12.4}_{-12.4}$	138.8	
KOI-0490	19 30 38.020	+38 20 43.40	14.02	11.83	4796 ± 96	$0.751^{+0.037}_{-0.037}$	$324.1^{+19.5}_{-16.2}$	330.0	(Kepler-167)
KOI-0500	19 44 27.019	+39 58 43.60	14.80	12.25	4040 ± 80	$0.588^{+0.029}_{-0.035}$	$272.4^{+19.1}_{-22.9}$	273.8	(Kepler-80)
KOI-0503	18 53 59.956	+40 33 10.08	15.00	12.31	4213 ± 84	$0.629^{+0.031}_{-0.037}$	$315.8^{+19.1}_{-22.9}$	315.8	
KOI-0505	19 03 59.971	+40 55 09.55	14.19	12.19	4997 ± 100	$0.796^{+0.042}_{-0.042}$	$413.2^{+29.2}_{-20.9}$	413.8	(Kepler-169)
KOI-0531	19 10 45.886	+47 32 48.85	14.42	11.61	4102 ± 82	$0.635^{+0.032}_{-0.032}$	$222.5^{+15.6}_{-15.6}$	222.5	
KOI-0554	19 21 24.272	+40 41 13.20	14.55	13.05	6103 ± 183	$1.007^{+0.150}_{-0.107}$	$916.8^{+259.1}_{-108.0}$	916.8	
KOI-0571	19 54 36.650	+43 57 18.08	14.62	11.60	3761 ± 80	$0.494^{+0.038}_{-0.053}$	$152.1^{+23.5}_{-23.5}$	152.3	(Kepler-186)
KOI-0588	18 49 48.142	+46 19 17.04	14.34	11.97	4525 ± 130	$0.549^{+0.040}_{-0.033}$	$240.2^{+20.2}_{-20.2}$	289.4	
KOI-0596	18 54 57.766	+47 30 58.64	14.82	11.57	3658 ± 80	$0.480^{+0.043}_{-0.060}$	$133.5^{+18.6}_{-18.6}$	133.5	
KOI-0610	18 57 54.836	+40 55 59.17	14.67	11.91	4103 ± 82	$0.615^{+0.031}_{-0.037}$	$246.3^{+17.8}_{-17.8}$	246.3	

TABLE 1
 KEPLER OBJECTS OF INTEREST

KOI-0623	19 40 54.346	+50 33 32.32	11.81	10.53	6004± 120	0.914 ^{+0.055} _{-0.066}	311.1 ^{+19.0} _{-15.8}	311.1	(Kepler-197)
KOI-0640	19 49 00.630	+40 17 18.96	13.33	11.48	5325± 106	0.915 ^{+0.046} _{-0.055}	363.2 ^{+32.9} _{-23.5}	508.1	
KOI-0650	19 21 35.083	+41 02 24.29	13.59	11.57	5050± 101	0.969 ^{+0.134} _{-0.048}	734.3 ^{+144.0} _{-82.3}	773.2	
KOI-0652	19 34 22.053	+41 05 42.58	13.65	11.58	5305± 106	0.857 ^{+0.044} _{-0.052}	351.7 ^{+32.4} _{-20.2}	456.7	
KOI-0657	18 51 53.621	+41 19 19.24	13.87	11.64	4668± 93	0.732 ^{+0.036} _{-0.036}	290.5 ^{+14.4} _{-17.3}	290.8	(Kepler-202)
KOI-0663	19 01 08.906	+41 51 40.22	13.51	10.83	4121± 82	0.567 ^{+0.028} _{-0.034}	142.4 ^{+8.9} _{-13.3}	142.6	(Kepler-205)
KOI-0674	19 21 18.560	+42 53 53.81	13.78	11.58	4883± 97	1.024 ^{+0.182} _{-0.061}	1037.9 ^{+94.0} _{-62.7}	1037.9	
KOI-0676	19 30 00.813	+43 04 59.34	13.82	11.31	3914± 80	0.556 ^{+0.028} _{-0.039}	155.5 ^{+14.2} _{-14.2}	155.5	(Kepler-210)
KOI-0678	19 01 45.396	+43 10 06.53	13.28	11.45	5290± 106	0.895 ^{+0.046} _{-0.055}	336.1 ^{+29.5} _{-16.4}	336.1	(Kepler-211)
KOI-0701	18 52 51.057	+45 20 59.50	13.73	11.66	4925± 98	0.691 ^{+0.042} _{-0.035}	284.0 ^{+17.3} _{-14.5}	287.8	(Kepler-62)
KOI-0707	19 16 18.611	+46 00 18.79	13.99	12.59	5904± 118	1.068 ^{+0.126} _{-0.090}	1002.6 ^{+246.5} _{-154.1}	1002.6	(Kepler-33)
KOI-0719	19 26 01.480	+46 53 44.67	13.18	10.55	4500± 90	0.656 ^{+0.032} _{-0.038}	153.8 ^{+7.7} _{-9.2}	153.8	(Kepler-220)
KOI-0781	19 44 53.269	+50 17 13.99	15.94	12.63	3637± 80	0.473 ^{+0.038} _{-0.061}	214.5 ^{+30.2} _{-36.2}	214.5	
KOI-0817	18 55 27.935	+39 53 53.08	15.41	12.31	3866± 80	0.562 ^{+0.028} _{-0.040}	246.2 ^{+32.3} _{-22.3}	246.2	(Kepler-236)
KOI-0818	19 15 14.883	+40 02 00.24	15.88	12.49	3610± 80	0.522 ^{+0.028} _{-0.064}	223.4 ^{+52.3} _{-33.5}	223.4	
KOI-0852	18 53 15.930	+41 50 13.63	15.26	13.56	5653± 175	0.953 ^{+0.106} _{-0.089}	1035.4 ^{+297.5} _{-114.4}	1035.4	
KOI-0854	19 18 02.036	+41 48 43.63	15.85	12.54	3670± 80	0.529 ^{+0.030} _{-0.048}	246.2 ^{+21.3} _{-31.9}	329.9	
KOI-0868	19 32 01.912	+42 18 25.92	15.17	12.52	4244± 85	0.672 ^{+0.028} _{-0.033}	373.0 ^{+18.0} _{-23.5}	373.0	
KOI-0886	19 39 05.742	+43 03 22.68	15.85	12.65	3797± 80	0.499 ^{+0.030} _{-0.052}	241.7 ^{+22.3} _{-34.7}	243.6	(Kepler-54)
KOI-0899	19 47 56.411	+43 39 30.67	15.23	11.97	3630± 80	0.420 ^{+0.044} _{-0.071}	136.1 ^{+22.3} _{-22.3}	136.3	(Kepler-249)
KOI-0908	19 54 32.556	+44 10 15.38	15.11	13.24	5559± 182	0.956 ^{+0.101} _{-0.084}	871.0 ^{+293.8} _{-91.8}	898.8	
KOI-0936	18 54 55.686	+45 57 31.58	15.07	11.72	3562± 80	0.463 ^{+0.042} _{-0.068}	131.7 ^{+20.7} _{-20.7}	131.7	
KOI-0947	19 27 27.085	+46 25 45.34	15.19	12.10	3792± 80	0.508 ^{+0.036} _{-0.050}	197.5 ^{+21.3} _{-25.6}	197.6	
KOI-0952	19 51 22.178	+46 34 27.36	15.80	12.76	3801± 80	0.544 ^{+0.033} _{-0.046}	285.8 ^{+26.1} _{-31.4}	285.8	(Kepler-32)
KOI-0961	19 28 52.573	+44 37 08.98	15.92	11.47	3068± 80	0.125 ^{+0.028} _{-0.010}	33.9 ^{+8.1} _{-2.7}	33.9	(Kepler-42)
KOI-0972	18 48 00.073	+48 32 32.00	9.27	8.74	7200± 144	1.849 ^{+0.175} _{-0.146}	417.9 ^{+66.8} _{-55.7}	417.9	
KOI-0974	19 43 12.642	+45 59 17.08	9.58	8.41	6253± 125	1.187 ^{+0.165} _{-0.082}	196.9 ^{+15.5} _{-12.9}	196.9	
KOI-0975	19 09 26.836	+38 42 50.46	8.22	6.95	6131± 122	1.134 ^{+0.164} _{-0.091}	95.5 ^{+6.7} _{-6.7}	96.6	(Kepler-21)
KOI-0984	19 24 11.712	+36 50 23.58	11.63	10.02	5295± 106	0.887 ^{+0.046} _{-0.055}	175.4 ^{+16.4} _{-10.2}	240.0	
KOI-0987	19 42 17.798	+42 48 23.18	12.55	10.78	5512± 110	0.933 ^{+0.047} _{-0.056}	273.6 ^{+27.5} _{-18.3}	290.4	
KOI-1078	19 59 19.299	+47 09 26.85	15.44	12.48	3868± 80	0.551 ^{+0.034} _{-0.041}	262.9 ^{+24.1} _{-28.9}	262.9	(Kepler-267)
KOI-1085	18 44 12.026	+47 11 17.33	15.23	12.25	3741± 80	0.444 ^{+0.043} _{-0.060}	168.9 ^{+27.9} _{-23.3}	168.9	
KOI-1146	19 02 30.850	+44 18 39.20	15.65	12.61	3787± 80	0.457 ^{+0.040} _{-0.055}	217.3 ^{+26.5} _{-31.8}	217.4	
KOI-1174	19 47 17.190	+47 21 14.51	13.45	10.84	4506± 128	0.738 ^{+0.040} _{-0.056}	196.7 ^{+12.3} _{-17.3}	197.8	
KOI-1201	19 30 18.486	+39 07 15.17	15.60	12.61	3661± 80	0.398 ^{+0.039} _{-0.079}	174.8 ^{+29.4} _{-35.3}	177.0	
KOI-1220	19 09 13.887	+39 08 41.03	12.99	11.07	5428± 109	0.940 ^{+0.073} _{-0.041}	376.7 ^{+133.3} _{-44.5}	376.7	
KOI-1221	19 20 25.723	+38 42 08.02	11.58	9.47	4991± 99	1.163 ^{+0.209} _{-0.119}	432.6 ^{+35.3} _{-130.7}	432.6	(Kepler-278)
KOI-1230	19 55 47.556	+41 48 43.74	12.26	9.99	5015± 100	1.247 ^{+0.264} _{-0.220}	1101.7 ^{+170.9} _{-91.0}	1102.8	
KOI-1241	19 35 02.007	+41 52 18.72	12.44	10.23	4840± 96	1.131 ^{+0.225} _{-0.125}	827.6 ^{+56.0} _{-45.5}	827.6	(Kepler-56)
KOI-1283	19 44 01.707	+44 51 12.51	11.73	10.13	5775± 115	0.889 ^{+0.083} _{-0.052}	274.0 ^{+65.0} _{-45.5}	274.0	
KOI-1298	19 34 27.290	+47 50 20.40	15.85	13.14	4141± 83	0.593 ^{+0.030} _{-0.036}	422.4 ^{+38.8} _{-30.8}	438.5	(Kepler-283)
KOI-1299	19 33 07.727	+48 17 09.24	12.18	10.12	4995± 99	1.064 ^{+0.247} _{-0.114}	815.8 ^{+77.1} _{-77.1}	819.1	(Kepler-432)
KOI-1300	19 26 22.581	+48 26 44.20	14.28	11.88	4449± 135	0.536 ^{+0.037} _{-0.037}	227.6 ^{+22.7} _{-27.3}	263.5	
KOI-1314	19 00 53.064	+47 52 52.96	13.24	11.19	5048± 100	1.136 ^{+0.185} _{-0.132}	1120.3 ^{+100.9} _{-86.5}	1120.3	
KOI-1316	19 22 12.568	+48 07 34.55	11.93	10.56	5859± 117	1.167 ^{+0.118} _{-0.088}	367.2 ^{+108.5} _{-39.5}	370.4	
KOI-1361	19 41 13.081	+42 28 31.04	14.99	12.27	4017± 80	0.607 ^{+0.030} _{-0.036}	283.4 ^{+18.7} _{-22.5}	293.6	(Kepler-61)
KOI-1393	18 54 13.330	+45 36 51.34	15.80	12.77	3764± 80	0.558 ^{+0.027} _{-0.048}	294.6 ^{+26.9} _{-32.2}	294.6	
KOI-1397	19 58 42.649	+45 58 20.38	15.37	12.43	3879± 80	0.508 ^{+0.038} _{-0.044}	234.6 ^{+24.1} _{-28.9}	334.5	
KOI-1408	19 21 10.693	+45 33 52.60	14.69	11.81	4100± 82	0.600 ^{+0.030} _{-0.036}	234.0 ^{+12.8} _{-19.2}	234.4	
KOI-1422	19 06 09.602	+49 26 14.38	15.92	12.60	3622± 80	0.438 ^{+0.040} _{-0.069}	189.1 ^{+30.0} _{-30.0}	219.1	(Kepler-296)
KOI-1426	18 52 50.200	+48 46 39.51	14.23	12.78	5619± 112	0.854 ^{+0.063} _{-0.045}	657.9 ^{+88.1} _{-52.9}	657.9	(Kepler-297)
KOI-1428	19 23 49.812	+49 12 13.72	14.63	12.52	4912± 143	0.809 ^{+0.050} _{-0.081}	477.6 ^{+43.7} _{-43.7}	485.5	
KOI-1431	19 08 05.347	+48 40 54.98	13.46	11.81	5618± 112	1.008 ^{+0.052} _{-0.062}	486.1 ^{+58.5} _{-39.0}	486.1	
KOI-1436	18 55 55.913	+49 13 58.76	14.27	12.71	5815± 164	0.905 ^{+0.116} _{-0.083}	689.7 ^{+197.8} _{-76.1}	689.7	(Kepler-301)
KOI-1442	19 04 08.723	+49 36 52.24	12.52	10.91	5476± 110	0.976 ^{+0.051} _{-0.051}	308.8 ^{+47.1} _{-21.4}	314.0	(Kepler-407)
KOI-1478	19 15 23.672	+51 12 32.58	12.45	10.86	5593± 112	0.906 ^{+0.056} _{-0.056}	279.1 ^{+39.3} _{-17.4}	279.1	
KOI-1515	18 52 32.512	+43 39 25.38	14.39	11.60	4045± 81	0.509 ^{+0.025} _{-0.035}	167.1 ^{+14.7} _{-17.6}	167.1	(Kepler-303)
KOI-1537	18 45 50.815	+46 47 23.62	11.74	10.51	6260± 125	1.357 ^{+0.067} _{-0.147}	514.5 ^{+30.5} _{-36.7}	514.5	
KOI-1588	19 24 36.709	+40 53 14.96	14.70	11.91	4131± 83	0.568 ^{+0.034} _{-0.034}	232.0 ^{+19.1} _{-19.1}	232.1	
KOI-1589	19 53 00.491	+40 29 45.88	14.76	13.19	6031± 121	0.991 ^{+0.070} _{-0.070}	962.5 ^{+205.9} _{-79.2}	1202.1	(Kepler-84)
KOI-1611	19 16 18.170	+51 45 26.78	11.76	9.00	4450± 89	0.632 ^{+0.031} _{-0.031}	73.2 ^{+3.7} _{-4.4}	73.2	(Kepler-16)

TABLE 1
KEPLER OBJECTS OF INTEREST

KOI-1612	18 59 08.687	+48 25 23.62	8.77	7.49	6104± 122	1.001 ^{+0.083} _{-0.070}	83.1 ^{+5.8} _{-4.1}	83.1	(Kepler-408)
KOI-1613	19 01 54.382	+41 37 57.78	11.05	10.28	6044± 120	0.989 ^{+0.072} _{-0.072}	329.8 ^{+20.4} _{-17.0}	376.6	
KOI-1615	19 41 17.402	+39 22 35.37	11.52	9.99	6002± 120	1.114 ^{+0.078} _{-0.078}	246.8 ^{+44.3} _{-19.7}	269.3	
KOI-1616	19 18 01.524	+45 22 15.59	11.54	10.27	6029± 121	1.109 ^{+0.081} _{-0.081}	287.3 ^{+55.2} _{-25.1}	287.3	
KOI-1618	19 44 11.367	+42 44 34.84	11.60	10.33	6173± 123	1.272 ^{+0.052} _{-0.114}	388.1 ^{+20.4} _{-24.4}	388.3	
KOI-1619	19 39 57.656	+39 20 46.96	11.76	9.59	4834± 97	0.687 ^{+0.041} _{-0.035}	109.8 ^{+6.5} _{-6.5}	117.7	
KOI-1621	19 54 21.409	+40 45 02.48	11.85	10.51	6081± 121	1.200 ^{+0.182} _{-0.083}	526.1 ^{+48.0} _{-27.4}	526.1	
KOI-1649	18 56 31.890	+49 08 33.39	14.96	11.79	3800± 80	0.459 ^{+0.037} _{-0.051}	148.6 ^{+19.3} _{-23.2}	148.6	
KOI-1681	19 25 08.401	+40 43 48.18	15.85	12.58	3700± 80	0.417 ^{+0.041} _{-0.072}	180.7 ^{+29.0} _{-29.0}	251.5	
KOI-1692	19 38 41.785	+42 04 32.09	12.56	10.78	5418± 108	0.949 ^{+0.041} _{-0.049}	270.4 ^{+31.3} _{-15.7}	270.7	(Kepler-314)
KOI-1702	19 50 55.020	+42 52 00.91	15.72	12.20	3404± 80	0.269 ^{+0.071} _{-0.071}	102.5 ^{+25.0} _{-25.0}	102.5	
KOI-1725	18 54 30.923	+48 23 27.61	13.50	9.80	3656± 80	0.417 ^{+0.048} _{-0.067}	51.9 ^{+8.7} _{-8.7}	51.9	
KOI-1738	19 26 59.612	+39 26 48.77	13.29	11.51	5301± 147	0.801 ^{+0.094} _{-0.078}	321.2 ^{+52.2} _{-32.6}	322.0	
KOI-1781	19 10 25.342	+49 31 23.73	12.23	10.06	4915± 98	0.790 ^{+0.041} _{-0.041}	152.8 ^{+10.9} _{-7.3}	161.6	(Kepler-411)
KOI-1788	19 10 57.012	+38 06 52.41	14.52	12.25	4844± 169	0.814 ^{+0.051} _{-0.062}	430.1 ^{+45.7} _{-38.1}	430.1	
KOI-1797	19 43 26.250	+47 56 22.24	12.97	10.84	4926± 99	0.784 ^{+0.039} _{-0.046}	218.7 ^{+13.1} _{-13.1}	218.7	
KOI-1800	19 01 04.460	+48 33 36.03	12.39	10.81	5541± 111	0.914 ^{+0.055} _{-0.055}	274.7 ^{+18.1} _{-18.1}	274.8	(Kepler-447)
KOI-1803	19 06 32.527	+39 29 19.04	13.26	11.14	4915± 98	0.766 ^{+0.039} _{-0.039}	246.4 ^{+12.0} _{-12.0}	246.4	
KOI-1815	18 45 49.724	+46 44 47.30	13.88	11.62	4855± 140	0.830 ^{+0.043} _{-0.043}	328.2 ^{+400.3} _{-22.5}	328.2	
KOI-1833	19 02 24.609	+50 06 43.35	14.27	11.83	4399± 126	0.572 ^{+0.058} _{-0.041}	243.6 ^{+23.5} _{-28.2}	273.9	
KOI-1835	19 37 18.127	+46 00 08.10	13.69	11.67	5105± 102	0.828 ^{+0.043} _{-0.043}	344.1 ^{+27.3} _{-17.1}	484.2	(Kepler-326)
KOI-1841	19 20 39.661	+49 55 25.89	13.22	11.30	5188± 104	0.828 ^{+0.043} _{-0.051}	298.3 ^{+20.8} _{-17.4}	319.1	
KOI-1843	19 00 03.142	+40 13 14.70	14.40	11.06	3600± 80	0.512 ^{+0.028} _{-0.056}	112.8 ^{+12.2} _{-17.1}	112.9	
KOI-1867	19 30 34.168	+44 05 15.61	15.02	11.96	3837± 80	0.551 ^{+0.028} _{-0.045}	200.7 ^{+20.8} _{-20.8}	200.7	(Kepler-327)
KOI-1877	18 57 43.272	+47 38 30.41	13.39	11.27	4979± 100	0.789 ^{+0.041} _{-0.041}	272.8 ^{+15.7} _{-15.7}	272.8	
KOI-1879	19 30 27.385	+44 23 40.78	15.97	12.73	3800± 80	0.570 ^{+0.029} _{-0.041}	295.3 ^{+27.4} _{-27.4}	295.5	
KOI-1880	19 16 17.336	+47 24 25.45	14.44	11.45	3855± 80	0.548 ^{+0.034} _{-0.040}	165.7 ^{+13.2} _{-18.5}	167.3	
KOI-1890	19 32 19.080	+43 04 25.36	11.70	10.37	6099± 121	1.130 ^{+0.139} _{-0.077}	402.1 ^{+26.0} _{-21.7}	431.8	
KOI-1894	19 49 26.228	+49 47 51.18	13.43	11.06	4992± 99	1.142 ^{+0.209} _{-0.131}	1081.5 ^{+110.0} _{-82.5}	1081.5	
KOI-1904	19 46 11.404	+44 56 30.94	13.40	11.38	4980± 100	0.772 ^{+0.038} _{-0.038}	279.7 ^{+20.1} _{-16.8}	279.7	
KOI-1907	18 51 26.382	+42 39 56.74	15.28	12.35	3971± 80	0.570 ^{+0.029} _{-0.035}	265.8 ^{+21.4} _{-25.7}	265.8	
KOI-1908	19 29 08.657	+40 54 48.92	14.73	12.12	4211± 84	0.608 ^{+0.030} _{-0.036}	278.1 ^{+16.8} _{-20.2}	285.2	(Kepler-333)
KOI-1925	19 34 43.008	+46 51 09.94	9.44	7.77	5460± 109	0.927 ^{+0.044} _{-0.066}	68.2 ^{+3.4} _{-3.4}	68.2	(Kepler-409)
KOI-1934	18 59 52.720	+39 21 37.05	14.65	12.27	4505± 129	0.605 ^{+0.068} _{-0.043}	317.7 ^{+30.3} _{-30.3}	317.7	
KOI-1937	18 54 52.207	+47 12 16.02	13.59	11.00	4345± 125	0.628 ^{+0.055} _{-0.066}	179.8 ^{+14.3} _{-21.4}	181.0	
KOI-1961	19 10 17.080	+42 48 50.11	12.85	11.12	5430± 109	0.915 ^{+0.046} _{-0.055}	299.8 ^{+28.6} _{-16.4}	409.9	
KOI-1962	18 56 56.155	+40 47 40.34	10.77	9.45	5904± 118	1.017 ^{+0.101} _{-0.068}	243.4 ^{+18.0} _{-15.0}	337.8	
KOI-1964	19 22 48.889	+43 36 25.95	10.69	8.95	5589± 112	0.899 ^{+0.055} _{-0.055}	116.7 ^{+14.1} _{-8.8}	126.4	
KOI-1967	19 28 31.912	+41 32 51.14	14.31	12.17	4910± 138	0.741 ^{+0.068} _{-0.068}	377.5 ^{+43.7} _{-36.4}	378.0	
KOI-1977	19 40 54.910	+45 58 15.67	14.03	11.55	4504± 90	0.694 ^{+0.036} _{-0.036}	255.7 ^{+15.2} _{-12.6}	351.6	(Kepler-345)
KOI-1985	18 43 42.268	+44 05 16.54	13.71	11.58	4931± 99	0.780 ^{+0.039} _{-0.039}	306.3 ^{+18.3} _{-18.3}	316.7	
KOI-1988	19 53 18.384	+45 18 55.84	14.15	11.75	4782± 138	0.808 ^{+0.076} _{-0.042}	336.0 ^{+48.2} _{-20.1}	336.3	
KOI-2001	19 48 05.061	+41 22 37.82	13.11	11.12	5115± 144	0.789 ^{+0.098} _{-0.082}	254.9 ^{+40.2} _{-25.1}	257.0	
KOI-2005	18 47 35.603	+42 09 56.85	14.83	12.45	4460± 129	0.581 ^{+0.058} _{-0.041}	329.5 ^{+34.5} _{-34.5}	410.9	
KOI-2006	19 09 23.218	+47 46 22.66	14.22	11.18	3859± 80	0.491 ^{+0.034} _{-0.041}	128.8 ^{+13.7} _{-16.4}	128.8	
KOI-2013	19 25 40.474	+39 07 38.71	13.16	10.59	4187± 126	0.534 ^{+0.060} _{-0.050}	118.6 ^{+16.7} _{-16.7}	118.6	
KOI-2029	19 59 35.164	+46 03 07.10	12.96	11.13	5212± 104	0.795 ^{+0.051} _{-0.042}	269.3 ^{+18.8} _{-15.7}	269.3	(Kepler-352)
KOI-2031	18 55 35.859	+41 13 17.80	14.80	12.33	4457± 127	0.680 ^{+0.046} _{-0.068}	354.7 ^{+30.8} _{-37.0}	374.9	
KOI-2032	19 22 06.423	+38 08 34.72	12.26	10.79	5564± 153	0.905 ^{+0.092} _{-0.092}	270.3 ^{+67.8} _{-30.8}	431.8	
KOI-2035	19 55 27.978	+46 30 08.06	13.01	11.36	5639± 159	0.868 ^{+0.106} _{-0.089}	335.3 ^{+109.0} _{-38.9}	335.3	
KOI-2036	19 47 25.591	+41 45 29.44	15.77	12.81	3909± 80	0.573 ^{+0.029} _{-0.041}	326.7 ^{+23.3} _{-35.0}	329.5	(Kepler-353)
KOI-2057	18 57 54.368	+46 15 09.28	15.03	12.07	3986± 80	0.580 ^{+0.030} _{-0.036}	244.5 ^{+19.5} _{-23.4}	244.5	
KOI-2059	19 10 21.621	+51 03 38.05	12.91	10.66	4999± 100	0.790 ^{+0.039} _{-0.039}	205.2 ^{+14.4} _{-10.3}	281.1	
KOI-2067	19 58 11.880	+45 46 11.10	12.58	11.06	5641± 113	0.970 ^{+0.096} _{-0.060}	433.0 ^{+91.0} _{-65.0}	532.1	
KOI-2079	19 39 54.917	+46 00 20.34	12.95	11.21	5582± 175	0.977 ^{+0.101} _{-0.084}	356.3 ^{+117.2} _{-36.6}	356.3	
KOI-2090	19 24 22.258	+49 11 24.22	15.53	12.39	3635± 80	0.497 ^{+0.039} _{-0.062}	204.9 ^{+23.6} _{-33.1}	204.9	
KOI-2124	19 41 09.251	+49 22 47.25	14.27	11.58	4132± 83	0.591 ^{+0.030} _{-0.036}	207.0 ^{+15.1} _{-15.1}	291.9	
KOI-2133	19 02 41.492	+44 07 00.23	12.49	10.14	4605± 92	1.198 ^{+0.227} _{-0.162}	1198.9 ^{+156.9} _{-67.2}	1198.9	(Kepler-91)
KOI-2149	19 51 08.782	+47 53 10.03	12.07	10.80	6166± 123	1.252 ^{+0.119} _{-0.119}	458.2 ^{+192.4} _{-61.2}	458.2	
KOI-2156	19 06 22.625	+37 53 28.53	15.96	12.83	3700± 80	0.387 ^{+0.045} _{-0.072}	182.2 ^{+30.6} _{-30.6}	184.6	
KOI-2158	19 50 36.343	+40 21 09.18	13.05	11.28	5428± 153	0.897 ^{+0.090} _{-0.090}	323.3 ^{+94.3} _{-33.7}	326.6	

TABLE 1
KEPLER OBJECTS OF INTEREST

KOI-2169	19 00 49.797	+45 23 03.66	12.40	10.66	5469± 109	0.928 ^{+0.046} _{-0.055}	254.9 ^{+22.8} _{-17.1}	264.6
KOI-2173	19 49 10.181	+49 58 53.86	12.88	10.67	4844± 97	0.759 ^{+0.039} _{-0.039}	194.2 ^{+11.4} _{-9.5}	194.2 (Kepler-367)
KOI-2175	19 27 31.208	+45 23 16.56	12.85	11.18	5502± 110	0.976 ^{+0.153} _{-0.051}	565.1 ^{+149.4} _{-83.0}	565.1 (Kepler-368)
KOI-2179	19 34 41.814	+47 54 30.45	15.67	12.40	3691± 80	0.479 ^{+0.037} _{-0.060}	204.2 ^{+25.1} _{-35.2}	262.8 (Kepler-369)
KOI-2181	20 05 22.288	+44 40 19.96	14.41	12.36	5104± 150	0.850 ^{+0.070} _{-0.084}	471.3 ^{+83.2} _{-37.8}	473.0
KOI-2191	19 00 20.772	+40 53 56.39	14.91	11.81	3800± 80	0.549 ^{+0.034} _{-0.041}	186.5 ^{+19.3} _{-19.3}	187.1
KOI-2208	19 22 10.474	+47 43 33.19	12.59	10.97	5818± 116	1.009 ^{+0.073} _{-0.073}	357.5 ^{+67.5} _{-33.7}	358.0
KOI-2225	19 46 53.877	+49 31 57.76	14.44	12.13	4820± 139	0.828 ^{+0.062} _{-0.051}	408.8 ^{+44.8} _{-28.0}	410.4
KOI-2238	19 21 44.165	+44 06 27.54	14.63	11.68	3900± 80	0.519 ^{+0.032} _{-0.045}	172.4 ^{+17.6} _{-21.1}	172.4
KOI-2287	19 39 47.659	+46 26 19.11	12.48	10.20	4661± 93	0.732 ^{+0.037} _{-0.037}	150.0 ^{+7.3} _{-8.8}	150.7 (Kepler-378)
KOI-2295	19 18 10.832	+39 09 51.94	11.67	9.68	5424± 108	0.815 ^{+0.050} _{-0.042}	147.2 ^{+14.3} _{-10.2}	176.0
KOI-2306	18 49 08.254	+42 09 15.08	14.78	11.83	3854± 80	0.624 ^{+0.021} _{-0.031}	234.5 ^{+11.8} _{-21.3}	234.5
KOI-2311	19 08 57.883	+39 19 57.94	12.57	10.98	5657± 113	0.948 ^{+0.057} _{-0.068}	308.7 ^{+37.3} _{-23.3}	309.9
KOI-2329	19 31 04.783	+48 53 58.63	15.65	12.67	3900± 80	0.535 ^{+0.033} _{-0.046}	280.1 ^{+25.4} _{-30.5}	280.1
KOI-2332	19 29 00.593	+40 47 33.80	13.02	11.17	5381± 108	0.906 ^{+0.052} _{-0.052}	332.3 ^{+100.4} _{-29.5}	332.5
KOI-2347	19 31 05.610	+44 10 41.27	14.93	12.06	4036± 81	0.614 ^{+0.032} _{-0.032}	264.6 ^{+22.1} _{-26.9}	264.6
KOI-2352	19 00 43.872	+43 49 51.88	10.42	9.50	6210± 124	1.078 ^{+0.057} _{-0.089}	321.0 ^{+26.9} _{-57.7}	321.0 (Kepler-381)
KOI-2390	19 48 51.790	+47 22 42.68	12.25	10.81	5824± 116	1.184 ^{+0.137} _{-0.117}	679.0 ^{+124.2} _{-124.2}	680.0
KOI-2418	19 49 56.807	+46 59 48.16	15.47	12.37	3577± 80	0.484 ^{+0.038} _{-0.068}	194.9 ^{+26.0} _{-31.2}	204.5
KOI-2453	19 37 52.434	+44 45 14.26	15.63	12.42	3643± 80	0.368 ^{+0.047} _{-0.070}	148.2 ^{+25.6} _{-25.6}	148.3
KOI-2462	19 55 58.008	+40 08 32.72	11.82	10.37	5869± 117	1.089 ^{+0.163} _{-0.091}	398.3 ^{+103.5} _{-57.5}	398.5
KOI-2479	19 31 32.468	+41 16 45.26	12.94	11.14	5418± 108	0.936 ^{+0.137} _{-0.032}	563.0 ^{+135.6} _{-84.8}	563.0
KOI-2481	19 39 07.764	+39 35 47.47	13.60	11.08	4553± 91	1.388 ^{+0.221} _{-0.265}	2761.6 ^{+332.4} _{-237.4}	2764.3
KOI-2486	18 42 45.710	+43 55 09.06	13.05	11.71	6388± 223	1.036 ^{+0.184} _{-0.123}	581.1 ^{+183.3} _{-91.7}	795.9
KOI-2522	19 57 31.582	+45 35 32.06	13.71	11.53	4849± 97	0.765 ^{+0.038} _{-0.038}	287.5 ^{+20.3} _{-14.5}	287.5
KOI-2527	19 08 34.248	+43 36 57.78	14.13	11.56	4240± 85	0.601 ^{+0.037} _{-0.030}	218.9 ^{+13.4} _{-16.1}	218.9
KOI-2533	19 06 51.753	+48 38 43.00	13.27	11.24	4929± 99	0.968 ^{+0.270} _{-0.052}	1166.7 ^{+302.6} _{-168.1}	1166.7
KOI-2541	19 22 29.238	+51 03 26.28	13.01	10.97	4940± 99	1.039 ^{+0.220} _{-0.094}	971.4 ^{+199.1} _{-132.8}	971.4 (Kepler-391)
KOI-2542	18 53 36.467	+41 30 58.79	15.53	12.03	3443± 80	0.295 ^{+0.078} _{-0.065}	94.0 ^{+29.6} _{-18.5}	112.2
KOI-2545	18 58 22.493	+46 26 59.21	11.75	10.45	6131± 122	1.458 ^{+0.070} _{-0.169}	597.2 ^{+27.7} _{-48.5}	597.2
KOI-2583	18 53 42.986	+47 35 33.04	12.62	11.08	5642± 113	0.946 ^{+0.058} _{-0.058}	334.3 ^{+44.5} _{-29.6}	334.3
KOI-2593	18 47 20.478	+44 09 21.30	11.71	10.48	6176± 124	1.230 ^{+0.088} _{-0.088}	361.4 ^{+66.0} _{-33.0}	362.5
KOI-2626	19 37 27.861	+49 54 54.21	15.93	12.64	3637± 80	0.389 ^{+0.045} _{-0.081}	163.8 ^{+29.7} _{-29.7}	233.3
KOI-2640	19 27 14.363	+45 26 07.72	13.23	10.99	4854± 97	0.949 ^{+0.403} _{-0.058}	2003.7 ^{+391.4} _{-130.5}	2003.7
KOI-2650	19 34 02.659	+45 08 11.72	15.99	12.95	3915± 80	0.560 ^{+0.034} _{-0.041}	340.0 ^{+26.7} _{-32.1}	340.1 (Kepler-395)
KOI-2657	19 31 02.820	+45 43 38.07	12.87	11.24	5486± 110	0.844 ^{+0.051} _{-0.051}	308.6 ^{+34.3} _{-21.5}	426.3
KOI-2662	19 03 42.935	+38 31 15.53	14.49	11.02	3444± 80	0.295 ^{+0.078} _{-0.065}	59.1 ^{+18.6} _{-11.6}	59.1
KOI-2672	19 44 31.875	+48 58 38.65	11.92	10.28	5591± 112	0.932 ^{+0.057} _{-0.057}	224.4 ^{+33.5} _{-16.7}	227.5 (Kepler-396)
KOI-2675	19 31 53.100	+41 02 08.77	12.43	10.91	5728± 115	0.962 ^{+0.060} _{-0.060}	309.5 ^{+38.1} _{-23.8}	309.5
KOI-2678	19 29 33.252	+42 13 59.74	11.80	10.09	5398± 108	0.861 ^{+0.054} _{-0.045}	183.1 ^{+19.2} _{-10.6}	183.1
KOI-2686	19 33 11.609	+43 33 21.13	13.85	11.56	4663± 93	0.732 ^{+0.036} _{-0.036}	273.8 ^{+16.6} _{-13.9}	273.8
KOI-2687	19 30 27.627	+42 45 51.31	10.16	8.69	5805± 116	0.962 ^{+0.061} _{-0.061}	111.8 ^{+15.6} _{-7.8}	111.8
KOI-2693	19 25 52.478	+40 20 37.86	13.26	10.79	4493± 90	0.681 ^{+0.035} _{-0.035}	179.8 ^{+8.4} _{-10.5}	179.8 (Kepler-398)
KOI-2704	19 54 56.668	+46 29 55.08	17.48	12.61	3327± 116	0.168 ^{+0.108} _{-0.039}	81.1 ^{+41.3} _{-19.3}	81.2 (Kepler-445)
KOI-2705	19 23 49.475	+49 21 59.03	14.72	10.73	3526± 58	0.412 ^{+0.038} _{-0.054}	74.8 ^{+9.3} _{-9.3}	78.0
KOI-2706	19 00 18.640	+46 25 10.56	10.27	9.11	6493± 176	1.351 ^{+0.121} _{-0.217}	271.5 ^{+22.6} _{-22.6}	272.6
KOI-2712	19 50 59.348	+48 41 39.51	11.12	9.95	6420± 128	1.341 ^{+0.084} _{-0.084}	312.0 ^{+53.6} _{-26.8}	312.0
KOI-2720	19 41 45.520	+44 02 20.98	10.34	9.00	6090± 161	0.976 ^{+0.108} _{-0.112}	197.6 ^{+17.9} _{-14.9}	197.6
KOI-2733	19 18 12.722	+41 17 52.27	14.01	11.76	4881± 139	0.829 ^{+0.069} _{-0.069}	343.3 ^{+43.0} _{-30.7}	493.5
KOI-2754	18 54 58.997	+48 22 24.36	12.30	10.63	5776± 116	0.937 ^{+0.059} _{-0.059}	273.1 ^{+42.0} _{-21.0}	302.5
KOI-2755	19 26 17.813	+38 39 21.42	12.15	10.71	5830± 117	0.935 ^{+0.058} _{-0.069}	275.4 ^{+42.4} _{-21.2}	275.4
KOI-2790	19 58 38.306	+40 50 37.86	13.38	11.49	5150± 103	0.775 ^{+0.049} _{-0.041}	301.4 ^{+21.3} _{-17.8}	385.5
KOI-2792	19 05 21.204	+48 44 38.76	11.13	9.76	5985± 160	0.930 ^{+0.147} _{-0.081}	242.3 ^{+21.4} _{-15.3}	242.3
KOI-2798	19 34 26.096	+42 11 51.65	14.11	11.47	4365± 126	0.606 ^{+0.063} _{-0.053}	218.9 ^{+19.9} _{-23.9}	218.9
KOI-2801	19 56 38.518	+41 08 37.43	10.79	9.47	6065± 121	1.058 ^{+0.124} _{-0.077}	225.1 ^{+53.5} _{-33.4}	225.1
KOI-2803	19 39 28.052	+46 47 26.02	12.26	10.64	5615± 112	0.994 ^{+0.052} _{-0.062}	283.8 ^{+34.9} _{-21.8}	296.3
KOI-2813	19 41 22.134	+48 51 22.15	13.59	11.51	5133± 151	0.636 ^{+0.052} _{-0.032}	242.9 ^{+28.1} _{-17.6}	266.1
KOI-2842	18 49 00.051	+44 55 15.99	16.26	12.83	3485± 121	0.441 ^{+0.063} _{-0.114}	196.8 ^{+49.1} _{-49.1}	196.8 (Kepler-446)
KOI-2862	19 11 47.666	+42 09 22.10	15.91	12.76	3744± 58	0.522 ^{+0.026} _{-0.031}	269.9 ^{+21.5} _{-21.5}	382.1
KOI-2867	19 40 36.123	+46 46 20.30	12.91	10.48	4945± 99	0.770 ^{+0.040} _{-0.040}	180.9 ^{+10.7} _{-8.9}	180.9
KOI-2948	19 17 34.739	+41 46 56.46	11.93	10.32	5562± 111	0.921 ^{+0.064} _{-0.054}	265.8 ^{+70.0} _{-31.8}	265.8

TABLE 1
KEPLER OBJECTS OF INTEREST

KOI-2992	19 46 56.939	+44 30 05.33	15.99	13.04	3984 ± 58	$0.591^{+0.022}_{-0.025}$	$388.1^{+19.0}_{-22.8}$	388.1
KOI-3075	19 08 49.409	+38 29 53.00	12.99	11.53	5699 ± 199	$0.865^{+0.114}_{-0.082}$	$378.6^{+130.9}_{-43.6}$	378.6
KOI-3097	18 44 26.960	+43 13 40.05	11.97	10.65	5993 ± 120	$1.052^{+0.124}_{-0.077}$	$393.3^{+91.7}_{-57.3}$	393.3 (Kepler-431)
KOI-3119	19 46 20.925	+40 43 22.76	16.95	13.54	3413 ± 58	$0.326^{+0.054}_{-0.065}$	$225.5^{+31.2}_{-43.6}$	228.7
KOI-3144	19 02 57.554	+40 58 48.18	16.11	12.74	3500 ± 58	$0.397^{+0.043}_{-0.060}$	$178.1^{+28.0}_{-23.4}$	178.1
KOI-3158	19 19 00.549	+41 38 04.58	8.72	6.70	5046 ± 74	$0.708^{+0.022}_{-0.017}$	$35.7^{+1.1}_{-1.1}$	37.9 (Kepler-444)
KOI-3179	19 57 12.671	+41 26 27.66	10.88	10.64	5719 ± 114	$0.944^{+0.069}_{-0.058}$	$273.9^{+44.2}_{-20.1}$	273.9
KOI-3184	19 13 34.871	+39 52 21.46	11.16	9.79	5789 ± 116	$1.039^{+0.098}_{-0.081}$	$241.1^{+54.5}_{-34.1}$	241.1
KOI-3194	19 06 30.850	+50 28 16.58	11.49	10.35	6377 ± 128	$1.343^{+0.101}_{-0.084}$	$397.2^{+75.9}_{-45.5}$	397.2
KOI-3196	18 53 24.111	+45 20 20.80	11.52	10.28	6129 ± 123	$1.068^{+0.113}_{-0.070}$	$299.2^{+70.1}_{-32.3}$	299.2
KOI-3208	19 46 43.162	+47 10 23.93	11.89	10.66	5851 ± 117	$0.962^{+0.060}_{-0.060}$	$291.7^{+44.3}_{-24.6}$	291.8
KOI-3232	18 48 28.279	+46 13 26.15	12.25	10.80	5733 ± 115	$0.972^{+0.062}_{-0.062}$	$301.5^{+43.4}_{-24.1}$	301.5
KOI-3237	19 01 19.350	+42 02 25.54	12.32	10.81	5733 ± 115	$0.982^{+0.074}_{-0.062}$	$319.1^{+54.6}_{-27.3}$	319.1
KOI-3246	19 17 41.748	+46 43 34.21	12.41	10.20	4871 ± 97	$0.792^{+0.041}_{-0.041}$	$163.4^{+9.0}_{-8.0}$	163.4
KOI-3255	19 49 23.372	+44 01 36.98	14.35	11.85	4551 ± 91	$0.707^{+0.036}_{-0.036}$	$299.2^{+17.8}_{-14.8}$	415.4 (Kepler-437)
KOI-3263	19 00 23.005	+50 06 03.46	15.95	12.73	3676 ± 58	$0.497^{+0.024}_{-0.039}$	$248.3^{+16.9}_{-25.4}$	263.1
KOI-3284	18 46 34.995	+41 57 03.93	14.47	11.20	3677 ± 58	$0.491^{+0.029}_{-0.035}$	$123.4^{+14.8}_{-12.6}$	136.5 (Kepler-438)
KOI-3309	19 55 52.390	+40 47 50.47	14.71	12.69	5279 ± 160	$0.843^{+0.087}_{-0.087}$	$557.2^{+111.3}_{-55.6}$	646.9
KOI-3414	18 57 59.106	+41 19 33.20	15.48	12.52	3784 ± 58	$0.533^{+0.026}_{-0.026}$	$257.5^{+15.3}_{-21.4}$	257.5
KOI-3425	20 01 15.886	+45 29 43.37	13.27	11.51	6124 ± 214	$1.092^{+0.212}_{-0.132}$	$530.9^{+246.2}_{-92.3}$	530.9
KOI-3444	19 49 43.008	+40 33 42.87	13.69	10.31	3608 ± 58	$0.460^{+0.032}_{-0.045}$	$71.6^{+7.8}_{-7.8}$	75.6
KOI-3497	19 17 05.881	+44 28 13.16	13.39	10.62	4627 ± 161	$0.723^{+0.056}_{-0.067}$	$176.8^{+16.6}_{-16.6}$	223.7
KOI-3506	20 04 35.046	+44 52 10.77	12.93	11.71	6882 ± 226	$1.118^{+0.246}_{-0.113}$	$656.2^{+267.1}_{-89.0}$	657.9
KOI-3663	19 19 03.267	+51 57 45.36	12.62	11.12	5728 ± 115	$0.950^{+0.058}_{-0.058}$	$338.3^{+45.1}_{-25.0}$	338.3 (Kepler-86)
KOI-3681	19 30 30.593	+37 51 36.51	11.69	10.69	6258 ± 125	$1.210^{+0.084}_{-0.101}$	$381.7^{+58.7}_{-35.2}$	382.5
KOI-3835	19 30 45.666	+37 50 05.93	12.86	10.84	4978 ± 100	$0.753^{+0.047}_{-0.040}$	$213.6^{+12.8}_{-12.8}$	213.6
KOI-3864	19 33 22.793	+39 15 28.11	12.91	10.91	5011 ± 100	$0.771^{+0.047}_{-0.040}$	$226.1^{+15.4}_{-11.0}$	226.1
KOI-3876	19 21 45.762	+38 31 24.82	12.62	11.11	5618 ± 112	$0.943^{+0.057}_{-0.057}$	$331.2^{+39.0}_{-24.4}$	331.2
KOI-3891	19 44 37.441	+44 55 12.32	13.73	11.67	5259 ± 163	$0.894^{+0.272}_{-0.136}$	$328.4^{+993.9}_{-32.9}$	332.6
KOI-3892	19 22 14.282	+49 56 34.83	12.74	11.19	5707 ± 114	$1.061^{+0.055}_{-0.066}$	$392.7^{+62.0}_{-31.0}$	395.9
KOI-3908	19 58 20.010	+47 26 53.08	12.07	10.45	5793 ± 116	$0.983^{+0.109}_{-0.062}$	$346.0^{+77.8}_{-48.6}$	476.5
KOI-3925	19 12 39.001	+48 09 54.54	14.03	12.30	5679 ± 198	$0.981^{+0.139}_{-0.100}$	$615.0^{+217.1}_{-83.5}$	615.0
KOI-3991	19 46 00.850	+47 29 12.91	13.14	11.41	5572 ± 164	$0.686^{+0.056}_{-0.035}$	$266.6^{+36.8}_{-22.1}$	298.8
KOI-4004	18 55 58.821	+39 55 01.20	12.70	11.11	5761 ± 169	$0.832^{+0.118}_{-0.074}$	$287.9^{+185.7}_{-29.0}$	303.5
KOI-4016	18 53 22.676	+41 12 06.26	14.07	11.52	4368 ± 125	$0.643^{+0.056}_{-0.056}$	$234.0^{+20.8}_{-24.9}$	235.2
KOI-4032	19 02 54.836	+42 39 16.31	12.64	10.99	5575 ± 111	$0.945^{+0.069}_{-0.057}$	$334.0^{+60.8}_{-30.4}$	344.1
KOI-4097	19 02 45.600	+40 59 40.31	13.44	10.84	4355 ± 124	$0.646^{+0.056}_{-0.067}$	$168.7^{+16.9}_{-16.9}$	171.7
KOI-4146	19 07 16.648	+46 54 42.08	13.63	11.66	5117 ± 147	$0.853^{+0.062}_{-0.087}$	$351.3^{+49.8}_{-33.2}$	351.3
KOI-4184	18 47 35.552	+42 17 09.13	13.47	11.37	4987 ± 143	$0.815^{+0.058}_{-0.082}$	$291.4^{+28.7}_{-28.7}$	407.2
KOI-4226	20 02 14.978	+46 02 16.15	12.83	11.20	5898 ± 118	$1.180^{+0.104}_{-0.074}$	$489.1^{+110.9}_{-59.2}$	494.6
KOI-4252	19 09 27.371	+47 47 06.76	13.98	10.87	3764 ± 58	$0.527^{+0.027}_{-0.032}$	$116.2^{+8.2}_{-9.9}$	149.3
KOI-4269	19 35 11.243	+45 09 38.62	13.26	11.14	5159 ± 152	$0.886^{+0.275}_{-0.106}$	$275.9^{+64.3}_{-25.2}$	275.9
KOI-4287	19 21 49.995	+48 39 40.93	11.27	10.04	6137 ± 123	$1.147^{+0.148}_{-0.093}$	$331.3^{+85.5}_{-47.5}$	377.1
KOI-4288	19 09 29.099	+39 36 12.85	12.40	11.02	5882 ± 118	$1.017^{+0.093}_{-0.067}$	$388.8^{+81.7}_{-40.8}$	389.2
KOI-4292	19 05 32.864	+47 00 59.86	12.90	11.28	5812 ± 171	$0.935^{+0.132}_{-0.095}$	$378.3^{+100.5}_{-50.3}$	380.8
KOI-4399	18 48 30.930	+44 18 11.38	11.97	10.35	5585 ± 112	$0.888^{+0.054}_{-0.054}$	$211.7^{+22.4}_{-12.4}$	214.7
KOI-4407	20 04 37.573	+44 22 46.32	11.18	9.78	6360 ± 127	$1.262^{+0.090}_{-0.108}$	$269.7^{+47.1}_{-26.2}$	291.4
KOI-4427	19 40 28.132	+39 16 26.72	15.65	12.50	3700 ± 58	$0.512^{+0.024}_{-0.039}$	$228.0^{+19.3}_{-23.1}$	228.2
KOI-4446	19 08 32.373	+47 29 19.04	12.43	10.59	5444 ± 158	$0.924^{+0.251}_{-0.090}$	$239.5^{+400.2}_{-30.0}$	239.9
KOI-4556	19 18 28.455	+47 33 28.68	11.98	10.35	5600 ± 112	$0.922^{+0.074}_{-0.053}$	$276.1^{+77.6}_{-38.8}$	276.3
KOI-4582	19 45 20.852	+43 36 00.32	11.76	10.22	5737 ± 115	$0.886^{+0.067}_{-0.056}$	$215.9^{+29.5}_{-16.4}$	220.9
KOI-4637	19 14 23.921	+46 01 54.16	10.44	9.23	6377 ± 167	$1.138^{+0.243}_{-0.152}$	$282.3^{+31.6}_{-22.5}$	282.3
KOI-4657	19 33 10.269	+41 59 51.32	13.24	11.42	5360 ± 153	$0.839^{+0.078}_{-0.094}$	$323.2^{+52.6}_{-37.6}$	349.7
KOI-4663	19 10 40.942	+43 11 50.06	12.72	11.09	5642 ± 157	$0.919^{+0.120}_{-0.085}$	$325.7^{+117.8}_{-36.8}$	325.7
KOI-4775	19 29 36.775	+44 46 55.23	13.00	11.07	5349 ± 187	$0.944^{+0.115}_{-0.072}$	$318.6^{+171.0}_{-32.9}$	319.5
KOI-4834	19 27 10.715	+44 11 36.71	13.10	10.96	5127 ± 153	$0.890^{+0.243}_{-0.072}$	$267.3^{+437.2}_{-20.8}$	267.3
KOI-4875	19 23 07.712	+38 11 16.04	15.78	12.64	3700 ± 58	$0.512^{+0.024}_{-0.039}$	$243.1^{+20.6}_{-24.7}$	245.6
<i>False Positives</i>								
KOI-0044	20 00 36.445	+45 05 22.60	13.48	11.66	5841 ± 204	$1.029^{+0.136}_{-0.113}$	$490.6^{+156.0}_{-65.0}$	497.9 (D. Latham, CFOP)
KOI-0064	19 46 02.538	+42 32 50.81	13.14	11.23	5302 ± 106	$1.231^{+0.085}_{-0.142}$	$872.8^{+40.1}_{-80.1}$	872.8 (G. Marcy, CFOP)
KOI-0113	19 29 05.698	+37 40 17.61	12.39	10.72	5543 ± 110	$1.090^{+0.138}_{-0.063}$	$459.4^{+34.7}_{-24.8}$	516.5 (Unknown, CFOP)

TABLE 1
KEPLER OBJECTS OF INTEREST

KOI-0189	18 59 31.194	+49 16 01.17	14.39	12.29	4939 ± 140	$0.775^{+0.069}_{-0.069}$	$425.9^{+39.7}_{-39.7}$	425.9	(Diaz et al. 2014)
KOI-0201	19 08 31.340	+42 21 00.54	14.01	12.35	5572 ± 111	$1.020^{+0.052}_{-0.052}$	$637.2^{+112.2}_{-43.2}$	639.1	(Slawson et al. 2011)
KOI-0256	19 00 44.429	+49 33 55.33	15.37	11.78	3450 ± 80	$0.441^{+0.044}_{-0.070}$	$125.3^{+18.8}_{-22.6}$	125.3	(Muirhead et al. 2013)
KOI-0263	18 45 05.713	+47 46 27.84	10.82	9.01	5784 ± 115	$1.002^{+0.071}_{-0.071}$	$213.4^{+13.0}_{-13.0}$	266.4	(Unknown, CFOP)
KOI-0302	19 42 26.111	+38 44 08.67	12.06	10.99	6954 ± 202	$1.375^{+0.242}_{-0.202}$	$578.8^{+205.7}_{-102.9}$	579.4	(Unknown, CFOP)
KOI-0371	19 58 42.275	+40 51 23.37	12.19	10.17	5198 ± 103	$1.499^{+0.107}_{-0.249}$	$655.5^{+54.1}_{-54.1}$	655.8	(Lillo-Box et al. 2015)
KOI-0969	19 10 27.920	+39 07 38.06	12.34	11.03	6220 ± 217	$0.999^{+0.164}_{-0.123}$	$386.8^{+129.1}_{-59.6}$	386.8	(Slawson et al. 2011)
KOI-0976	19 23 46.648	+38 32 19.92	9.73	9.10	7240 ± 253	$1.518^{+0.233}_{-0.166}$	$280.3^{+90.2}_{-41.0}$	358.6	(Slawson et al. 2011)
KOI-0981	18 54 56.741	+44 42 47.92	10.73	8.72	5066 ± 101	$1.125^{+0.246}_{-0.164}$	$526.8^{+64.8}_{-43.2}$	526.8	(Unknown, CFOP)
KOI-1019	19 45 55.650	+44 00 32.94	10.27	8.21	5009 ± 100	$1.101^{+0.210}_{-0.116}$	$290.6^{+25.9}_{-25.9}$	290.9	(Unknown, CFOP)
KOI-1054	19 14 43.821	+41 18 26.35	11.90	10.07	5235 ± 104	$1.580^{+0.187}_{-0.485}$	$2072.5^{+378.7}_{-378.7}$	2072.5	(Unknown, CFOP)
KOI-1164	19 30 57.341	+47 29 26.63	14.96	11.80	3684 ± 80	$0.510^{+0.035}_{-0.049}$	$166.9^{+18.8}_{-22.6}$	166.9	(Unknown, CFOP)
KOI-1222	19 29 59.231	+39 11 35.41	12.20	10.21	5055 ± 101	$1.122^{+0.205}_{-0.128}$	$721.4^{+64.2}_{-53.5}$	723.9	(Unknown, CFOP)
KOI-1686	19 54 01.743	+41 28 44.58	15.89	12.49	3500 ± 80	$0.333^{+0.074}_{-0.074}$	$145.6^{+28.5}_{-34.2}$	193.8	(Unknown, CFOP)
KOI-1701	19 50 04.578	+42 46 37.42	11.04	10.22	7288 ± 255	$1.517^{+0.266}_{-0.166}$	$441.7^{+177.5}_{-68.3}$	441.7	(Slawson et al. 2011)
KOI-1902	19 47 30.439	+41 04 50.10	14.65	11.45	3743 ± 58	$0.520^{+0.026}_{-0.031}$	$147.5^{+11.8}_{-11.8}$	147.5	(Swift et al. 2015)
KOI-1924	19 37 08.855	+40 12 49.72	7.84	6.49	5844 ± 116	$1.347^{+0.213}_{-0.067}$	$103.2^{+9.3}_{-5.2}$	103.2	(D. Latham, CFOP)
KOI-2659	18 59 11.265	+45 05 56.73	13.00	10.91	5193 ± 104	$1.224^{+0.144}_{-0.209}$	$579.7^{+158.8}_{-70.5}$	579.7	(Beck et al. 2014)
KOI-3334	19 45 21.270	+48 45 27.29	14.40	11.84	4529 ± 128	$0.663^{+0.058}_{-0.058}$	$281.4^{+25.3}_{-25.3}$	281.4	(M. Omohundro, CFOP)
KOI-3528	19 18 47.292	+39 22 17.90	12.72	10.84	6049 ± 211	$0.809^{+0.122}_{-0.056}$	$275.4^{+178.1}_{-29.7}$	275.4	(Slawson et al. 2011)
KOI-3782	19 40 20.940	+49 10 11.64	13.53	11.35	5014 ± 148	$0.861^{+0.294}_{-0.061}$	$311.5^{+707.0}_{-26.2}$	311.7	(M. Omohundro, CFOP)

^a Distances are listed both with and without the luminosity correction applied for flux contributions for companions that were unresolved in 2MASS. Targets were selected for observation using uncorrected distances, mostly the spectrophotometric distances described in Section 2, while isochronal distances that were corrected for multiplicity are used to calculate physical projected separations. Binary systems are weighted by a $1/V_{max}$ weighting in our analysis to avoid Malmquist bias.

TABLE 2
 KECK/NIRC2 NRM DETECTION LIMITS

Name	MJD	UT Date	N_{frames}	Limit	(mag)	at Sep.	(mas)
				15	20	30	40–160
KOI-0001	56114.59	120706	6	2.43	3.16	4.11	4.46
KOI-0002	56882.48	140813	8	2.90	3.63	4.56	4.81
KOI-0003	56113.59	120705	5	2.49	3.22	4.17	4.55
KOI-0005	56153.45	120814	4	0.11	0.36	1.12	1.44
KOI-0012	56153.52	120814	6	1.42	2.15	3.10	3.37
KOI-0013	56511.35	130807	8	1.74	2.47	3.41	3.69
KOI-0041	56116.60	120708	6	2.55	3.28	4.23	4.54
KOI-0042	56869.36	140731	8	2.31	3.04	3.97	4.24
KOI-0044	56882.53	140813	7	3.03	3.76	4.69	4.93
KOI-0063	56153.44	120814	3	0.46	1.14	2.11	2.44
KOI-0064	56151.50	120812	6	1.40	2.13	3.08	3.44
KOI-0069	56113.61	120705	6	2.22	2.94	3.87	4.16
KOI-0070	56053.60	120506	6	3.33	4.06	5.00	5.21
KOI-0072	56153.34	120814	6	2.65	3.39	4.34	4.64
KOI-0075	56116.60	120708	6	2.55	3.28	4.23	4.54
KOI-0082	56053.60	120506	6	3.33	4.06	4.99	5.21
KOI-0084	56152.33	120813	6	3.83	4.56	5.49	5.68
KOI-0085	56153.42	120814	6	1.94	2.67	3.60	3.87
KOI-0087	56153.45	120814	5	1.42	2.15	3.07	3.33
KOI-0089	56114.63	120706	6	2.64	3.38	4.32	4.64
KOI-0092	56510.43	130806	8	3.52	4.25	5.20	5.50
KOI-0094	56115.62	120707	6	2.89	3.62	4.55	4.82
KOI-0099	56152.49	120813	4	1.57	2.30	3.24	3.55
KOI-0103	56152.42	120813	6	2.14	2.88	3.81	4.06
KOI-0104	56152.38	120813	6	3.03	3.76	4.70	4.96
KOI-0105	56152.51	120813	6	2.23	2.96	3.89	4.18
KOI-0116	56115.63	120707	6	2.19	2.93	3.88	4.18
KOI-0117	56152.52	120813	6	2.22	2.95	3.89	4.13
KOI-0118	56152.43	120813	6	2.67	3.40	4.33	4.56
KOI-0119	56882.38	140813	8	2.02	2.75	3.69	3.95
KOI-0122	56510.48	130806	8	3.43	4.16	5.11	5.37
KOI-0137	56882.52	140813	8	2.97	3.70	4.64	4.90
KOI-0141	56882.37	140813	8	2.54	3.27	4.20	4.45
KOI-0144	56151.50	120812	6	1.61	2.34	3.29	3.62
KOI-0148	56152.52	120813	4	1.21	1.94	2.89	3.20
KOI-0153	56510.50	130806	8	3.08	3.82	4.76	5.04
KOI-0156	56151.40	120812	6	1.71	2.44	3.38	3.67
KOI-0157	56053.62	120506	6	1.74	2.47	3.41	3.68
KOI-0161	56511.48	130807	8	1.67	2.40	3.36	3.71
KOI-0174	56882.41	140813	8	2.98	3.70	4.63	4.86
KOI-0189	56880.44	140811	8	2.82	3.55	4.48	4.74
KOI-0197	56882.25	140813	8	2.68	3.40	4.34	4.66
KOI-0201	56880.46	140811	8	2.79	3.52	4.45	4.71
KOI-0205	56868.39	140730	8	2.44	3.17	4.11	4.37
KOI-0214	56882.30	140813	8	2.46	3.19	4.13	4.40
KOI-0216	56882.31	140813	8	1.68	2.42	3.38	3.73
KOI-0232	56053.61	120506	6	0.57	1.30	2.24	2.52
KOI-0242	56880.50	140811	8	1.92	2.66	3.60	3.90
KOI-0244	56153.41	120814	3	1.28	2.00	2.93	3.20
KOI-0245	56053.64	120506	6	2.64	3.37	4.30	4.51
KOI-0246	56153.33	120814	6	2.67	3.40	4.34	4.66
KOI-0247	56151.36	120812	6	1.27	2.00	2.95	3.26
KOI-0249	56151.36	120812	6	1.21	1.95	2.90	3.22
KOI-0251	56491.54	130718	8	2.21	2.95	3.90	4.28
KOI-0252	56868.34	140730	7	0.99	1.73	2.68	3.04
KOI-0253	56867.47	140729	8	1.87	2.60	3.55	3.85
KOI-0254	56491.47	130718	8	2.21	2.94	3.88	4.19
KOI-0255	56868.47	140730	7	1.78	2.51	3.47	3.79
KOI-0256	56490.47	130717	6	1.87	2.61	3.55	3.86
KOI-0257	56153.39	120814	4	1.76	2.49	3.43	3.71
KOI-0260	56153.42	120814	4	1.68	2.41	3.35	3.62
KOI-0261	56114.62	120706	6	2.96	3.69	4.64	4.93
KOI-0262	56153.33	120814	6	2.67	3.40	4.34	4.66
KOI-0268	56153.47	120814	6	1.59	2.32	3.26	3.56
KOI-0269	56153.38	120814	4	1.79	2.52	3.48	3.75
KOI-0271	56510.44	130806	7	3.37	4.11	5.04	5.30
KOI-0273	56153.46	120814	6	1.90	2.64	3.59	3.89
KOI-0274	56153.48	120814	6	2.53	3.27	4.23	4.52
KOI-0275	56153.48	120814	6	2.61	3.34	4.29	4.54
KOI-0276	56881.45	140812	8	3.18	3.91	4.85	5.11
KOI-0280	56153.41	120814	6	1.83	2.56	3.48	3.71
KOI-0281	56153.48	120814	6	1.64	2.37	3.32	3.58
KOI-0282	56866.48	140728	6	2.98	3.72	4.65	4.96
KOI-0283	56153.46	120814	6	2.24	2.97	3.92	4.20

TABLE 2
KECK/NIRC2 NRM DETECTION LIMITS

KOI-0284	56869.45	140731	7	2.46	3.18	4.11	4.32
KOI-0285	56866.47	140728	8	2.71	3.44	4.37	4.62
KOI-0289	56882.46	140813	8	2.40	3.13	4.06	4.31
KOI-0291	56881.51	140812	8	1.11	1.83	2.76	3.02
KOI-0298	56868.53	140730	8	1.31	2.04	2.98	3.31
KOI-0299	56869.47	140731	8	2.97	3.70	4.64	4.90
KOI-0302	56116.61	120708	6	2.09	2.82	3.76	4.04
KOI-0303	56152.46	120813	6	2.76	3.49	4.43	4.71
KOI-0305	56152.39	120813	6	2.76	3.48	4.41	4.67
KOI-0306	56115.63	120707	6	2.65	3.38	4.32	4.63
KOI-0313	56152.47	120813	6	2.52	3.25	4.20	4.47
KOI-0314	56152.39	120813	6	2.87	3.60	4.53	4.78
KOI-0315	56263.21	121202	6	2.22	2.96	3.91	4.20
KOI-0316	56869.40	140731	8	2.79	3.52	4.46	4.76
KOI-0321	56152.46	120813	6	2.80	3.54	4.48	4.78
KOI-0323	56152.44	120813	6	2.49	3.22	4.17	4.45
KOI-0338	56510.53	130806	8	2.25	2.98	3.91	4.20
KOI-0345	56151.46	120812	6	2.45	3.19	4.13	4.43
KOI-0346	56882.42	140813	8	3.08	3.81	4.74	5.00
KOI-0348	56881.49	140812	4	1.19	1.91	2.91	3.38
KOI-0356	56882.52	140813	7	1.57	2.29	3.22	3.44
KOI-0365	56153.44	120814	4	0.90	1.63	2.57	2.77
KOI-0366	56153.47	120814	6	2.61	3.34	4.28	4.58
KOI-0367	56153.40	120814	4	1.51	2.25	3.20	3.50
KOI-0370	56881.47	140812	8	3.26	3.99	4.92	5.16
KOI-0371	56882.43	140813	8	3.18	3.91	4.85	5.11
KOI-0372	56881.53	140812	7	3.33	4.06	5.00	5.26
KOI-0387	56882.33	140813	8	2.44	3.17	4.12	4.40
KOI-0421	56880.53	140811	13	1.28	2.00	2.94	3.23
KOI-0435	56867.44	140729	8	1.31	2.03	2.96	3.24
KOI-0438	56867.46	140729	6	1.76	2.50	3.44	3.76
KOI-0463	56491.59	130718	8	1.75	2.48	3.43	3.77
KOI-0464	56882.27	140813	8	2.60	3.33	4.28	4.56
KOI-0478	56491.54	130718	8	2.45	3.18	4.12	4.43
KOI-0490	56882.27	140813	8	2.67	3.41	4.35	4.63
KOI-0503	56868.44	140730	8	1.65	2.40	3.36	3.73
KOI-0505	56868.48	140730	8	2.16	2.89	3.84	4.18
KOI-0531	56151.38	120812	6	0.42	1.13	2.09	2.45
KOI-0554	56868.42	140730	8	1.87	2.60	3.55	3.82
KOI-0571	56490.59	130717	7	2.03	2.76	3.71	4.07
KOI-0596	56490.45	130717	6	2.42	3.15	4.08	4.37
KOI-0610	56868.49	140730	8	2.29	3.01	3.96	4.29
KOI-0623	56153.51	120814	6	1.43	2.17	3.13	3.43
KOI-0640	56882.43	140813	8	0.62	1.36	2.32	2.62
KOI-0650	56869.53	140731	8	2.28	3.01	3.94	4.20
KOI-0652	56882.35	140813	8	2.25	2.99	3.94	4.18
KOI-0657	56869.41	140731	8	2.42	3.14	4.07	4.35
KOI-0663	56151.48	120812	6	2.21	2.95	3.90	4.23
KOI-0674	56869.52	140731	8	2.36	3.09	4.03	4.31
KOI-0676	56151.42	120812	6	1.57	2.30	3.24	3.54
KOI-0678	56869.43	140731	8	2.56	3.29	4.23	4.52
KOI-0701	56869.42	140731	14	2.29	3.01	3.94	4.24
KOI-0707	56053.61	120506	6	1.17	1.90	2.83	3.04
KOI-0719	56151.43	120812	6	2.01	2.75	3.73	4.11
KOI-0781	56491.53	130718	8	1.84	2.57	3.52	3.82
KOI-0817	56501.49	130728	6	1.26	2.00	2.97	3.34
KOI-0818	56867.41	140729	6	1.39	2.12	3.08	3.41
KOI-0852	56491.45	130718	8	2.11	2.84	3.79	4.09
KOI-0854	56490.53	130717	6	1.92	2.65	3.59	3.89
KOI-0868	56880.52	140811	8	1.67	2.40	3.33	3.64
KOI-0886	56491.56	130718	7	2.31	3.05	3.99	4.31
KOI-0899	56491.58	130718	7	2.14	2.87	3.81	4.12
KOI-0908	56880.53	140811	8	1.28	2.01	2.96	3.24
KOI-0936	56490.44	130717	8	2.42	3.15	4.08	4.37
KOI-0947	56490.50	130717	6	3.10	3.83	4.77	5.03
KOI-0952	56868.37	140730	8	2.12	2.85	3.79	4.08
KOI-0961	56490.50	130717	6	2.81	3.54	4.47	4.78
KOI-0972	56153.35	120814	6	2.92	3.65	4.59	4.83
KOI-0974	56113.62	120705	6	2.23	2.95	3.88	4.20
KOI-0981	56153.37	120814	4	2.15	2.88	3.81	4.07
KOI-0984	56882.50	140813	8	1.97	2.70	3.64	3.91
KOI-0987	56882.40	140813	8	2.88	3.61	4.54	4.72
KOI-1019	56113.62	120705	5	2.23	2.96	3.90	4.22
KOI-1054	56152.34	120813	6	4.02	4.75	5.68	5.91
KOI-1078	56491.55	130718	7	2.10	2.83	3.78	4.10
KOI-1085	56867.48	140729	8	1.92	2.65	3.58	3.89
KOI-1146	56868.43	140730	8	1.83	2.56	3.50	3.79

TABLE 2
KECK/NIRC2 NRM DETECTION LIMITS

KOI-1164	56491.50	130718	8	1.74	2.47	3.41	3.75
KOI-1174	56882.40	140813	8	2.95	3.68	4.63	4.87
KOI-1201	56868.41	140730	8	2.30	3.03	3.97	4.25
KOI-1220	56152.48	120813	6	2.17	2.90	3.82	4.07
KOI-1221	56114.60	120706	6	3.04	3.77	4.72	5.00
KOI-1222	56152.32	120813	6	3.68	4.41	5.34	5.56
KOI-1230	56116.62	120708	5	1.53	2.27	3.21	3.52
KOI-1241	56152.35	120813	6	3.66	4.39	5.33	5.61
KOI-1283	56152.36	120813	6	4.12	4.85	5.78	6.00
KOI-1298	56868.40	140730	8	1.81	2.54	3.48	3.78
KOI-1299	56152.37	120813	5	3.50	4.23	5.18	5.47
KOI-1314	56510.49	130806	8	3.30	4.03	4.97	5.26
KOI-1316	56882.48	140813	8	2.88	3.61	4.55	4.82
KOI-1361	56882.28	140813	8	2.48	3.21	4.17	4.48
KOI-1393	56867.43	140729	8	1.72	2.45	3.40	3.71
KOI-1397	56501.57	130728	10	0.14	0.64	1.59	2.04
KOI-1408	56490.49	130717	6	2.91	3.64	4.58	4.85
KOI-1428	56882.49	140813	7	1.98	2.71	3.66	3.98
KOI-1431	56882.37	140813	8	3.38	4.11	5.04	5.22
KOI-1436	56151.35	120812	6	0.71	1.44	2.37	2.66
KOI-1442	56152.45	120813	6	2.69	3.42	4.36	4.65
KOI-1478	56511.42	130807	7	2.50	3.23	4.17	4.44
KOI-1515	56151.34	120812	6	1.27	2.00	2.94	3.27
KOI-1537	56869.35	140731	8	3.24	3.97	4.91	5.21
KOI-1588	56490.54	130717	6	2.00	2.73	3.67	3.96
KOI-1611	56114.59	120706	6	2.57	3.30	4.23	4.51
KOI-1612	56153.35	120814	6	2.92	3.65	4.59	4.89
KOI-1613	56882.45	140813	8	0.14	0.65	1.58	1.81
KOI-1615	56114.62	120706	6	1.16	1.79	2.73	3.01
KOI-1616	56153.49	120814	4	1.82	2.56	3.51	3.81
KOI-1618	56511.39	130807	8	3.91	4.64	5.57	5.82
KOI-1619	56114.61	120706	6	2.81	3.54	4.48	4.75
KOI-1621	56611.27	131115	6	2.11	2.84	3.79	4.12
KOI-1649	56490.46	130717	6	1.64	2.37	3.31	3.60
KOI-1686	56491.49	130718	8	1.59	2.32	3.27	3.60
KOI-1692	56116.61	120708	5	1.79	2.52	3.44	3.69
KOI-1701	56113.63	120705	3	1.61	2.34	3.29	3.57
KOI-1702	56491.58	130718	8	2.22	2.96	3.90	4.20
KOI-1725	56152.38	120813	6	1.43	2.18	3.16	3.55
KOI-1738	56882.33	140813	8	2.49	3.22	4.16	4.46
KOI-1781	56152.37	120813	6	2.94	3.68	4.61	4.88
KOI-1788	56880.47	140811	8	1.92	2.66	3.60	3.90
KOI-1797	56152.40	120813	6	1.11	1.85	2.81	3.17
KOI-1800	56152.45	120813	6	1.83	2.56	3.50	3.79
KOI-1803	56151.48	120812	6	2.15	2.88	3.82	4.08
KOI-1815	56869.39	140731	8	2.73	3.47	4.41	4.69
KOI-1833	56867.46	140729	8	2.09	2.83	3.78	4.08
KOI-1835	56868.54	140730	8	0.00	0.02	0.33	0.55
KOI-1843	56491.56	130718	7	2.08	2.81	3.76	4.06
KOI-1867	56490.56	130717	8	2.45	3.17	4.11	4.40
KOI-1877	56510.50	130806	8	2.71	3.45	4.39	4.68
KOI-1879	56490.55	130717	8	2.09	2.83	3.78	4.11
KOI-1880	56867.44	140729	8	0.92	1.63	2.61	3.02
KOI-1890	56882.51	140813	8	2.23	2.96	3.90	4.13
KOI-1894	56152.40	120813	5	1.32	2.05	3.00	3.32
KOI-1902	56491.48	130718	8	2.21	2.94	3.88	4.20
KOI-1904	56867.55	140729	8	1.32	2.05	2.99	3.30
KOI-1908	56882.26	140813	8	2.70	3.44	4.37	4.63
KOI-1924	56113.59	120705	6	2.29	3.01	3.94	4.24
KOI-1925	56153.32	120814	6	2.60	3.34	4.31	4.67
KOI-1937	56151.47	120812	6	1.60	2.34	3.29	3.59
KOI-1961	56869.49	140731	8	1.07	0.69	0.97	1.12
KOI-1967	56151.42	120812	5	0.12	0.67	1.59	1.89
KOI-1977	56867.54	140729	8	0.00	0.02	0.33	0.69
KOI-1985	56869.39	140731	8	2.34	3.07	4.02	4.31
KOI-1988	56867.56	140729	7	1.29	2.02	2.96	3.25
KOI-2001	56151.51	120812	6	2.22	2.95	3.90	4.20
KOI-2005	56501.51	130728	12	1.18	1.88	2.84	3.19
KOI-2006	56151.37	120812	6	1.44	2.18	3.12	3.45
KOI-2013	56115.60	120707	6	2.58	3.31	4.25	4.55
KOI-2029	56152.50	120813	6	1.99	2.72	3.66	3.94
KOI-2031	56501.50	130728	12	1.29	2.03	2.99	3.35
KOI-2032	56882.50	140813	7	0.00	0.12	0.90	1.16
KOI-2035	56152.50	120813	5	1.61	2.34	3.28	3.59
KOI-2036	56491.48	130718	8	2.57	3.29	4.22	4.50
KOI-2057	56490.47	130717	6	2.25	2.98	3.92	4.21
KOI-2067	56869.56	140731	7	1.50	2.23	3.17	3.51

TABLE 2
KECK/NIRC2 NRM DETECTION LIMITS

KOI-2079	56882.38	140813	8	3.18	3.91	4.84	5.05
KOI-2090	56491.50	130718	6	2.42	3.15	4.09	4.38
KOI-2124	56868.36	140730	8	0.00	0.01	0.38	0.71
KOI-2133	56152.34	120813	6	3.62	4.35	5.28	5.53
KOI-2149	56153.51	120814	5	1.00	1.73	2.66	2.94
KOI-2156	56490.53	130717	6	1.43	2.16	3.11	3.43
KOI-2158	56151.52	120812	6	2.22	2.95	3.90	4.20
KOI-2169	56152.43	120813	6	2.43	3.15	4.09	4.38
KOI-2173	56152.41	120813	6	2.28	3.01	3.95	4.24
KOI-2175	56263.20	121202	6	2.22	2.95	3.90	4.20
KOI-2181	56501.57	130728	10	1.33	2.06	3.02	3.35
KOI-2191	56491.46	130718	8	2.53	3.26	4.21	4.51
KOI-2208	56881.46	140812	8	2.92	3.65	4.58	4.80
KOI-2225	56501.56	130728	8	1.67	2.41	3.36	3.69
KOI-2238	56490.51	130717	6	2.71	3.45	4.39	4.70
KOI-2287	56152.36	120813	6	3.41	4.14	5.07	5.33
KOI-2306	56491.44	130718	8	2.64	3.37	4.31	4.61
KOI-2311	56152.43	120813	6	2.03	2.75	3.68	3.94
KOI-2329	56491.51	130718	8	1.91	2.65	3.59	3.91
KOI-2332	56115.61	120707	6	2.61	3.35	4.29	4.58
KOI-2347	56490.56	130717	8	2.44	3.17	4.11	4.40
KOI-2352	56153.37	120814	6	2.29	3.02	3.96	4.25
KOI-2390	56152.47	120813	6	2.86	3.59	4.53	4.83
KOI-2418	56868.36	140730	8	1.90	2.63	3.56	3.86
KOI-2453	56491.57	130718	8	1.91	2.64	3.58	3.91
KOI-2462	56153.52	120814	18	1.34	2.09	3.05	3.37
KOI-2479	56152.49	120813	6	2.42	3.16	4.09	4.35
KOI-2481	56115.61	120707	6	1.94	2.67	3.62	3.92
KOI-2522	56882.42	140813	8	3.30	4.03	4.96	5.23
KOI-2527	56490.51	130717	6	2.97	3.70	4.64	4.92
KOI-2533	56151.46	120812	6	2.33	3.06	4.00	4.27
KOI-2541	56151.45	120812	6	2.66	3.39	4.33	4.61
KOI-2542	56868.46	140730	8	1.43	2.16	3.11	3.46
KOI-2545	56152.35	120813	6	3.46	4.19	5.12	5.35
KOI-2583	56152.44	120813	6	2.73	3.46	4.40	4.73
KOI-2593	56510.42	130806	8	2.99	3.72	4.66	4.91
KOI-2640	56151.44	120812	5	2.53	3.26	4.21	4.52
KOI-2650	56490.57	130717	8	1.69	2.43	3.39	3.75
KOI-2657	56881.48	140812	8	2.48	3.21	4.14	4.36
KOI-2659	56510.48	130806	7	3.47	4.21	5.15	5.41
KOI-2662	56490.52	130717	6	2.10	2.83	3.77	4.07
KOI-2672	56511.40	130807	8	3.11	3.84	4.77	5.03
KOI-2675	56869.54	140731	8	2.98	3.71	4.64	4.83
KOI-2678	56511.52	130807	7	0.86	1.58	2.54	2.84
KOI-2686	56882.35	140813	8	2.87	3.60	4.54	4.83
KOI-2687	56511.33	130807	8	3.02	3.75	4.69	4.95
KOI-2693	56511.48	130807	8	2.04	2.79	3.77	4.20
KOI-2704	56490.48	130717	6	2.03	2.77	3.72	4.10
KOI-2705	56868.34	140730	8	1.95	2.68	3.62	3.93
KOI-2706	56511.34	130807	7	3.08	3.81	4.75	5.02
KOI-2712	56881.52	140812	6	3.18	3.91	4.86	5.12
KOI-2720	56511.37	130807	8	3.75	4.49	5.43	5.67
KOI-2754	56510.47	130806	8	3.31	4.04	4.97	5.24
KOI-2755	56511.49	130807	3	2.15	2.88	3.82	4.10
KOI-2792	56869.37	140731	8	3.24	3.97	4.91	5.21
KOI-2798	56867.53	140729	8	1.65	2.38	3.31	3.59
KOI-2801	56511.38	130807	8	3.72	4.45	5.39	5.64
KOI-2803	56511.40	130807	8	3.23	3.96	4.90	5.16
KOI-2813	56882.39	140813	8	2.39	3.13	4.06	4.31
KOI-2842	56867.49	140729	8	1.20	1.93	2.88	3.22
KOI-2867	56510.53	130806	8	2.76	3.49	4.43	4.74
KOI-2948	56866.49	140728	8	2.73	3.45	4.40	4.74
KOI-2992	56868.37	140730	8	2.23	2.96	3.90	4.19
KOI-3075	56511.44	130807	8	3.10	3.84	4.79	5.12
KOI-3097	56510.46	130806	8	3.27	4.01	4.95	5.20
KOI-3119	56868.38	140730	8	1.27	2.01	2.95	3.24
KOI-3144	56511.28	130807	7	1.77	2.49	3.42	3.69
KOI-3158	56511.33	130807	8	2.77	3.50	4.44	4.79
KOI-3179	56611.27	131115	5	1.89	2.62	3.57	3.94
KOI-3184	56869.49	140731	8	2.65	3.38	4.30	4.51
KOI-3194	56882.46	140813	8	2.28	3.01	3.94	4.18
KOI-3196	56510.44	130806	8	3.19	3.92	4.85	5.13
KOI-3208	56868.55	140730	7	1.99	2.72	3.67	4.04
KOI-3232	56510.46	130806	8	3.24	3.97	4.91	5.15
KOI-3237	56869.44	140731	8	2.50	3.23	4.16	4.39
KOI-3246	56511.41	130807	8	3.45	4.18	5.12	5.43
KOI-3263	56868.33	140730	8	1.19	1.92	2.86	3.17

TABLE 2
KECK/NIRC2 NRM DETECTION LIMITS

KOI-3309	56882.30	140813	8	1.92	2.65	3.59	3.90
KOI-3334	56867.54	140729	8	1.13	1.87	2.82	3.15
KOI-3414	56867.52	140729	8	0.65	1.38	2.32	2.62
KOI-3425	56510.54	130806	8	2.36	3.10	4.04	4.32
KOI-3444	56882.29	140813	8	2.36	3.09	4.03	4.35
KOI-3506	56511.45	130807	8	3.13	3.86	4.82	5.15
KOI-3528	56511.44	130807	8	3.68	4.42	5.37	5.70
KOI-3663	56882.47	140813	8	3.23	3.95	4.88	5.06
KOI-3681	56881.51	140812	7	3.16	3.89	4.84	5.11
KOI-3782	56881.50	140812	6	1.50	2.23	3.22	3.68
KOI-3835	56511.45	130807	7	2.71	3.44	4.39	4.73
KOI-3864	56511.46	130807	8	2.98	3.72	4.67	4.99
KOI-3876	56869.54	140731	8	2.67	3.40	4.33	4.57
KOI-3891	56882.44	140813	8	2.92	3.65	4.59	4.91
KOI-3892	56881.47	140812	8	3.22	3.94	4.88	5.16
KOI-3908	56868.56	140730	7	0.09	0.21	0.78	1.01
KOI-3925	56880.46	140811	8	2.47	3.20	4.13	4.41
KOI-4004	56869.45	140731	8	2.88	3.61	4.55	4.81
KOI-4016	56867.50	140729	8	1.72	2.44	3.38	3.69
KOI-4032	56511.43	130807	7	2.17	2.91	3.87	4.25
KOI-4097	56511.47	130807	8	1.78	2.53	3.50	3.87
KOI-4146	56881.44	140812	8	2.50	3.23	4.17	4.50
KOI-4226	56510.55	130806	8	3.02	3.75	4.69	4.97
KOI-4252	56880.45	140811	8	0.82	0.70	1.17	1.45
KOI-4269	56510.52	130806	8	2.81	3.54	4.49	4.81
KOI-4287	56881.45	140812	8	2.68	3.41	4.35	4.61
KOI-4288	56511.49	130807	8	2.13	2.87	3.82	4.18
KOI-4292	56880.49	140811	8	1.58	2.32	3.27	3.60
KOI-4399	56510.45	130806	8	3.49	4.22	5.16	5.41
KOI-4407	56511.39	130807	8	3.45	4.18	5.11	5.35
KOI-4427	56868.39	140730	8	2.19	2.92	3.85	4.15
KOI-4446	56511.41	130807	8	3.03	3.77	4.72	5.08
KOI-4556	56868.52	140730	8	2.18	2.91	3.86	4.22
KOI-4567	56882.53	140813	8	2.74	3.47	4.40	4.60
KOI-4582	56611.26	131115	4	1.85	2.58	3.51	3.71
KOI-4637	56511.34	130807	8	2.65	3.38	4.32	4.54
KOI-4657	56882.34	140813	8	2.40	3.14	4.08	4.41
KOI-4663	56511.43	130807	8	2.78	3.52	4.46	4.80
KOI-4775	56510.52	130806	8	3.02	3.75	4.69	4.97
KOI-4834	56510.51	130806	7	3.04	3.77	4.72	5.00
KOI-4875	56868.41	140730	8	2.30	3.04	3.98	4.25

TABLE 3
KECK/NIRC2 NRM CANDIDATE COMPANIONS

Name	MJD	$\Delta K'$ (mag)	ρ (mas)	PA (deg)
KOI-0005	56153.45	0.400± 0.062	28.548± 0.590	142.109± 2.019
KOI-0214	56882.30	3.706± 0.097	70.938± 1.596	196.658± 1.289
KOI-0289	56882.46	0.189± 0.091	16.940± 0.985	233.485± 3.805
KOI-0291	56881.51	1.349± 0.022	66.170± 0.335	316.688± 0.262
KOI-0854	56490.53	0.299± 0.231	16.089± 0.980	209.435± 4.706
KOI-1316	56882.48	4.749± 0.181	48.403± 3.276	101.567± 3.121
KOI-1397	56501.57	0.001± 0.119	26.760± 1.537	211.818± 2.220
KOI-1613	56882.45	1.291± 0.022	208.520± 0.363	184.646± 0.097
KOI-1615	56114.62	1.810± 0.100	31.798± 1.571	121.956± 1.605
KOI-1833	56867.46	1.443± 0.456	17.150± 1.452	75.868± 3.606
KOI-1835	56868.54	0.026± 0.006	51.188± 1.994	170.482± 2.638
KOI-1902	56491.48	1.944± 0.084	30.821± 1.124	27.391± 0.686
KOI-1961	56869.49	0.152± 0.006	34.606± 0.107	258.834± 0.326
KOI-1977	56867.54	0.125± 0.014	80.728± 0.152	77.556± 0.243
KOI-2005	56501.51	0.644± 0.186	22.628± 0.830	58.000± 3.724
KOI-2031	56501.50	2.330± 0.085	55.640± 1.406	246.163± 1.306
KOI-2036	56491.48	4.415± 0.199	45.220± 5.033	210.132± 3.565
KOI-2124	56868.36	0.011± 0.008	56.828± 0.436	53.958± 1.414
KOI-2418	56868.36	2.509± 0.062	105.672± 0.873	3.229± 0.464
KOI-3892	56881.47	4.482± 0.116	116.599± 1.579	339.262± 0.935
KOI-3908	56868.56	0.126± 0.029	38.784± 0.383	43.140± 1.086
KOI-4032	56511.43	3.025± 0.059	125.077± 0.883	30.312± 0.454
KOI-4252	56880.45	0.468± 0.006	43.029± 0.081	348.651± 0.113
False Positives				
KOI-1222	56152.32	5.390± 0.278	34.472± 7.090	303.330± 4.243
KOI-1686	56491.49	0.284± 0.054	22.268± 0.385	40.924± 1.658
Duplicate Detections				
KOI-2032 B-C	56882.50	0.243± 0.009	62.441± 0.122	127.711± 0.087

NOTE. — KOI-2032 B-C was also detected as part of a triple system in imaging data; we use the imaging results to achieve consistent astrometry and photometry across all three components, but we list the NRM detection here for completeness. KOI-1613 was previously identified as a candidate companion by Law et al. (2013).

TABLE 4
 KECK/NIRC2 IMAGING DETECTION LIMITS

Name	MJD	Filter + Coronagraph	N_{fram}	t_{int}	Limit (mag) at							Separation (mas)			
					150	200	250	300	400	500	700	1000	1500	2000	
KOI-0001	56114.59	Kp	1	10.00	4.4	5.3	5.4	5.8	5.8	5.9	6.1	6.0	6.1	6.0	
KOI-0001	56114.59	Kp+C06	2	40.00	7.2	7.6	8.5	7.6	10.1	10.3	
KOI-0002	56153.43	Kp	1	10.00	3.8	4.4	5.1	5.3	5.6	5.8	6.4	6.8	6.9	6.9	
KOI-0002	56153.43	Kp+C06	2	40.00	7.2	7.2	8.1	9.2	10.2	10.3	
KOI-0003	56113.59	Kp+C06	4	60.00	7.2	7.7	8.8	10.0	11.2	12.1	
KOI-0005	56153.45	Kp	2	40.00	4.5	5.3	5.6	6.0	6.3	6.7	7.4	7.9	8.1	8.1	
KOI-0012	56153.52	Kp	2	40.00	4.9	5.8	6.1	6.2	6.6	6.9	7.8	8.4	8.7	8.7	
KOI-0013	56511.35	Kp	5	100.00	3.8	5.0	5.7	6.0	6.5	7.0	7.3	7.4	7.7	7.8	
KOI-0041	56116.59	Kp	1	10.00	4.8	5.5	5.9	5.9	6.1	6.5	6.7	6.7	6.8	6.7	
KOI-0041	56116.60	Kp+C06	2	40.00	7.6	7.9	9.0	10.0	10.6	10.7	
KOI-0042	56053.64	Kp	2	20.00	5.5	5.9	6.3	6.8	7.1	7.4	8.0	8.4	7.8	8.6	
KOI-0063	56153.44	Kp	2	40.00	4.0	4.9	5.3	5.6	6.1	6.3	7.2	7.8	7.9	7.9	
KOI-0069	56113.61	Kp	1	10.00	4.3	5.1	5.5	5.8	6.4	6.2	6.5	6.7	6.6	6.6	
KOI-0069	56113.61	Kp+C06	2	40.00	7.2	7.8	9.1	10.0	11.2	11.8	
KOI-0070	56053.60	Kp	1	10.00	4.9	5.2	5.4	5.4	5.7	5.5	5.6	5.6	5.5	5.7	
KOI-0070	56053.60	Kp+C06	2	40.00	7.8	8.1	9.3	10.0	10.2	10.2	
KOI-0072	56153.34	Kp	2	30.00	4.6	5.3	5.5	5.5	6.1	6.5	7.0	7.5	8.3	8.4	
KOI-0072	56153.34	Kp+C06	2	40.00	7.5	7.9	9.0	10.2	10.8	10.8	
KOI-0075	56116.60	Kp	2	20.00	4.9	5.8	6.1	6.3	6.6	6.9	7.3	7.6	7.7	7.6	
KOI-0075	56116.60	Kp+C06	2	40.00	7.5	7.8	8.9	10.0	10.8	10.9	
KOI-0082	56053.60	Kp	1	10.00	5.2	5.7	6.0	6.5	6.8	7.1	7.2	7.3	7.2	7.4	
KOI-0082	56053.60	Kp+C06	2	40.00	7.9	8.5	9.7	10.7	11.4	11.8	
KOI-0084	56152.33	Kp	1	10.00	5.5	6.2	6.6	6.8	7.4	7.6	7.7	7.8	7.9	7.9	
KOI-0084	56152.33	Kp+C06	2	40.00	8.1	8.6	9.8	10.5	10.7	10.8	
KOI-0085	56153.42	Kp	1	10.00	3.7	4.3	4.7	5.1	5.2	5.6	5.9	6.0	6.0	6.0	
KOI-0085	56153.42	Kp+C06	2	40.00	7.2	7.2	7.2	8.2	8.7	8.8	
KOI-0087	56153.45	Kp	2	40.00	2.9	3.9	4.6	4.8	5.0	5.5	6.0	6.5	6.6	6.6	
KOI-0089	56114.62	Kp	1	10.00	4.4	5.0	5.2	5.2	5.3	5.2	5.1	5.1	5.2	5.1	
KOI-0089	56114.63	Kp+C06	2	40.00	7.7	8.1	9.0	9.3	9.3	9.3	
KOI-0092	56510.43	Kp	2	20.00	5.9	6.3	6.6	7.1	7.6	7.8	8.1	8.1	8.2	8.2	
KOI-0092	56510.43	Kp+C06	2	40.00	7.9	8.4	9.3	10.0	10.4	10.6	
KOI-0094	56115.62	Kp	2	40.00	5.8	6.6	6.8	7.2	7.9	8.2	8.5	8.8	8.9	8.9	
KOI-0098	56866.50	Kp	12	210.00	5.4	6.0	6.6	6.6	7.1	7.2	7.9	8.4	8.5	8.5	
KOI-0099	56152.49	Kp	3	50.00	6.1	6.7	7.1	7.3	7.6	7.6	7.8	8.0	8.1	8.1	
KOI-0103	56152.42	Kp	3	50.00	5.7	6.5	6.9	7.0	7.6	7.7	8.0	8.3	8.3	8.3	
KOI-0104	56152.38	Kp	1	10.00	5.0	5.6	6.3	6.7	7.1	7.2	7.7	8.1	8.2	8.2	
KOI-0104	56152.38	Kp+C06	2	40.00	7.9	8.2	9.5	10.2	10.2	10.3	
KOI-0105	56152.51	Kp	3	50.00	6.0	6.7	7.0	7.3	7.5	7.6	7.9	8.2	8.5	8.5	
KOI-0112	56869.32	Kp	12	240.00	5.2	5.9	6.6	6.9	7.7	8.0	8.6	8.8	8.9	8.9	
KOI-0116	56115.63	Kp	2	40.00	5.3	6.2	6.8	7.1	7.5	7.9	8.4	8.8	8.9	9.0	
KOI-0117	56152.51	Kp	3	50.00	5.3	6.0	6.5	6.9	7.2	7.6	7.7	8.0	8.0	8.1	
KOI-0118	56152.42	Kp	3	50.00	5.8	6.4	6.9	7.1	7.4	7.7	8.0	8.2	8.3	8.3	
KOI-0119	56263.20	Kp	3	30.00	4.3	4.9	5.2	5.3	5.6	5.9	6.0	5.5	6.1	6.2	
KOI-0122	56510.47	Kp	2	20.00	5.9	6.3	6.3	6.7	7.0	6.9	7.2	7.2	7.4	7.4	
KOI-0122	56510.47	Kp+C06	2	40.00	7.5	7.9	9.0	9.5	9.8	9.7	
KOI-0137	56882.52	Kp	4	80.00	6.1	6.6	7.0	7.2	7.7	8.0	8.1	8.3	8.4	8.4	
KOI-0141	56882.37	Kp	4	80.00	5.6	6.3	6.7	6.9	7.4	7.6	7.8	8.1	8.1	8.1	
KOI-0144	56151.49	Kp	3	50.00	5.5	6.2	6.7	6.8	7.3	7.6	8.1	8.4	8.5	8.4	
KOI-0148	56152.52	Kp	3	50.00	4.5	5.1	5.4	5.7	6.1	6.3	6.6	6.8	6.8	6.8	
KOI-0152	56868.57	Kp	8	160.00	4.5	5.6	5.9	6.3	6.9	7.4	7.9	8.0	8.0	8.0	
KOI-0153	56510.50	Kp	2	40.00	5.5	6.3	6.5	6.9	7.5	7.5	8.0	8.1	8.0	8.1	
KOI-0156	56151.40	Kp	3	50.00	4.9	6.1	6.4	6.5	7.2	7.6	8.1	8.3	8.5	8.5	
KOI-0157	56053.62	Kp	2	40.00	4.8	5.6	6.1	6.4	7.0	7.4	8.2	8.6	8.7	8.7	
KOI-0161	56511.48	Kp	3	60.00	6.1	6.9	7.1	7.3	8.1	8.1	8.5	8.8	8.8	8.9	
KOI-0174	56263.21	Kp	4	40.00	3.3	4.3	4.5	4.9	5.4	5.5	5.7	5.8	5.9	5.9	
KOI-0177	56869.51	Kp	15	300.00	5.5	6.4	6.5	6.7	7.4	7.8	8.3	8.7	8.7	8.7	
KOI-0197	56882.25	Kp	5	100.00	6.0	6.7	7.2	7.4	7.8	8.0	8.2	8.5	8.5	8.5	
KOI-0205	56868.39	Kp	4	80.00	5.5	6.3	6.7	7.0	7.6	7.7	8.2	8.5	8.5	8.5	
KOI-0214	56882.30	Kp	4	80.00	5.6	6.3	6.9	7.0	7.7	7.9	8.2	8.6	8.7	8.6	
KOI-0216	56882.31	Kp	4	80.00	5.3	6.1	6.6	6.7	7.5	7.7	7.9	8.0	8.1	8.1	
KOI-0227	56501.50	Kp	8	80.00	4.6	5.7	5.9	6.3	6.9	7.1	7.6	7.7	7.8	7.8	
KOI-0232	56053.61	Kp	2	40.00	4.4	5.3	5.7	5.9	6.7	7.0	7.3	7.3	7.3	7.4	
KOI-0242	56880.50	Kp	4	80.00	4.9	5.8	6.3	6.5	7.0	7.2	7.4	7.6	7.6	7.6	
KOI-0244	56153.41	Kp	1	10.00	4.0	4.7	5.3	5.3	5.6	5.9	6.2	6.4	6.5	6.5	
KOI-0244	56153.41	Kp+C06	2	40.00	7.2	7.2	7.2	8.3	9.1	9.1	
KOI-0245	56053.64	Kp	1	10.00	2.9	3.6	4.3	4.8	6.1	6.7	7.5	7.8	7.7	7.8	
KOI-0245	56053.64	Kp+C06	2	40.00	7.2	7.9	9.1	10.5	12.1	12.7	
KOI-0246	56153.33	Kp	2	20.00	4.9	5.6	5.7	6.0	6.6	6.7	7.1	7.4	7.5	7.5	
KOI-0246	56153.33	Kp+C06	2	40.00	7.6	7.9	9.0	10.3	11.1	11.7	
KOI-0247	56151.36	Kp	3	50.00	5.8	6.3	6.6	7.0	7.5	7.7	7.9	8.1	8.1	8.1	
KOI-0249	56151.35	Kp	3	50.00	5.2	6.0	6.4	6.8	7.2	7.5	7.8	7.9	8.0	8.0	
KOI-0251	56491.54	Kp	3	60.00	4.8	6.0	6.4	6.5	7.1	7.2	7.6	7.7	7.8	7.7	
KOI-0252	56868.34	Kp	4	80.00	4.6	5.7	6.2	6.5	7.1	7.3	7.7	8.0	8.0	8.0	
KOI-0253	56867.47	Kp	4	80.00	4.7	6.0	6.4	6.8	7.4	7.7	8.2	8.6	8.6	8.6	

TABLE 4
KECK/NIRC2 IMAGING DETECTION LIMITS

KOI-0254	56491.47	Kp	3	60.00	5.6	6.4	6.7	7.0	7.3	7.5	7.9	8.1	8.2	8.1
KOI-0255	56868.47	Kp	5	100.00	5.7	6.6	7.0	7.1	7.8	8.0	8.3	8.6	8.7	8.7
KOI-0257	56153.39	Kp	1	10.00	3.3	4.4	4.7	4.9	5.1	5.4	5.9	6.0	6.0	5.9
KOI-0257	56153.39	Kp+C06	2	40.00	7.2	7.2	8.1	9.0	9.8	9.8
KOI-0260	56153.42	Kp	1	10.00	4.2	5.4	5.8	6.0	6.3	6.5	7.2	7.8	7.8	7.9
KOI-0260	56153.42	Kp+C06	2	40.00	7.2	7.2	7.9	9.1	9.9	10.2
KOI-0261	56114.62	Kp	1	10.00	4.8	5.7	6.0	6.4	6.8	7.0	7.3	7.4	7.5	7.6
KOI-0261	56114.62	Kp+C06	2	40.00	7.9	8.1	9.5	10.5	11.0	11.3
KOI-0262	56153.33	Kp	1	10.00	4.3	5.2	5.6	5.7	6.0	6.3	6.3	6.3	6.4	6.3
KOI-0262	56153.33	Kp+C06	2	40.00	7.4	7.7	8.9	10.0	10.8	10.9
KOI-0268	56153.40	Kp	3	50.00	4.7	5.4	6.0	6.1	6.7	7.0	7.8	8.2	8.3	8.3
KOI-0268	56153.40	Kp+C06	2	40.00	7.2	7.2	7.2	7.3	8.0	8.0
KOI-0269	56153.38	Kp	1	10.00	4.0	4.6	5.3	5.5	5.9	6.1	6.6	6.8	6.8	6.9
KOI-0269	56153.38	Kp+C06	2	40.00	7.2	7.4	8.5	9.3	9.9	10.1
KOI-0270	56869.27	Kp	12	120.00	5.4	6.4	6.6	7.0	7.8	8.0	8.3	8.5	8.6	8.6
KOI-0271	56510.44	Kp	2	20.00	5.9	6.4	6.8	7.2	7.7	7.9	8.0	8.1	8.2	8.2
KOI-0271	56510.44	Kp+C06	2	40.00	7.6	8.1	9.2	9.8	10.2	10.2
KOI-0273	56153.46	Kp	2	40.00	5.0	5.8	6.1	6.3	7.1	7.2	8.1	8.6	9.0	9.1
KOI-0274	56153.47	Kp	2	40.00	5.1	5.8	6.6	6.8	7.3	7.7	8.5	9.0	9.3	9.4
KOI-0275	56153.48	Kp	2	40.00	5.7	6.4	6.6	6.7	7.3	7.8	8.4	8.7	9.1	9.2
KOI-0276	56881.44	Kp	2	40.00	5.5	6.1	6.4	6.5	7.2	7.7	8.0	8.3	8.4	8.4
KOI-0276	56881.45	Kp+C06	2	40.00	7.9	8.1	9.2	10.2	10.4	10.6
KOI-0280	56153.41	Kp	1	10.00	4.2	5.0	5.7	6.1	6.4	6.7	7.1	7.2	7.2	7.1
KOI-0280	56153.41	Kp+C06	2	40.00	7.2	7.2	7.9	9.0	9.4	9.6
KOI-0281	56153.48	Kp	2	40.00	4.7	5.3	5.8	5.9	6.3	6.6	7.2	7.8	8.0	8.0
KOI-0282	56265.18	Kp	3	50.00	4.6	5.3	5.7	5.9	6.4	6.7	7.0	7.1	7.2	7.2
KOI-0283	56153.46	Kp	2	40.00	5.0	6.1	6.3	6.8	7.1	7.3	8.3	8.7	9.0	9.1
KOI-0284	56869.45	Kp	4	80.00	6.0	6.3	6.7	6.8	7.0	7.0	7.8	6.7	8.3	8.4
KOI-0285	56153.49	Kp	2	40.00	4.8	5.3	6.0	6.0	6.6	6.8	7.4	7.9	7.2	8.2
KOI-0288	56153.43	Kp	3	30.00	4.6	5.3	5.8	6.3	6.7	6.7	7.3	7.6	7.5	7.6
KOI-0289	56882.46	Kp	4	80.00	6.1	6.8	7.0	7.2	7.8	8.1	8.4	9.0	9.1	9.1
KOI-0291	56881.50	Kp	8	160.00	4.9	6.3	6.6	7.0	7.8	8.0	8.2	8.7	8.7	8.7
KOI-0298	56152.48	Kp	3	50.00	4.7	5.5	6.2	6.3	6.9	7.1	7.4	7.7	7.6	7.7
KOI-0299	56869.46	Kp	4	80.00	5.7	6.3	6.8	7.2	7.9	7.9	8.3	8.7	8.7	8.7
KOI-0303	56152.46	Kp	3	50.00	6.0	6.8	7.1	7.3	7.7	8.0	8.3	8.6	8.8	8.8
KOI-0305	56152.39	Kp	1	10.00	5.0	5.7	6.3	6.6	6.8	7.1	7.6	7.9	7.9	7.9
KOI-0305	56152.39	Kp+C06	2	40.00	7.2	7.6	8.7	9.5	9.8	9.8
KOI-0306	56115.62	Kp	2	40.00	5.4	6.4	6.8	7.1	7.7	8.1	8.6	8.8	8.9	8.4
KOI-0313	56152.47	Kp	3	50.00	5.2	5.9	6.3	6.6	7.0	7.2	7.4	7.6	7.6	7.6
KOI-0314	56152.39	Kp	1	10.00	5.0	6.0	6.5	6.6	7.0	7.2	7.5	7.6	7.7	7.7
KOI-0314	56152.39	Kp+C06	2	40.00	7.2	8.5	9.5	10.5	11.1	11.3
KOI-0315	56116.62	Kp	2	20.00	4.1	4.8	5.2	5.3	5.9	6.3	6.9	7.0	6.9	7.0
KOI-0315	56116.62	Kp+C06	2	40.00	7.2	7.2	8.1	8.8	8.9	8.9
KOI-0316	56869.40	Kp	4	80.00	5.6	6.2	6.7	6.8	7.5	7.7	8.4	8.8	8.9	8.9
KOI-0321	56152.46	Kp	3	50.00	5.9	6.6	7.0	7.3	7.6	7.8	7.9	8.1	8.2	8.3
KOI-0323	56152.44	Kp	3	50.00	5.9	6.8	7.2	7.3	7.5	7.6	8.0	8.4	8.4	8.4
KOI-0338	56510.53	Kp	3	60.00	5.4	6.0	6.1	6.2	6.9	7.0	7.7	7.6	7.6	7.6
KOI-0345	56151.45	Kp	3	50.00	5.4	6.3	6.7	7.0	7.5	7.6	8.1	8.9	9.2	9.2
KOI-0345	56151.46	Kp+C06	2	40.00	8.2	8.9	9.8	10.2	10.3	10.3
KOI-0346	56882.41	Kp	4	80.00	6.3	7.0	7.4	7.4	8.0	8.1	8.4	8.8	8.8	8.8
KOI-0348	56881.49	Kp	4	80.00	5.2	6.1	6.2	6.6	7.4	7.7	8.3	8.8	8.9	8.9
KOI-0356	56882.51	Kp	4	80.00	5.8	6.2	6.3	6.8	7.2	7.4	8.0	8.5	8.5	8.5
KOI-0365	56153.44	Kp	3	50.00	3.5	4.6	5.2	5.5	5.6	5.9	6.5	7.3	7.6	7.7
KOI-0366	56153.47	Kp	2	40.00	4.9	5.4	6.0	6.4	6.9	7.2	7.7	8.1	8.2	8.3
KOI-0367	56153.39	Kp	1	10.00	3.1	3.6	3.8	4.0	4.6	4.6	4.9	4.9	5.0	4.9
KOI-0367	56153.40	Kp+C06	2	40.00	7.2	7.2	7.2	7.2	7.2	7.2
KOI-0370	56881.47	Kp	2	40.00	5.5	6.7	6.8	6.8	7.7	7.8	8.0	8.2	8.2	8.2
KOI-0370	56881.47	Kp+C06	2	40.00	7.8	8.1	9.2	10.0	10.4	10.6
KOI-0372	56881.53	Kp	2	40.00	6.2	6.6	6.7	6.9	7.4	7.5	7.7	7.8	7.9	7.9
KOI-0372	56881.53	Kp+C06	2	40.00	7.4	7.9	8.9	9.5	9.7	9.7
KOI-0387	56151.49	Kp	3	30.00	5.8	6.6	6.7	7.0	7.3	7.3	7.7	7.7	7.8	7.9
KOI-0421	56880.53	Kp	4	80.00	5.6	6.1	6.5	6.7	7.4	7.5	7.7	7.8	7.8	7.8
KOI-0435	56867.44	Kp	4	80.00	5.6	6.4	6.8	6.9	7.5	7.7	7.9	8.0	8.0	8.0
KOI-0438	56867.45	Kp	4	80.00	4.5	5.6	6.1	6.3	7.1	7.3	7.8	8.1	8.2	8.2
KOI-0463	56491.59	Kp	2	40.00	5.2	6.0	6.5	6.7	7.1	7.3	7.7	7.7	7.9	7.8
KOI-0464	56882.27	Kp	4	80.00	5.7	6.8	7.0	7.2	7.7	7.9	8.2	8.3	8.3	8.3
KOI-0478	56491.53	Kp	3	60.00	5.6	6.2	6.6	6.8	7.1	7.3	8.0	8.2	8.3	8.3
KOI-0490	56882.27	Kp	4	80.00	5.8	6.5	7.0	7.2	7.8	7.9	8.1	8.3	8.5	8.4
KOI-0500	56053.62	Kp	2	40.00	3.6	4.5	5.2	5.5	5.9	6.6	7.1	7.2	7.2	7.3
KOI-0503	56501.48	Kp	4	60.00	5.0	6.1	6.5	6.7	7.4	7.7	8.0	8.2	8.1	8.2
KOI-0505	56868.48	Kp	5	100.00	5.6	6.7	7.0	7.2	7.8	8.0	8.4	8.6	8.6	8.6
KOI-0531	56151.38	Kp	3	50.00	5.0	5.4	5.7	6.0	6.6	7.0	7.4	7.5	7.5	7.5
KOI-0554	56868.42	Kp	4	80.00	4.8	5.7	6.4	6.6	7.1	7.4	7.7	7.9	7.9	7.9
KOI-0571	56490.59	Kp	3	60.00	5.1	6.2	6.6	6.8	7.1	7.4	7.7	7.7	7.7	7.8
KOI-0588	56151.33	Kp	3	30.00	4.8	5.3	5.6	6.0	6.4	6.8	7.0	7.0	7.0	7.0
KOI-0596	56490.45	Kp	3	60.00	5.8	6.6	7.0	7.3	7.8	8.1	8.6	8.9	9.0	9.0
KOI-0610	56501.48	Kp	3	50.00	4.5	5.7	6.1	6.5	7.4	7.7	8.1	8.4	8.5	8.4

TABLE 4
KECK/NIRC2 IMAGING DETECTION LIMITS

KOI-0623	56153.51	Kp	1	20.00	4.5	5.3	5.6	5.8	6.2	6.7	7.1	7.5	7.7	7.7
KOI-0640	56882.43	Kp	4	80.00	5.5	5.7	6.0	6.2	6.9	7.1	7.4	7.9	8.1	8.1
KOI-0650	56869.53	Kp	4	80.00	5.2	6.1	6.4	6.7	7.4	7.7	8.3	8.8	8.9	8.9
KOI-0652	56265.20	Kp	3	50.00	3.5	4.6	5.0	5.2	5.6	6.0	6.2	6.3	6.5	6.4
KOI-0657	56869.40	Kp	4	80.00	5.1	6.2	6.2	6.6	7.3	7.6	8.5	8.9	9.1	9.0
KOI-0663	56151.48	Kp	1	10.00	5.0	5.9	6.2	6.5	6.6	7.1	7.2	7.5	7.5	7.4
KOI-0663	56151.48	Kp+C06	2	40.00	7.2	7.2	8.5	9.0	9.2	9.2
KOI-0674	56869.52	Kp	4	80.00	4.8	5.9	6.0	6.3	7.1	7.4	8.1	8.5	8.5	8.5
KOI-0676	56151.42	Kp	3	50.00	4.8	5.8	6.1	6.3	7.0	7.5	8.1	8.3	8.4	8.4
KOI-0678	56869.42	Kp	4	80.00	5.5	6.5	6.7	6.9	7.7	7.8	8.1	8.2	8.2	8.2
KOI-0701	56869.41	Kp	11	220.00	5.6	6.4	6.7	7.0	7.8	8.2	8.8	9.1	9.2	9.2
KOI-0707	56053.61	Kp	3	50.00	4.2	5.1	5.6	5.9	6.5	7.0	7.4	7.6	7.6	7.6
KOI-0719	56151.43	Kp	1	10.00	5.4	5.9	6.4	6.6	7.1	7.3	7.2	7.4	7.4	7.4
KOI-0719	56151.43	Kp+C06	2	40.00	7.8	8.4	9.5	10.2	10.3	10.4
KOI-0781	56491.53	Kp	3	60.00	5.5	6.4	6.6	6.9	7.1	7.3	7.5	7.6	7.6	7.6
KOI-0817	56501.49	Kp	4	60.00	5.3	6.4	6.7	6.9	7.5	7.7	7.8	8.0	8.1	8.1
KOI-0818	56867.41	Kp	5	100.00	5.5	6.2	6.6	6.8	7.6	7.9	8.3	8.7	8.7	8.7
KOI-0852	56491.45	Kp	3	60.00	4.9	6.0	6.3	6.5	6.8	6.8	6.9	6.9	6.9	6.9
KOI-0854	56490.53	Kp	3	60.00	5.0	6.0	6.5	6.8	7.2	7.4	8.0	8.0	8.1	8.1
KOI-0868	56880.51	Kp	3	60.00	5.3	5.9	6.4	6.7	7.1	7.3	7.8	8.0	8.0	8.0
KOI-0886	56491.56	Kp	2	40.00	4.5	5.6	6.1	6.2	6.9	7.0	7.3	7.4	7.4	7.4
KOI-0899	56491.58	Kp	2	40.00	4.9	5.8	6.1	6.3	6.7	7.0	7.5	7.7	7.8	7.8
KOI-0908	56880.52	Kp	4	80.00	5.2	6.0	6.1	6.5	7.0	7.2	7.4	7.4	7.5	7.5
KOI-0936	56490.44	Kp	3	45.00	5.8	6.6	6.7	6.9	7.8	8.1	8.4	8.7	8.6	8.8
KOI-0947	56490.49	Kp	3	60.00	6.0	6.9	7.2	7.4	7.9	8.1	8.2	8.4	8.4	8.4
KOI-0952	56868.37	Kp	4	80.00	5.3	5.9	6.6	6.7	7.3	7.4	7.8	8.0	8.1	8.1
KOI-0961	56490.50	Kp	3	60.00	6.1	6.8	7.1	7.4	8.1	8.3	8.6	8.9	9.1	9.1
KOI-0972	56153.35	Kp	1	10.00	4.0	5.3	5.7	5.8	6.2	6.4	6.6	6.7	6.7	6.7
KOI-0972	56153.35	Kp+C06	2	40.00	7.2	7.2	8.4	9.8	10.8	11.2
KOI-0974	56113.62	Kp	1	10.00	5.2	5.8	6.4	6.5	6.9	7.3	7.8	7.8	7.8	7.8
KOI-0974	56113.62	Kp+C06	2	40.00	7.2	7.4	8.5	9.8	11.0	11.3
KOI-0975	56113.60	Kp	1	10.00	3.8	4.8	5.2	5.5	6.1	5.9	6.4	7.3	7.5	7.5
KOI-0975	56113.60	Kp+C06	2	40.00	7.2	7.2	7.5	9.1	10.3	11.3
KOI-0984	56153.50	Kp	2	40.00	3.7	4.6	5.1	5.4	5.6	6.0	6.4	6.6	6.7	6.2
KOI-0987	56115.62	Kp	2	40.00	5.3	6.4	6.7	6.7	7.5	8.1	8.5	8.7	8.7	8.2
KOI-1078	56491.55	Kp	3	60.00	4.6	5.6	6.2	6.5	6.9	7.0	7.4	7.6	7.7	7.6
KOI-1085	56867.48	Kp	4	80.00	5.3	6.3	6.5	6.7	7.6	7.8	8.2	8.5	8.6	8.7
KOI-1146	56868.42	Kp	4	80.00	5.2	6.0	6.5	6.8	7.3	7.4	7.8	8.1	8.1	8.2
KOI-1174	56151.41	Kp	3	30.00	4.9	5.5	6.0	6.4	7.2	7.5	8.1	8.3	8.3	8.3
KOI-1201	56868.40	Kp	4	80.00	4.7	5.6	6.3	6.4	7.1	7.3	7.6	7.8	7.9	7.9
KOI-1220	56152.48	Kp	3	50.00	5.6	6.0	6.6	6.8	7.2	7.4	7.6	7.8	7.8	7.9
KOI-1221	56114.60	Kp	1	10.00	5.0	5.8	6.1	6.4	6.3	6.5	6.5	6.6	6.6	6.6
KOI-1221	56114.60	Kp+C06	2	40.00	7.2	7.7	8.6	10.0	10.5	10.8
KOI-1230	56116.62	Kp	2	20.00	5.2	5.8	6.1	6.3	6.5	7.0	7.4	7.6	7.7	7.6
KOI-1230	56116.62	Kp+C06	2	40.00	7.2	7.2	8.4	9.3	9.8	9.9
KOI-1241	56152.35	Kp	1	10.00	5.3	6.4	6.7	7.0	7.4	7.6	7.9	7.9	7.8	7.8
KOI-1241	56152.35	Kp+C06	2	40.00	7.9	8.5	9.8	10.5	10.5	10.7
KOI-1283	56152.36	Kp	1	10.00	5.6	6.3	6.3	6.7	7.3	7.5	7.8	8.0	8.1	8.2
KOI-1283	56152.36	Kp+C06	2	40.00	8.1	8.6	9.7	10.7	10.8	11.2
KOI-1298	56868.40	Kp	4	80.00	5.1	6.0	6.6	6.7	7.2	7.3	6.8	7.7	7.8	7.8
KOI-1299	56152.37	Kp	1	10.00	6.0	6.4	6.6	7.0	7.3	7.6	7.7	7.9	8.0	8.0
KOI-1299	56152.37	Kp+C06	2	40.00	8.6	9.0	10.0	10.3	10.8	10.9
KOI-1300	56868.35	Kp	4	80.00	5.4	6.2	6.6	6.9	7.4	7.8	7.8	8.1	8.3	8.3
KOI-1314	56510.49	Kp	4	60.00	5.9	6.4	6.8	7.0	7.9	7.9	8.3	8.4	8.4	8.4
KOI-1316	56882.48	Kp	2	40.00	6.1	6.8	7.0	7.3	8.0	8.0	8.3	8.7	8.8	8.7
KOI-1316	56882.48	Kp+C06	2	40.00	8.1	8.5	9.5	10.3	10.7	10.8
KOI-1361	56882.28	Kp	4	80.00	5.9	6.5	6.9	7.0	7.7	7.8	8.1	8.3	8.5	8.6
KOI-1393	56867.43	Kp	4	80.00	5.0	5.7	6.3	6.5	7.1	7.3	7.7	7.9	8.0	7.9
KOI-1397	56501.57	Kp	2	20.00	4.5	5.4	5.8	6.1	6.8	6.8	7.2	7.2	7.3	7.2
KOI-1408	56490.49	Kp	3	60.00	5.7	6.9	7.3	7.6	7.9	8.1	8.5	8.6	8.7	8.6
KOI-1422	56490.48	Kp	3	60.00	5.0	5.9	6.3	6.7	7.2	7.5	7.9	8.0	8.0	8.0
KOI-1426	56151.34	Kp	3	50.00	5.0	5.8	6.3	6.6	7.0	7.2	7.5	7.5	7.5	7.4
KOI-1428	56501.53	Kp	14	240.00	5.8	6.5	6.9	7.1	7.6	7.8	8.1	8.2	8.2	8.2
KOI-1431	56882.36	Kp	4	80.00	6.3	6.9	7.2	7.4	7.9	8.0	8.3	8.5	8.5	8.5
KOI-1436	56151.35	Kp	3	50.00	4.3	4.8	5.4	5.6	6.4	6.7	7.1	7.1	7.1	7.0
KOI-1442	56152.45	Kp	3	50.00	5.8	6.4	6.9	7.1	7.4	7.6	7.9	8.1	8.2	8.1
KOI-1478	56511.42	Kp	3	60.00	6.3	6.8	7.1	7.3	7.8	7.9	8.2	8.3	8.4	8.4
KOI-1515	56151.33	Kp	3	50.00	5.2	5.9	6.4	6.7	7.1	7.4	8.0	8.1	8.1	8.0
KOI-1537	56869.34	Kp	3	60.00	4.2	5.5	5.6	6.1	7.0	7.5	8.2	9.0	9.2	9.2
KOI-1537	56869.35	Kp+C06	2	40.00	7.9	8.1	9.2	10.2	10.8	10.8
KOI-1588	56490.54	Kp	3	60.00	5.6	6.5	6.8	7.1	7.4	7.7	8.2	8.3	8.4	8.4
KOI-1589	56053.63	Kp	2	40.00	3.9	4.7	4.9	5.0	5.6	6.0	6.4	6.4	6.4	6.5
KOI-1611	56114.59	Kp	1	10.00	5.0	5.8	6.2	6.6	6.4	6.5	7.2	7.4	7.3	7.3
KOI-1611	56114.59	Kp+C06	2	40.00	7.2	7.2	8.1	9.2	10.2	10.7
KOI-1612	56153.35	Kp	2	20.00	4.3	5.3	5.6	6.0	6.3	6.7	7.4	8.1	8.2	8.2
KOI-1612	56153.35	Kp+C06	2	40.00	7.2	7.6	9.0	10.2	11.3	12.2
KOI-1613	56153.39	Kp	3	30.00	4.8	5.4	5.7	5.8	6.1	6.3	6.8	7.0	7.1	7.1

TABLE 4
KECK/NIRC2 IMAGING DETECTION LIMITS

KOI-1615	56114.61	Kp	1	10.00	4.6	5.4	5.5	5.7	5.8	6.0	6.2	6.1	6.1	6.1
KOI-1615	56114.61	Kp+C06	2	40.00	7.5	7.9	9.0	9.8	10.0	10.2
KOI-1616	56153.49	Kp	2	40.00	5.2	6.2	6.5	6.5	7.2	7.7	8.3	8.7	8.9	9.0
KOI-1618	56511.39	Kp	3	60.00	6.7	7.2	7.5	7.9	8.6	8.6	8.8	9.0	9.1	9.0
KOI-1619	56114.61	Kp	1	10.00	3.8	4.9	5.3	5.0	5.5	5.9	6.1	5.9	6.1	6.0
KOI-1619	56114.61	Kp+C06	2	40.00	7.2	7.5	8.6	9.6	9.8	9.0
KOI-1621	56611.26	Kp	2	20.00	5.4	6.0	6.4	6.6	6.9	7.0	7.2	7.4	7.4	7.5
KOI-1621	56611.26	Kp+C06	2	40.00	8.1	8.5	9.3	10.0	10.2	10.3
KOI-1649	56490.46	Kp	4	80.00	5.3	6.1	6.7	7.0	7.6	7.9	8.4	8.6	8.7	8.7
KOI-1681	56490.54	Kp	3	60.00	4.8	5.9	6.2	6.2	6.8	6.9	7.1	7.3	7.3	7.3
KOI-1692	56116.61	Kp	2	20.00	4.9	5.3	5.8	6.1	6.6	6.9	7.3	7.4	7.5	7.5
KOI-1692	56116.61	Kp+C06	2	40.00	7.2	7.2	8.1	8.8	9.0	8.9
KOI-1702	56491.58	Kp	3	60.00	5.2	6.1	6.4	6.9	7.2	7.5	7.8	7.9	8.0	8.0
KOI-1725	56152.38	Kp	1	10.00	5.1	5.7	6.2	6.3	6.7	6.9	6.9	7.1	7.2	7.2
KOI-1725	56152.38	Kp+C06	2	40.00	7.4	7.9	9.0	10.0	10.6	10.7
KOI-1738	56882.32	Kp	5	100.00	5.4	6.3	6.7	7.3	8.0	8.1	8.4	8.8	8.9	8.8
KOI-1781	56152.37	Kp	1	10.00	5.9	6.4	6.6	7.1	7.3	7.6	7.7	7.9	8.0	8.1
KOI-1781	56152.37	Kp+C06	2	40.00	8.8	9.0	10.0	10.3	10.8	11.1
KOI-1788	56880.47	Kp	4	80.00	5.6	6.2	6.7	7.0	7.6	7.7	8.0	8.2	8.2	8.2
KOI-1797	56152.40	Kp	3	50.00	5.5	6.1	6.6	6.8	7.2	7.7	8.0	8.2	8.3	8.3
KOI-1800	56152.45	Kp	3	50.00	5.8	6.5	7.0	7.3	7.6	7.8	8.0	8.4	8.4	8.4
KOI-1803	56151.48	Kp	3	50.00	5.6	6.6	7.1	7.3	7.4	7.7	8.1	8.2	8.2	8.3
KOI-1815	56869.38	Kp	6	120.00	6.1	6.6	7.0	7.2	7.9	8.2	8.7	9.1	9.2	9.2
KOI-1833	56867.46	Kp	4	80.00	5.9	6.6	6.9	6.9	7.7	7.9	8.3	8.6	8.7	8.7
KOI-1835	56151.40	Kp	3	30.00	4.5	5.3	5.5	5.9	6.8	7.0	7.5	7.6	7.6	7.6
KOI-1841	56151.45	Kp	3	30.00	5.3	6.0	6.3	6.6	7.2	7.4	7.6	7.8	7.8	7.8
KOI-1843	56491.56	Kp	3	60.00	5.1	6.1	6.4	6.7	7.2	7.5	8.0	8.3	8.3	8.4
KOI-1867	56490.55	Kp	3	60.00	5.8	6.5	7.0	7.3	7.6	7.9	8.3	8.4	8.5	8.5
KOI-1877	56510.50	Kp	2	40.00	4.9	5.9	6.3	6.4	7.3	7.5	7.9	8.0	8.0	8.0
KOI-1879	56490.55	Kp	3	60.00	5.2	6.4	6.9	7.3	7.6	7.6	7.9	8.0	8.1	8.1
KOI-1880	56151.39	Kp	3	50.00	4.9	5.5	5.9	6.2	6.6	7.0	7.6	7.7	7.7	7.8
KOI-1890	56882.51	Kp	4	80.00	6.0	6.6	6.9	7.1	7.9	8.1	8.6	8.9	9.0	9.0
KOI-1894	56152.40	Kp	3	50.00	5.3	5.9	6.5	6.6	6.9	7.5	8.1	8.4	8.4	8.4
KOI-1902	56491.48	Kp	3	60.00	5.0	6.2	6.6	6.8	7.3	7.4	7.8	7.8	7.9	7.9
KOI-1904	56151.51	Kp	3	50.00	5.1	6.4	6.8	7.1	7.5	8.0	8.2	8.5	8.6	8.6
KOI-1907	56501.52	Kp	5	80.00	4.7	5.6	6.0	6.3	7.0	7.0	7.6	7.6	7.7	7.7
KOI-1908	56882.26	Kp	4	80.00	5.6	6.3	6.6	7.0	7.6	7.8	8.2	8.6	8.6	8.7
KOI-1925	56153.32	Kc	1	10.00	3.1	3.8	4.6	5.2	5.4	5.9	5.9	6.1	6.2	6.2
KOI-1934	56501.47	Kp	5	70.00	5.1	5.7	6.1	6.4	7.1	7.3	7.9	8.1	8.2	8.2
KOI-1937	56151.47	Kp	3	50.00	5.1	5.8	6.0	6.3	7.1	7.3	7.7	7.8	7.8	7.9
KOI-1961	56869.48	Kp	10	200.00	5.9	7.0	7.2	7.5	8.1	8.2	8.7	9.0	9.1	9.1
KOI-1962	56153.38	Kp	3	30.00	4.2	5.0	5.4	5.8	6.0	6.3	7.0	8.3	8.5	8.6
KOI-1964	56114.60	Kp	3	30.00	5.0	5.8	6.2	6.3	6.6	6.8	7.2	7.4	7.4	7.4
KOI-1967	56151.42	Kp	3	50.00	4.3	5.2	5.4	5.7	6.2	6.6	7.2	7.2	7.3	7.2
KOI-1977	56151.39	Kp	3	30.00	4.2	5.3	5.7	6.0	6.8	7.1	7.2	7.4	7.5	7.5
KOI-1985	56869.39	Kp	4	80.00	5.5	6.1	6.4	6.7	7.5	7.7	8.4	8.8	8.9	9.0
KOI-1988	56867.56	Kp	4	80.00	5.1	6.0	6.6	6.7	7.4	7.7	8.1	8.4	8.4	8.4
KOI-2001	56151.51	Kp	3	50.00	6.1	6.8	7.2	7.4	7.6	8.0	8.2	8.3	8.4	8.4
KOI-2005	56501.51	Kp	4	60.00	5.5	6.4	6.7	7.0	7.3	7.5	7.7	7.8	7.8	7.8
KOI-2006	56151.37	Kp	3	50.00	5.7	6.2	6.5	7.1	7.4	7.6	7.9	8.0	8.0	8.0
KOI-2013	56115.60	Kp	3	60.00	5.3	5.7	5.9	6.5	6.9	7.7	8.4	9.3	9.5	9.6
KOI-2029	56152.50	Kp	3	50.00	5.7	6.4	6.9	7.1	7.6	7.7	7.9	8.4	8.5	8.5
KOI-2031	56501.50	Kp	4	60.00	5.2	6.3	6.7	7.0	7.4	7.5	8.0	8.0	8.1	8.1
KOI-2032	56152.42	Kp	3	30.00	3.7	4.9	5.3	5.8	6.3	6.5	6.8	4.6	6.8	6.9
KOI-2035	56152.50	Kp	3	50.00	5.6	6.2	6.7	7.0	7.3	7.7	7.9	8.2	8.3	8.3
KOI-2036	56491.47	Kp	3	60.00	5.5	6.4	6.8	7.0	7.2	7.5	8.0	8.2	8.3	8.2
KOI-2057	56490.47	Kp	3	60.00	5.4	6.2	6.7	7.1	7.6	8.0	8.3	8.6	8.7	8.7
KOI-2059	56152.41	Kp	3	30.00	5.1	5.5	5.8	6.3	6.6	6.8	7.2	7.5	7.6	7.6
KOI-2067	56869.55	Kp	4	80.00	5.1	5.5	6.0	6.3	6.5	6.9	7.4	7.7	7.7	7.7
KOI-2079	56882.38	Kp	4	80.00	6.6	6.9	7.0	7.3	8.0	8.3	8.9	9.1	9.2	9.2
KOI-2090	56491.49	Kp	3	60.00	4.3	5.0	5.7	6.0	6.2	6.5	6.8	7.0	6.9	7.0
KOI-2124	56151.41	Kp	3	50.00	3.6	4.8	5.3	5.5	6.1	6.4	7.0	7.1	7.1	7.1
KOI-2133	56152.34	Kp	1	10.00	5.0	6.2	6.5	6.8	7.1	7.4	7.7	7.9	7.9	7.9
KOI-2133	56152.34	Kp+C06	2	40.00	8.2	8.9	9.8	10.7	10.9	11.2
KOI-2149	56153.51	Kp	2	40.00	4.5	5.3	5.5	5.7	6.2	6.7	7.0	7.6	7.6	7.6
KOI-2156	56490.53	Kp	2	40.00	5.4	5.9	6.3	6.6	6.9	7.2	7.6	7.7	7.7	7.7
KOI-2158	56151.52	Kp	3	50.00	5.9	6.8	7.1	7.5	7.8	8.1	8.4	8.8	9.0	9.0
KOI-2169	56152.43	Kp	3	50.00	5.6	6.4	6.9	6.8	7.3	7.5	8.0	8.2	8.3	8.4
KOI-2173	56152.41	Kp	3	50.00	5.3	6.2	6.6	7.0	7.6	7.9	8.2	8.6	8.7	8.8
KOI-2175	56263.20	Kp	3	50.00	5.3	6.0	6.2	6.3	6.7	7.1	7.3	7.4	7.5	7.5
KOI-2179	56491.52	Kp	2	40.00	4.1	5.1	5.7	6.2	6.6	6.7	6.8	6.8	6.9	7.0
KOI-2181	56501.57	Kp	4	60.00	5.0	5.8	6.3	6.6	7.1	7.3	7.8	8.0	8.0	8.0
KOI-2191	56491.46	Kp	4	80.00	5.8	6.3	6.6	6.9	7.6	7.8	8.5	8.8	8.8	8.9
KOI-2208	56881.46	Kp	4	80.00	6.0	6.8	7.1	7.2	8.1	8.2	8.5	9.0	9.0	9.1
KOI-2225	56501.56	Kp	5	50.00	5.5	6.5	6.7	6.9	7.6	7.8	8.4	8.5	8.5	8.5
KOI-2238	56115.60	Kp	2	40.00	3.4	4.5	5.0	5.0	5.3	6.2	6.6	6.7	6.6	6.7
KOI-2287	56152.36	Kp	1	10.00	5.3	6.4	6.8	7.0	7.3	7.6	7.5	7.8	7.9	7.9

TABLE 4
KECK/NIRC2 IMAGING DETECTION LIMITS

KOI-2287	56152.36	Kp+C06	2	40.00	7.9	8.6	9.5	10.3	10.6	10.8
KOI-2295	56116.59	Kp	2	20.00	3.2	3.9	4.4	4.8	5.2	5.8	6.3	6.3	6.3	6.2
KOI-2306	56491.44	Kp	4	65.00	5.6	6.2	6.5	6.8	7.5	7.8	8.3	8.6	8.7	8.7
KOI-2311	56152.43	Kp	3	50.00	5.6	6.3	6.8	6.9	7.4	7.5	7.8	7.9	8.1	8.1
KOI-2329	56491.51	Kp	4	106.45	5.3	6.1	6.5	6.8	7.2	7.4	7.7	7.9	8.0	8.0
KOI-2332	56115.61	Kp	2	40.00	5.3	6.1	6.8	7.1	7.5	7.7	8.4	8.8	9.0	9.1
KOI-2347	56490.56	Kp	3	60.00	5.4	6.6	7.0	7.3	7.7	7.8	8.1	8.2	8.3	8.3
KOI-2352	56153.37	Kp	1	10.00	3.5	4.1	4.9	5.0	5.3	5.6	5.6	5.8	5.7	5.7
KOI-2352	56153.37	Kp+C06	2	40.00	7.2	7.4	8.5	9.3	10.2	10.2
KOI-2390	56152.47	Kp	3	50.00	6.0	6.8	7.2	7.6	7.8	8.0	8.2	8.5	8.6	8.6
KOI-2418	56868.36	Kp	4	80.00	5.2	6.2	6.6	6.9	7.4	7.7	8.2	8.4	8.4	8.4
KOI-2453	56490.57	Kp	3	60.00	5.6	6.5	6.9	7.0	7.4	7.7	8.1	8.2	8.4	8.3
KOI-2462	56153.52	Kp	2	40.00	4.6	5.6	5.9	6.1	6.5	6.9	7.5	8.1	8.1	8.2
KOI-2479	56152.49	Kp	3	50.00	5.5	6.2	6.8	6.9	7.2	7.4	7.6	7.7	7.7	7.7
KOI-2481	56115.61	Kp	2	40.00	4.8	5.7	6.2	6.4	6.8	7.1	7.8	7.9	8.0	8.0
KOI-2486	56868.51	Kp	12	240.00	5.3	6.1	6.4	6.5	7.0	7.3	8.2	8.5	8.6	8.6
KOI-2522	56151.52	Kp	3	50.00	5.2	5.8	6.4	6.6	7.1	7.4	8.0	8.2	8.2	8.2
KOI-2527	56490.51	Kp	3	60.00	5.9	6.9	7.2	7.4	7.9	8.2	8.5	8.8	8.9	9.0
KOI-2533	56151.46	Kp	3	50.00	5.8	6.4	6.9	7.3	7.7	7.8	8.2	8.0	8.1	8.1
KOI-2541	56151.44	Kp	4	60.00	5.5	6.2	6.5	6.8	7.2	7.7	8.0	8.7	9.1	9.2
KOI-2541	56151.45	Kp+C06	2	40.00	7.9	8.4	9.5	9.8	9.9	9.9
KOI-2542	56868.46	Kp	17	340.00	5.8	6.5	7.0	7.2	7.9	8.1	8.2	8.5	8.8	8.8
KOI-2545	56152.34	Kp	3	50.00	4.6	5.2	5.7	6.0	6.8	7.0	7.6	8.5	8.9	9.1
KOI-2545	56152.35	Kp+C06	2	40.00	8.1	8.4	9.5	10.3	10.7	10.7
KOI-2583	56152.44	Kp	3	50.00	5.9	6.3	6.7	6.9	7.3	7.4	7.9	8.0	8.1	8.1
KOI-2593	56510.42	Kp	2	20.00	5.2	6.0	6.2	6.3	6.8	7.2	7.8	7.9	7.8	7.9
KOI-2593	56510.42	Kp+C06	2	40.00	7.6	7.9	9.0	10.0	10.2	10.2
KOI-2626	56491.52	Kp	3	60.00	3.8	4.4	4.8	5.1	6.0	6.2	6.5	6.4	6.4	6.5
KOI-2640	56151.44	Kp	2	30.00	5.5	5.9	6.5	6.9	7.1	7.5	7.6	7.8	8.0	8.0
KOI-2640	56151.44	Kp+C06	2	40.00	7.9	8.5	9.5	9.8	9.9	9.9
KOI-2650	56490.57	Kp	3	60.00	5.1	6.2	6.8	7.1	7.2	7.4	7.8	7.8	7.9	7.8
KOI-2657	56881.48	Kp	4	80.00	4.6	5.5	5.9	6.2	6.8	6.8	7.3	7.6	7.7	7.8
KOI-2662	56115.59	Kp	3	50.00	4.7	5.4	5.8	6.2	6.4	7.2	7.9	8.3	8.3	8.3
KOI-2672	56511.40	Kp	3	60.00	5.8	6.6	6.8	7.3	8.0	8.3	7.2	8.7	8.8	8.8
KOI-2675	56869.54	Kp	4	80.00	5.4	6.1	6.5	6.9	7.5	7.9	8.4	9.0	9.0	9.1
KOI-2678	56511.52	Kp	5	100.00	4.8	5.4	5.5	6.0	6.5	6.7	6.7	6.7	6.7	6.8
KOI-2686	56882.34	Kp	3	60.00	5.7	6.5	6.9	7.3	8.0	8.1	8.4	8.6	8.6	8.6
KOI-2687	56511.32	Kp	8	160.00	5.6	6.6	7.2	7.4	8.1	8.1	8.7	9.0	9.1	9.1
KOI-2693	56511.48	Kp	3	60.00	5.8	6.6	6.8	7.1	7.9	8.0	8.2	8.3	8.4	8.5
KOI-2704	56490.48	Kp	3	60.00	5.2	6.3	6.8	6.9	7.5	7.8	8.1	8.3	8.3	8.3
KOI-2705	56868.34	Kp	4	80.00	5.0	6.2	6.6	7.0	7.6	7.9	8.4	8.8	8.9	8.9
KOI-2706	56511.34	Kp	3	60.00	5.4	6.4	6.7	7.2	7.9	8.0	8.6	9.1	9.4	9.4
KOI-2712	56881.52	Kp	2	40.00	5.4	6.0	6.3	6.5	7.1	7.3	7.7	7.9	7.9	8.0
KOI-2712	56881.52	Kp+C06	2	40.00	7.5	7.9	9.0	9.8	10.7	10.8
KOI-2720	56511.37	Kp	4	80.00	6.6	7.2	7.3	7.6	8.0	8.0	8.2	8.4	8.4	8.4
KOI-2733	56867.52	Kp	4	80.00	4.8	5.5	5.9	6.4	7.0	7.2	7.5	7.8	7.9	7.9
KOI-2754	56510.47	Kp	2	20.00	6.1	6.4	6.5	6.6	7.1	6.8	7.2	7.1	7.4	7.4
KOI-2754	56510.47	Kp+C06	2	40.00	7.2	7.4	7.2	9.2	9.7	9.8
KOI-2755	56511.49	Kp	3	60.00	6.0	6.6	6.9	7.1	7.8	7.9	8.1	8.3	8.3	8.4
KOI-2790	56869.32	Kp	12	240.00	5.4	5.9	6.3	6.6	7.3	7.7	8.3	8.5	8.5	8.5
KOI-2792	56869.37	Kp	2	40.00	4.9	6.3	6.6	6.6	7.5	7.5	8.1	8.5	8.6	8.6
KOI-2792	56869.37	Kp+C06	2	40.00	7.9	8.2	9.5	10.5	11.2	11.3
KOI-2798	56867.53	Kp	4	80.00	5.3	6.2	6.5	6.9	7.5	7.8	8.3	8.6	8.7	8.7
KOI-2801	56511.38	Kp	3	60.00	6.6	7.2	7.4	7.6	8.3	8.3	8.6	9.0	9.1	9.1
KOI-2803	56511.40	Kp	3	60.00	6.1	7.0	7.1	7.5	7.9	8.0	8.1	8.1	8.2	8.2
KOI-2813	56882.39	Kp	4	80.00	5.4	5.7	6.2	6.3	7.5	7.6	8.0	7.1	8.4	8.5
KOI-2842	56867.42	Kp	8	160.00	5.2	6.1	6.5	6.8	7.4	7.6	8.0	8.1	8.1	8.1
KOI-2862	56867.41	Kp	4	80.00	5.6	6.0	6.5	6.5	6.8	7.0	7.3	7.4	7.6	7.6
KOI-2867	56510.53	Kp	3	60.00	5.5	6.3	6.7	7.2	7.6	7.9	8.4	8.8	8.9	8.9
KOI-2948	56511.51	Kp	3	60.00	4.4	5.4	6.1	6.5	6.8	7.0	7.2	7.2	7.3	7.3
KOI-2992	56868.37	Kp	4	80.00	5.7	6.4	6.7	6.8	7.4	7.7	8.0	8.1	8.2	8.1
KOI-3075	56511.44	Kp	3	60.00	6.1	6.8	7.0	7.2	7.7	7.6	8.4	8.6	8.7	8.7
KOI-3097	56510.45	Kp	4	60.00	6.2	6.8	7.2	7.4	7.9	8.0	8.4	8.6	9.1	9.0
KOI-3097	56510.46	Kp+C06	2	40.00	7.5	8.1	9.1	9.7	9.8	9.9
KOI-3119	56868.38	Kp	4	80.00	5.2	6.0	6.0	6.2	6.8	7.1	7.1	7.2	7.2	7.2
KOI-3144	56511.28	Kp	5	80.00	4.9	5.8	6.2	6.4	7.3	7.6	8.0	8.1	8.2	8.2
KOI-3158	56511.33	Kp	3	60.00	4.8	6.0	6.7	6.9	7.8	8.2	8.7	9.0	9.1	8.5
KOI-3179	56511.54	Kp	3	60.00	5.3	6.2	6.8	7.0	7.3	7.6	8.2	8.4	8.4	8.4
KOI-3184	56511.51	Kp	3	60.00	5.1	6.1	6.6	6.8	7.2	7.3	7.5	7.6	7.6	7.6
KOI-3194	56882.46	Kp	2	40.00	6.2	6.6	6.7	6.8	7.5	7.7	8.1	8.2	8.2	8.2
KOI-3194	56882.46	Kp+C06	2	40.00	7.9	8.1	9.3	10.2	10.7	10.8
KOI-3196	56510.43	Kp	4	40.00	6.0	6.8	7.0	7.5	7.9	7.9	8.3	8.4	8.5	8.6
KOI-3196	56510.44	Kp+C06	2	40.00	7.5	8.1	9.1	10.0	10.3	10.3
KOI-3208	56868.54	Kp	2	20.00	4.9	5.5	5.8	6.0	6.7	6.9	7.4	7.3	7.6	7.5
KOI-3208	56868.55	Kp+C06	2	40.00	7.2	7.7	8.6	9.5	9.8	9.9
KOI-3232	56510.46	Kp	2	20.00	5.8	6.3	6.4	6.7	6.9	6.9	7.2	7.3	7.5	7.5
KOI-3232	56510.46	Kp+C06	2	40.00	7.6	8.1	9.0	9.7	9.8	9.8

TABLE 4
KECK/NIRC2 IMAGING DETECTION LIMITS

KOI-3237	56869.44	Kp	4	80.00	5.6	6.4	6.7	6.9	7.9	8.1	8.6	9.2	9.3	9.3
KOI-3246	56511.41	Kp	3	60.00	6.7	7.5	7.5	7.8	8.4	8.6	8.6	9.0	9.0	9.0
KOI-3255	56867.55	Kp	4	80.00	3.3	4.1	4.6	4.9	6.0	6.5	7.2	7.3	7.3	7.3
KOI-3263	56868.33	Kp	4	80.00	4.9	5.9	6.3	6.6	7.1	7.5	7.7	7.9	8.0	8.0
KOI-3284	56867.49	Kp	6	120.00	5.6	6.4	6.8	7.0	7.5	7.8	8.3	8.5	8.6	8.6
KOI-3309	56882.30	Kp	4	80.00	5.6	6.2	6.5	6.8	7.1	7.4	7.4	7.8	7.8	7.8
KOI-3414	56867.51	Kp	4	80.00	5.0	5.8	6.3	6.7	7.3	7.5	8.0	8.3	8.3	8.3
KOI-3425	56510.54	Kp	3	60.00	5.6	6.1	6.3	6.5	7.0	7.1	7.5	7.6	7.6	7.6
KOI-3444	56882.29	Kp	2	40.00	4.7	5.3	5.9	6.2	7.0	7.3	7.8	7.5	8.4	8.5
KOI-3444	56882.29	Kp+C06	2	40.00	7.8	8.1	9.3	7.6	10.6	10.7
KOI-3497	56510.51	Kp	5	100.00	5.7	6.4	6.5	6.9	7.6	7.7	6.5	8.5	8.7	8.7
KOI-3506	56511.45	Kp	3	60.00	6.3	7.0	7.1	7.3	7.8	7.8	7.8	7.9	7.9	7.9
KOI-3663	56882.47	Kp	4	80.00	6.3	7.1	7.3	7.6	8.4	8.4	8.7	9.1	9.2	9.2
KOI-3681	56881.51	Kp	2	40.00	6.2	6.7	6.8	6.9	7.4	7.5	7.7	8.1	8.1	8.0
KOI-3681	56881.51	Kp+C06	2	40.00	7.2	7.8	8.9	9.8	10.2	10.2
KOI-3835	56511.45	Kp	3	60.00	6.8	7.3	7.6	7.8	8.5	8.6	8.5	8.7	8.7	8.7
KOI-3864	56511.46	Kp	3	60.00	6.7	7.3	7.7	8.0	8.4	8.5	8.4	8.7	8.8	8.8
KOI-3876	56869.54	Kp	4	80.00	5.5	6.3	6.6	6.8	7.4	8.0	8.4	8.8	8.8	8.9
KOI-3891	56882.44	Kp	4	80.00	5.6	6.4	7.0	7.4	7.8	8.0	8.4	8.1	8.7	8.7
KOI-3892	56881.47	Kp	2	40.00	5.7	6.8	6.9	6.8	7.7	7.7	7.9	8.3	8.4	8.4
KOI-3908	56868.56	Kp	2	20.00	4.1	5.1	5.1	5.6	6.4	6.6	7.2	7.4	7.5	7.5
KOI-3908	56868.56	Kp+C06	2	40.00	7.2	7.6	8.8	9.8	10.2	10.3
KOI-3925	56880.45	Kp	4	80.00	5.6	6.1	6.6	6.7	7.4	7.6	7.9	8.1	8.1	8.2
KOI-3991	56869.55	Kp	6	120.00	5.0	5.8	6.3	6.6	7.2	7.5	7.8	8.0	8.0	8.0
KOI-4004	56869.45	Kp	4	80.00	5.7	6.4	6.8	7.1	7.8	8.1	8.4	8.8	8.8	8.8
KOI-4016	56510.41	Kp	3	60.00	4.5	5.2	5.5	5.9	6.7	7.2	8.3	8.7	9.0	9.0
KOI-4032	56511.43	Kp	3	60.00	6.4	6.9	7.2	7.3	7.6	7.8	7.9	8.0	7.9	8.0
KOI-4097	56511.47	Kp	3	60.00	6.2	6.5	7.0	7.4	8.0	8.0	8.2	8.4	8.4	8.4
KOI-4146	56881.44	Kp	4	80.00	5.7	6.6	6.7	6.9	7.7	7.8	8.1	8.3	8.4	8.4
KOI-4184	56511.47	Kp	3	60.00	5.7	5.8	5.9	6.4	6.9	7.3	7.8	8.1	8.2	8.2
KOI-4226	56510.54	Kp	3	60.00	5.4	6.1	6.5	7.0	7.4	7.6	7.9	8.0	8.2	8.1
KOI-4252	56880.45	Kp	4	80.00	4.9	5.6	5.9	6.4	7.2	7.4	8.0	8.4	8.5	8.4
KOI-4269	56510.52	Kp	3	60.00	5.6	6.2	6.3	6.6	7.2	7.4	8.0	8.1	8.1	8.1
KOI-4287	56881.45	Kp	4	80.00	5.5	6.3	6.5	6.8	7.3	7.4	7.5	8.0	8.1	8.1
KOI-4288	56511.49	Kp	3	60.00	5.9	6.6	7.0	7.3	7.6	7.8	8.3	8.4	8.5	8.5
KOI-4292	56869.50	Kp	13	260.00	5.8	6.9	7.2	7.4	8.0	8.2	8.6	8.8	8.8	8.8
KOI-4399	56510.45	Kp	2	20.00	6.0	6.6	7.0	7.2	7.6	7.7	7.9	8.0	8.0	7.9
KOI-4399	56510.45	Kp+C06	2	40.00	7.9	8.4	9.5	10.2	10.3	10.3
KOI-4407	56511.38	Kp	3	60.00	6.5	7.1	7.5	7.9	8.5	8.6	8.8	9.0	9.2	9.1
KOI-4427	56868.39	Kp	4	80.00	4.8	5.9	6.3	6.6	7.2	7.5	7.9	8.1	8.1	8.1
KOI-4446	56511.41	Kp	3	60.00	6.9	7.5	7.7	7.8	8.5	8.7	8.8	9.0	9.1	9.1
KOI-4556	56868.52	Kp	2	20.00	4.8	5.7	6.0	6.3	7.2	7.6	8.0	8.1	8.2	8.0
KOI-4556	56868.52	Kp+C06	2	40.00	7.4	7.8	9.1	10.0	10.5	10.7
KOI-4582	56611.26	Kp	2	20.00	5.0	5.7	6.0	6.1	6.7	6.8	7.3	7.5	7.4	7.5
KOI-4582	56611.26	Kp+C06	2	40.00	7.9	8.2	9.0	9.8	10.3	10.4
KOI-4637	56511.34	Kp	3	60.00	5.5	6.5	6.8	7.1	8.0	8.0	8.6	9.1	9.2	9.2
KOI-4657	56882.34	Kp	4	80.00	6.0	6.7	7.1	7.3	8.1	8.2	8.6	8.8	8.9	8.9
KOI-4663	56511.43	Kp	3	60.00	6.8	7.6	7.5	7.8	8.2	8.3	8.5	8.5	8.5	8.5
KOI-4775	56510.52	Kp	2	40.00	5.4	6.0	6.3	6.5	7.1	7.4	8.0	8.2	8.2	8.2
KOI-4834	56510.51	Kp	2	40.00	5.5	6.1	6.1	6.7	7.5	7.7	8.1	8.3	8.3	8.3
KOI-4875	56868.41	Kp	4	80.00	4.9	5.6	6.4	6.5	7.1	7.4	7.6	7.9	7.9	7.9
False Positives														
KOI-0044	56882.53	Kp	4	80.00	6.2	6.7	7.0	7.4	7.9	8.1	8.2	8.5	8.6	8.6
KOI-0064	56151.50	Kp	3	50.00	6.1	6.9	7.3	7.4	7.6	8.0	8.1	8.2	8.3	8.3
KOI-0113	56869.27	Kp	12	120.00	5.8	6.6	7.0	7.4	8.0	8.2	8.5	8.7	8.7	8.7
KOI-0189	56880.44	Kp	4	80.00	5.7	6.1	6.7	7.0	7.6	7.9	8.3	8.5	8.6	8.6
KOI-0201	56880.46	Kp	4	80.00	5.4	6.1	6.4	6.8	7.4	7.6	7.9	8.2	8.2	8.2
KOI-0256	56490.47	Kp	3	60.00	5.3	6.2	6.7	7.0	7.7	7.9	8.1	8.3	8.4	8.4
KOI-0263	56869.25	Kp	10	100.00	5.0	5.5	5.6	6.2	6.7	6.8	7.5	7.6	7.6	7.6
KOI-0302	56116.61	Kp	1	10.00	5.1	5.7	6.1	6.2	6.4	6.7	7.0	7.3	7.3	7.3
KOI-0302	56116.61	Kp+C06	2	40.00	7.2	7.2	8.2	9.0	9.1	9.2
KOI-0371	56114.63	Kp	1	10.00	3.3	4.4	5.1	5.2	5.3	5.7	5.8	5.8	5.8	5.9
KOI-0371	56114.63	Kp+C06	2	40.00	7.2	7.2	7.8	9.0	9.8	9.9
KOI-0969	56511.50	Kp	3	60.00	4.7	5.2	5.3	5.2	5.2	5.3	5.4	5.3	5.4	5.4
KOI-0976	56113.61	Kp	3	30.00	4.4	5.3	5.8	5.7	5.7	5.7	6.1	6.2	6.2	6.2
KOI-0981	56153.36	Kp	1	10.00	4.5	5.6	5.9	5.9	6.6	6.6	7.1	7.1	7.2	7.1
KOI-0981	56153.37	Kp+C06	2	40.00	7.2	7.6	8.5	9.7	10.8	11.1
KOI-1019	56113.62	Kp	1	10.00	5.0	5.3	5.8	5.9	6.2	6.4	6.9	7.0	7.2	7.1
KOI-1019	56113.62	Kp+C06	2	40.00	7.7	8.1	9.1	10.3	11.6	11.9
KOI-1054	56152.33	Kp	1	10.00	5.3	6.1	6.5	6.8	7.3	7.5	7.7	8.1	8.1	8.2
KOI-1054	56152.33	Kp+C06	2	40.00	8.5	9.0	10.0	10.7	11.0	11.2
KOI-1164	56491.50	Kp	3	60.00	5.1	6.0	6.4	6.4	6.9	7.1	7.3	7.3	7.4	7.4
KOI-1222	56152.32	Kp	1	10.00	5.2	6.1	6.9	6.8	7.5	7.7	7.8	8.0	8.2	8.2
KOI-1222	56152.32	Kp+C06	2	40.00	8.2	8.6	9.8	10.5	10.8	10.9
KOI-1686	56491.49	Kp	3	60.00	4.6	6.1	6.4	6.5	6.9	7.1	7.4	7.5	7.6	7.5
KOI-1701	56113.63	Kp	1	10.00	4.7	5.3	5.3	5.5	5.5	5.7	5.5	5.5	5.5	5.5
KOI-1701	56113.63	Kp+C06	2	40.00	7.2	8.1	9.0	10.0	10.2	10.2

TABLE 4
KECK/NIRC2 IMAGING DETECTION LIMITS

KOI-1924	56113.59	Kp	2	18.10	4.1	4.9	5.4	5.7	5.9	6.4	7.2	8.1	8.4	8.6
KOI-1924	56113.59	Kp+C06	1	20.00	7.8	8.1	9.1	10.3	11.6	12.4
KOI-2659	56510.48	Kp	4	60.00	5.9	6.5	6.7	7.1	7.7	7.9	8.4	8.6	8.7	8.6
KOI-2659	56510.48	Kp+C06	1	20.00	7.2	7.5	8.2	8.1	8.2	8.2
KOI-3334	56867.54	Kp	4	80.00	5.3	6.1	6.5	6.8	7.2	7.6	8.0	8.2	8.3	8.2
KOI-3528	56511.44	Kp	3	60.00	6.6	7.2	7.5	7.9	8.4	8.5	8.6	8.7	8.8	8.8
KOI-3782	56881.49	Kp	4	80.00	5.8	6.6	6.7	7.1	7.8	8.0	8.2	8.5	8.5	8.5

TABLE 5
 KECK/NIRC2 IMAGING CANDIDATE COMPANIONS

Name	MJD	Filter + Coronagraph	N_{frames}	ρ (mas)	PA (deg)	Δm (mag)	Refs
KOI-0001	56114.59	Kp	1	1103.7 ± 1.5	136.803 ± 0.080	2.359 ± 0.006	6, 13
KOI-0001	56114.59	Kp+C06	2	5960.6 ± 2.7	112.205 ± 0.025	8.484 ± 0.119	
KOI-0002	56153.43	Kp+C06	2	3093.2 ± 1.9	266.385 ± 0.035	7.525 ± 0.114	14
KOI-0002	56153.43	Kp	1	3872.1 ± 2.8	90.419 ± 0.041	5.965 ± 0.045	14
KOI-0012	56153.52	Kp	2	603.3 ± 1.5	345.657 ± 0.146	3.835 ± 0.007	
KOI-0012	56153.52	Kp	2	1903.4 ± 2.7	320.307 ± 0.080	7.539 ± 0.043	
KOI-0013	56511.35	Kp	5	1150.2 ± 1.5	280.780 ± 0.076	0.157 ± 0.005	1, 2, 6
KOI-0041	56116.60	Kp+C06	2	3434.0 ± 6.0	195.844 ± 0.100	10.049 ± 0.162	
KOI-0042	56053.64	Kp	2	1667.2 ± 1.5	35.975 ± 0.052	1.873 ± 0.002	1, 2
KOI-0069	56113.61	Kp+C06	2	2288.4 ± 2.5	234.536 ± 0.063	10.282 ± 0.118	
KOI-0069	56113.61	Kp+C06	2	5109.0 ± 5.7	68.542 ± 0.064	11.664 ± 0.155	
KOI-0070	56053.60	Kp	1	3792.9 ± 2.1	53.160 ± 0.031	4.140 ± 0.025	2, 9
KOI-0072	56153.34	Kp	2	2000.1 ± 2.9	296.373 ± 0.083	6.844 ± 0.048	
KOI-0075	56116.60	Kp	2	3533.9 ± 2.5	127.359 ± 0.040	6.532 ± 0.038	2
KOI-0082	56053.60	Kp+C06	2	5226.7 ± 2.7	195.623 ± 0.028	10.286 ± 0.117	
KOI-0082	56053.60	Kp+C06	2	5550.6 ± 3.3	195.989 ± 0.033	10.778 ± 0.123	
KOI-0084	56152.33	Kp+C06	2	3070.1 ± 2.5	231.863 ± 0.046	8.981 ± 0.118	
KOI-0085	56153.42	Kp+C06	2	2979.5 ± 4.2	300.896 ± 0.080	8.110 ± 0.143	2
KOI-0087	56153.45	Kp	2	5396.6 ± 3.5	177.769 ± 0.037	5.710 ± 0.060	2, 9
KOI-0089	56114.63	Kp+C06	2	4419.5 ± 2.2	208.378 ± 0.027	6.942 ± 0.117	
KOI-0089	56114.63	Kp+C06	2	5565.7 ± 4.3	27.287 ± 0.044	8.648 ± 0.138	
KOI-0092	56510.43	Kp+C06	2	6413.0 ± 4.1	148.931 ± 0.036	9.671 ± 0.133	
KOI-0099	56152.49	Kp	3	3483.8 ± 1.8	47.996 ± 0.028	5.129 ± 0.012	3
KOI-0103	56152.42	Kp	3	3953.4 ± 3.1	46.693 ± 0.044	7.403 ± 0.051	
KOI-0104	56152.38	Kp+C06	2	6087.4 ± 5.2	64.949 ± 0.048	9.866 ± 0.148	
KOI-0105	56152.51	Kp	3	883.7 ± 1.5	158.597 ± 0.099	3.736 ± 0.006	
KOI-0105	56152.51	Kp	3	3965.6 ± 2.1	20.502 ± 0.030	6.438 ± 0.026	
KOI-0105	56152.51	Kp	3	5591.0 ± 4.2	155.816 ± 0.043	7.903 ± 0.076	
KOI-0116	56115.63	Kp	2	1690.4 ± 4.8	312.480 ± 0.163	8.476 ± 0.092	
KOI-0116	56115.63	Kp	2	3019.5 ± 3.5	270.712 ± 0.066	8.119 ± 0.062	
KOI-0116	56115.63	Kp	2	4681.0 ± 4.1	276.886 ± 0.050	8.384 ± 0.075	
KOI-0118	56152.42	Kp	3	1338.4 ± 1.5	214.624 ± 0.066	3.854 ± 0.005	2
KOI-0119	56263.20	Kp	3	1034.5 ± 1.5	119.644 ± 0.085	0.063 ± 0.006	6
KOI-0122	56510.47	Kp	2	4176.4 ± 3.2	213.148 ± 0.043	6.306 ± 0.054	2, 9
KOI-0137	56882.52	Kp	4	5078.1 ± 3.6	136.935 ± 0.040	7.382 ± 0.063	2, 9
KOI-0141	56882.37	Kp	4	1126.4 ± 1.5	12.103 ± 0.077	1.347 ± 0.002	2, 6
KOI-0144	56151.49	Kp	3	3311.2 ± 2.7	327.324 ± 0.046	7.111 ± 0.043	
KOI-0144	56151.49	Kp	3	3573.6 ± 4.8	336.924 ± 0.077	8.074 ± 0.090	
KOI-0144	56151.49	Kp	3	4771.4 ± 2.8	291.595 ± 0.033	7.188 ± 0.044	
KOI-0144	56151.49	Kp	3	5812.4 ± 5.7	252.578 ± 0.055	8.310 ± 0.107	
KOI-0148	56152.52	Kp	3	2544.2 ± 2.0	248.072 ± 0.045	4.892 ± 0.026	2, 9
KOI-0148	56152.52	Kp	3	4443.2 ± 1.8	222.238 ± 0.022	3.269 ± 0.011	2, 9
KOI-0152	56868.57	Kp	8	2505.7 ± 1.8	29.705 ± 0.040	5.464 ± 0.016	
KOI-0152	56868.57	Kp	8	4206.1 ± 2.4	21.749 ± 0.032	6.455 ± 0.034	
KOI-0152	56868.57	Kp	8	4232.4 ± 2.8	151.141 ± 0.037	6.489 ± 0.044	
KOI-0152	56868.57	Kp	8	4635.2 ± 1.9	133.796 ± 0.022	4.746 ± 0.011	
KOI-0152	56868.57	Kp	8	4967.2 ± 2.0	151.932 ± 0.021	5.111 ± 0.015	
KOI-0157	56053.62	Kp	2	1269.2 ± 1.6	178.384 ± 0.074	4.574 ± 0.013	
KOI-0157	56053.62	Kp	2	3871.5 ± 3.1	310.341 ± 0.045	7.205 ± 0.051	
KOI-0157	56053.62	Kp	2	4047.9 ± 1.8	238.936 ± 0.024	4.293 ± 0.011	
KOI-0157	56053.62	Kp	2	4703.0 ± 2.0	263.651 ± 0.023	5.257 ± 0.017	
KOI-0157	56053.62	Kp	2	5088.7 ± 4.7	342.298 ± 0.052	8.004 ± 0.087	
KOI-0157	56053.62	Kp	2	6036.8 ± 7.6	313.118 ± 0.072	8.384 ± 0.148	
KOI-0161	56511.48	Kp	3	2691.8 ± 1.7	172.570 ± 0.035	5.075 ± 0.010	
KOI-0161	56511.48	Kp	3	3204.8 ± 2.7	269.660 ± 0.048	7.811 ± 0.044	
KOI-0177	56869.51	Kp	15	2285.5 ± 1.7	258.374 ± 0.041	5.870 ± 0.012	
KOI-0177	56869.51	Kp	15	2870.7 ± 2.7	134.326 ± 0.054	7.535 ± 0.045	
KOI-0177	56869.51	Kp	14	4222.6 ± 1.9	132.206 ± 0.025	6.101 ± 0.016	
KOI-0177	56869.51	Kp	2	5730.6 ± 5.1	11.825 ± 0.050	7.480 ± 0.094	
KOI-0177	56869.51	Kp	4	6543.2 ± 2.0	110.415 ± 0.016	3.201 ± 0.005	
KOI-0177	56869.51	Kp	4	7535.1 ± 4.6	74.370 ± 0.035	7.745 ± 0.082	
KOI-0177	56869.51	Kp	2	7949.4 ± 2.9	61.219 ± 0.019	6.295 ± 0.037	
KOI-0205	56868.39	Kp	4	2262.3 ± 2.3	157.819 ± 0.059	6.795 ± 0.035	
KOI-0214	56882.30	Kp	4	3805.7 ± 1.8	120.162 ± 0.026	5.367 ± 0.013	
KOI-0216	56882.31	Kp	4	1829.2 ± 1.6	0.586 ± 0.050	4.342 ± 0.009	
KOI-0216	56882.31	Kp	4	5070.3 ± 2.7	344.868 ± 0.029	6.684 ± 0.039	
KOI-0216	56882.31	Kp	4	5846.2 ± 1.9	166.454 ± 0.017	2.748 ± 0.005	
KOI-0227	56501.50	Kp	8	3351.1 ± 2.5	149.056 ± 0.042	6.437 ± 0.037	
KOI-0227	56501.50	Kp	8	6548.5 ± 2.0	189.978 ± 0.016	2.715 ± 0.005	
KOI-0232	56053.61	Kp	2	5219.2 ± 4.4	12.685 ± 0.048	6.708 ± 0.080	
KOI-0242	56880.50	Kp	4	4505.1 ± 1.8	131.105 ± 0.022	3.680 ± 0.009	
KOI-0249	56151.35	Kp	3	4331.9 ± 1.7	28.589 ± 0.022	0.804 ± 0.003	2
KOI-0251	56491.54	Kp	3	3566.6 ± 1.7	123.470 ± 0.026	4.158 ± 0.007	2
KOI-0252	56868.34	Kp	2	5327.6 ± 2.1	350.011 ± 0.021	4.234 ± 0.019	

TABLE 5
KECK/NIRC2 IMAGING CANDIDATE COMPANIONS

KOI-0252	56868.34	Kp	4	5450.1 \pm 1.9	147.052 \pm 0.019	4.321 \pm 0.011	
KOI-0253	56867.47	Kp	4	4594.5 \pm 1.8	163.464 \pm 0.021	1.576 \pm 0.003	
KOI-0253	56867.47	Kp	4	4735.3 \pm 1.9	171.784 \pm 0.022	5.481 \pm 0.016	
KOI-0254	56491.47	Kp	3	2724.6 \pm 2.6	7.588 \pm 0.055	6.720 \pm 0.042	
KOI-0254	56491.47	Kp	3	3298.2 \pm 2.2	68.380 \pm 0.037	6.151 \pm 0.029	
KOI-0254	56491.47	Kp	3	6086.6 \pm 2.4	311.005 \pm 0.021	6.100 \pm 0.028	
KOI-0255	56868.47	Kp	5	3382.1 \pm 1.7	357.638 \pm 0.027	3.664 \pm 0.005	
KOI-0257	56153.39	Kp+C06	2	1868.6 \pm 2.8	87.195 \pm 0.087	8.415 \pm 0.124	
KOI-0257	56153.39	Kp+C06	2	4404.0 \pm 3.3	116.011 \pm 0.042	8.635 \pm 0.127	
KOI-0261	56114.62	Kp+C06	2	3355.4 \pm 2.3	330.443 \pm 0.039	9.771 \pm 0.116	
KOI-0261	56114.62	Kp+C06	2	5437.4 \pm 1.9	65.394 \pm 0.019	6.667 \pm 0.111	2
KOI-0268	56153.40	Kp+C06	2	1764.2 \pm 1.6	268.016 \pm 0.051	2.476 \pm 0.126	2, 6, 11
KOI-0268	56153.40	Kp+C06	2	2527.2 \pm 1.7	310.194 \pm 0.037	3.657 \pm 0.127	2, 11
KOI-0269	56153.38	Kp+C06	2	2641.4 \pm 2.3	280.530 \pm 0.050	8.105 \pm 0.118	2
KOI-0282	56265.18	Kp	3	4181.4 \pm 1.9	210.499 \pm 0.025	4.683 \pm 0.015	
KOI-0283	56153.46	Kp	2	6103.6 \pm 2.9	272.451 \pm 0.026	7.930 \pm 0.042	2, 9
KOI-0285	56153.49	Kp	2	1491.5 \pm 1.6	139.105 \pm 0.061	4.215 \pm 0.010	2
KOI-0285	56153.49	Kp	2	2327.1 \pm 3.0	28.817 \pm 0.073	7.077 \pm 0.051	2
KOI-0289	56882.46	Kp	4	3259.6 \pm 2.5	52.179 \pm 0.044	7.796 \pm 0.038	9
KOI-0298	56152.48	Kp	3	1995.8 \pm 1.6	273.549 \pm 0.044	0.195 \pm 0.004	3
KOI-0299	56869.46	Kp	4	2565.3 \pm 3.9	351.220 \pm 0.087	8.199 \pm 0.072	
KOI-0303	56152.46	Kp	3	6491.9 \pm 2.0	272.757 \pm 0.016	3.799 \pm 0.004	
KOI-0305	56152.39	Kp+C06	2	5533.5 \pm 2.0	97.343 \pm 0.019	6.172 \pm 0.115	
KOI-0306	56115.62	Kp	2	2100.1 \pm 1.6	246.803 \pm 0.042	2.039 \pm 0.002	2, 6
KOI-0306	56115.62	Kp	2	5495.0 \pm 2.1	140.919 \pm 0.021	6.653 \pm 0.020	2
KOI-0314	56152.39	Kp+C06	2	4098.4 \pm 5.5	103.082 \pm 0.076	11.051 \pm 0.152	
KOI-0314	56152.39	Kp+C06	2	5944.5 \pm 3.9	236.974 \pm 0.037	10.398 \pm 0.130	
KOI-0315	56116.62	Kp	2	4105.6 \pm 2.1	213.982 \pm 0.028	4.664 \pm 0.024	
KOI-0315	56116.62	Kp+C06	2	5407.6 \pm 2.1	85.916 \pm 0.021	5.873 \pm 0.121	
KOI-0316	56869.40	Kp	4	5100.7 \pm 2.2	9.484 \pm 0.024	7.139 \pm 0.026	2
KOI-0346	56882.41	Kp	4	1608.8 \pm 1.6	353.103 \pm 0.057	5.570 \pm 0.009	
KOI-0348	56881.49	Kp	4	2237.9 \pm 4.7	266.452 \pm 0.119	8.633 \pm 0.088	
KOI-0348	56881.49	Kp	4	4829.0 \pm 2.2	86.547 \pm 0.025	7.065 \pm 0.027	
KOI-0356	56882.51	Kp	4	4080.6 \pm 3.2	227.705 \pm 0.045	7.562 \pm 0.054	
KOI-0366	56153.47	Kp	2	1049.1 \pm 2.6	339.267 \pm 0.143	7.054 \pm 0.043	
KOI-0370	56881.47	Kp+C06	2	1450.7 \pm 2.2	241.316 \pm 0.088	8.475 \pm 0.117	
KOI-0372	56881.53	Kp+C06	2	2634.7 \pm 3.6	162.402 \pm 0.078	8.965 \pm 0.130	2
KOI-0372	56881.53	Kp+C06	2	3553.6 \pm 2.7	61.125 \pm 0.043	8.412 \pm 0.121	2
KOI-0372	56881.53	Kp	2	5975.7 \pm 1.9	36.756 \pm 0.017	4.057 \pm 0.006	2, 3
KOI-0387	56151.49	Kp	3	1900.5 \pm 2.6	223.171 \pm 0.077	6.651 \pm 0.041	
KOI-0421	56880.53	Kp	4	2383.6 \pm 2.1	214.341 \pm 0.051	5.950 \pm 0.029	
KOI-0421	56880.53	Kp	4	3021.9 \pm 5.0	11.138 \pm 0.094	7.411 \pm 0.094	
KOI-0421	56880.53	Kp	4	3771.4 \pm 2.4	130.295 \pm 0.036	6.154 \pm 0.035	
KOI-0421	56880.53	Kp	4	4005.8 \pm 3.7	85.954 \pm 0.052	6.982 \pm 0.065	
KOI-0438	56867.45	Kp	4	3265.4 \pm 1.6	181.995 \pm 0.028	2.160 \pm 0.003	
KOI-0490	56882.27	Kp	4	2219.9 \pm 1.6	63.087 \pm 0.040	3.608 \pm 0.004	
KOI-0500	56053.62	Kp	2	1697.6 \pm 2.2	158.973 \pm 0.076	5.240 \pm 0.033	
KOI-0500	56053.62	Kp	2	3865.5 \pm 6.1	212.087 \pm 0.090	6.763 \pm 0.117	
KOI-0505	56868.48	Kp	5	1969.8 \pm 1.8	201.777 \pm 0.053	6.479 \pm 0.020	
KOI-0554	56868.42	Kp	3	4058.6 \pm 6.7	230.780 \pm 0.094	7.728 \pm 0.130	
KOI-0554	56868.42	Kp	4	5563.4 \pm 1.9	211.978 \pm 0.018	1.937 \pm 0.007	
KOI-0554	56868.42	Kp	4	5734.6 \pm 1.9	205.430 \pm 0.018	3.065 \pm 0.008	
KOI-0571	56490.59	Kp	3	2557.4 \pm 4.1	58.744 \pm 0.091	7.474 \pm 0.075	
KOI-0571	56490.59	Kp	3	3856.1 \pm 3.1	233.620 \pm 0.046	7.077 \pm 0.053	
KOI-0623	56153.51	Kp	1	5618.1 \pm 1.9	202.138 \pm 0.018	1.960 \pm 0.009	3
KOI-0640	56882.43	Kp	4	1167.9 \pm 1.8	308.389 \pm 0.088	5.908 \pm 0.019	
KOI-0650	56869.53	Kp	4	2618.5 \pm 1.6	269.222 \pm 0.034	2.414 \pm 0.003	8
KOI-0657	56869.40	Kp	4	1190.8 \pm 2.0	81.111 \pm 0.097	7.008 \pm 0.027	
KOI-0663	56151.48	Kp+C06	2	1768.8 \pm 4.3	125.545 \pm 0.139	8.329 \pm 0.141	
KOI-0663	56151.48	Kp	1	3229.9 \pm 3.5	62.187 \pm 0.062	6.681 \pm 0.062	
KOI-0663	56151.48	Kp	1	4980.9 \pm 2.8	353.107 \pm 0.031	5.969 \pm 0.043	
KOI-0676	56151.42	Kp	3	7298.2 \pm 2.7	307.828 \pm 0.020	6.821 \pm 0.034	
KOI-0678	56869.42	Kp	4	6036.1 \pm 3.4	97.564 \pm 0.032	7.377 \pm 0.057	
KOI-0701	56869.41	Kp	11	2110.3 \pm 3.3	302.786 \pm 0.090	8.348 \pm 0.059	
KOI-0701	56869.41	Kp	11	2945.2 \pm 1.6	106.758 \pm 0.031	4.158 \pm 0.004	
KOI-0701	56869.41	Kp	11	3484.6 \pm 1.7	358.690 \pm 0.027	5.797 \pm 0.009	
KOI-0701	56869.41	Kp	11	6465.0 \pm 2.2	163.644 \pm 0.018	6.762 \pm 0.018	
KOI-0852	56491.45	Kp	3	4459.2 \pm 2.6	175.912 \pm 0.033	5.644 \pm 0.038	
KOI-0852	56491.45	Kp	3	5964.3 \pm 1.9	220.611 \pm 0.017	1.288 \pm 0.004	
KOI-0868	56880.51	Kp	3	4388.7 \pm 3.9	341.419 \pm 0.050	7.221 \pm 0.069	
KOI-0886	56491.56	Kp	2	3688.1 \pm 1.8	355.996 \pm 0.027	4.550 \pm 0.014	
KOI-0899	56491.58	Kp	2	2995.7 \pm 3.0	218.152 \pm 0.056	6.891 \pm 0.049	
KOI-0908	56880.52	Kp	4	1077.9 \pm 1.6	254.137 \pm 0.085	3.848 \pm 0.010	
KOI-0908	56880.52	Kp	4	1461.2 \pm 1.6	198.189 \pm 0.064	4.041 \pm 0.012	
KOI-0908	56880.52	Kp	4	2623.6 \pm 2.8	330.258 \pm 0.060	6.210 \pm 0.045	
KOI-0908	56880.52	Kp	4	3020.0 \pm 2.0	226.976 \pm 0.038	5.360 \pm 0.025	
KOI-0908	56880.52	Kp	4	3028.3 \pm 4.8	309.624 \pm 0.091	6.995 \pm 0.091	

TABLE 5
KECK/NIRC2 IMAGING CANDIDATE COMPANIONS

KOI-0908	56880.52	Kp	4	5831.9 ± 3.2	319.381 ± 0.031	6.374 ± 0.053	
KOI-0947	56490.49	Kp	3	3884.3 ± 3.5	128.055 ± 0.051	7.800 ± 0.061	
KOI-0947	56490.49	Kp	3	5117.4 ± 2.9	218.972 ± 0.031	7.276 ± 0.044	
KOI-0961	56490.50	Kp	3	6580.6 ± 3.2	298.346 ± 0.027	8.205 ± 0.049	
KOI-0975	56113.60	Kp	1	764.9 ± 1.5	129.600 ± 0.115	4.111 ± 0.006	2, 9
KOI-0975	56113.60	Kp+C06	2	1083.9 ± 4.2	126.768 ± 0.221	8.963 ± 0.135	
KOI-0975	56113.60	Kp+C06	2	6222.3 ± 2.4	182.264 ± 0.021	9.602 ± 0.114	
KOI-0984	56153.50	Kp	2	1751.0 ± 1.6	222.441 ± 0.052	0.148 ± 0.009	6
KOI-0984	56265.19	Kp	2	4809.1 ± 3.7	145.967 ± 0.044	7.145 ± 0.065	
KOI-0987	56115.62	Kp	2	1966.6 ± 1.6	226.239 ± 0.045	2.272 ± 0.003	6
KOI-0987	56115.62	Kp	2	2175.3 ± 1.9	143.040 ± 0.049	6.658 ± 0.021	
KOI-0987	56115.62	Kp	2	5327.9 ± 2.8	156.874 ± 0.030	7.528 ± 0.043	
KOI-0987	56882.40	Kp	4	6020.8 ± 4.2	1.108 ± 0.039	8.868 ± 0.074	
KOI-1146	56868.42	Kp	4	3868.1 ± 5.2	35.830 ± 0.076	7.729 ± 0.098	
KOI-1174	56151.41	Kp	3	3093.8 ± 2.7	5.338 ± 0.049	7.153 ± 0.043	
KOI-1174	56151.41	Kp	3	3480.1 ± 2.5	317.186 ± 0.040	7.041 ± 0.036	
KOI-1174	56151.41	Kp	3	4962.4 ± 1.9	237.864 ± 0.020	4.922 ± 0.010	8
KOI-1201	56868.40	Kp	4	2773.9 ± 1.7	238.543 ± 0.034	4.276 ± 0.011	
KOI-1201	56868.40	Kp	4	3810.0 ± 2.1	266.937 ± 0.030	5.794 ± 0.025	
KOI-1201	56868.40	Kp	4	5235.3 ± 2.6	106.114 ± 0.027	6.256 ± 0.037	
KOI-1221	56114.60	Kp+C06	2	1984.6 ± 3.8	10.101 ± 0.110	9.831 ± 0.131	
KOI-1230	56116.62	Kp	2	2765.6 ± 2.9	109.014 ± 0.059	6.910 ± 0.048	8
KOI-1241	56152.35	Kp+C06	2	3428.2 ± 2.6	105.165 ± 0.044	9.097 ± 0.119	
KOI-1241	56152.35	Kp+C06	2	7222.4 ± 2.9	186.076 ± 0.022	9.058 ± 0.119	
KOI-1298	56868.40	Kp	4	725.0 ± 1.5	235.351 ± 0.121	2.770 ± 0.006	
KOI-1299	56152.37	Kp	1	876.6 ± 1.6	20.983 ± 0.107	5.252 ± 0.013	
KOI-1300	56868.35	Kp	4	759.7 ± 1.5	357.966 ± 0.114	1.168 ± 0.003	
KOI-1316	56882.48	Kp	2	2878.3 ± 1.9	106.500 ± 0.038	6.537 ± 0.022	5
KOI-1316	56882.48	Kp	2	2990.3 ± 2.2	107.965 ± 0.041	6.858 ± 0.030	
KOI-1361	56882.28	Kp	4	883.6 ± 1.5	311.642 ± 0.098	2.865 ± 0.004	
KOI-1361	56882.28	Kp	4	1104.9 ± 3.0	60.147 ± 0.155	7.447 ± 0.052	
KOI-1361	56882.28	Kp	4	6344.0 ± 4.5	353.755 ± 0.040	8.069 ± 0.081	
KOI-1393	56867.43	Kp	4	5523.6 ± 2.5	196.819 ± 0.025	5.764 ± 0.033	
KOI-1397	56501.57	Kp	2	1701.1 ± 3.1	60.782 ± 0.103	6.119 ± 0.053	
KOI-1397	56501.57	Kp	2	2201.2 ± 1.7	233.016 ± 0.045	3.953 ± 0.016	
KOI-1397	56501.57	Kp	2	3455.9 ± 5.4	154.658 ± 0.089	7.011 ± 0.102	
KOI-1397	56501.57	Kp	2	3590.6 ± 3.1	263.747 ± 0.048	6.079 ± 0.051	
KOI-1408	56490.49	Kp	3	2467.6 ± 2.4	158.953 ± 0.055	7.202 ± 0.036	
KOI-1408	56490.49	Kp	3	3462.4 ± 2.2	3.958 ± 0.036	7.024 ± 0.030	
KOI-1408	56490.49	Kp	3	4324.5 ± 3.0	185.073 ± 0.039	7.658 ± 0.049	
KOI-1428	56501.53	Kp	14	2632.5 ± 1.6	170.328 ± 0.034	3.695 ± 0.005	
KOI-1431	56882.36	Kp	4	4980.4 ± 2.3	166.262 ± 0.025	6.758 ± 0.028	
KOI-1436	56151.35	Kp	3	5784.3 ± 2.0	243.276 ± 0.019	3.723 ± 0.016	
KOI-1442	56152.45	Kp	3	2102.8 ± 1.6	71.138 ± 0.042	3.679 ± 0.005	6, 9
KOI-1515	56151.33	Kp	3	1108.8 ± 4.1	112.792 ± 0.214	7.627 ± 0.077	
KOI-1588	56490.54	Kp	3	1493.0 ± 2.5	237.270 ± 0.095	7.205 ± 0.039	
KOI-1588	56490.54	Kp	3	4752.2 ± 2.0	172.349 ± 0.022	5.602 ± 0.016	
KOI-1588	56490.54	Kp	3	4853.5 ± 3.1	173.217 ± 0.035	7.020 ± 0.050	
KOI-1589	56053.63	Kp	2	3949.4 ± 6.8	212.800 ± 0.097	6.169 ± 0.131	
KOI-1589	56053.63	Kp	2	5750.7 ± 3.3	268.273 ± 0.032	4.837 ± 0.055	
KOI-1589	56053.63	Kp	2	5776.7 ± 2.7	266.424 ± 0.026	4.394 ± 0.039	
KOI-1589	56053.63	Kp	2	6254.1 ± 4.6	301.513 ± 0.041	5.564 ± 0.083	
KOI-1615	56114.61	Kp+C06	2	2958.3 ± 1.7	358.140 ± 0.033	6.751 ± 0.113	
KOI-1615	56114.61	Kp+C06	2	3079.9 ± 3.4	94.185 ± 0.063	9.155 ± 0.127	
KOI-1615	56114.61	Kp	1	4777.6 ± 4.5	267.238 ± 0.054	5.914 ± 0.083	
KOI-1615	56114.61	Kp+C06	2	5548.2 ± 2.5	136.714 ± 0.024	8.174 ± 0.116	
KOI-1618	56511.39	Kp	3	3266.0 ± 2.5	158.037 ± 0.044	7.950 ± 0.038	
KOI-1619	56114.61	Kp+C06	2	945.9 ± 3.4	333.790 ± 0.207	8.984 ± 0.128	
KOI-1619	56114.61	Kp	1	2061.6 ± 1.6	227.111 ± 0.043	2.069 ± 0.006	6
KOI-1621	56611.26	Kp	2	5137.2 ± 2.2	160.475 ± 0.023	5.626 ± 0.024	
KOI-1621	56611.26	Kp+C06	2	5995.2 ± 2.6	76.786 ± 0.024	8.359 ± 0.118	
KOI-1681	56490.54	Kp	3	4071.7 ± 2.2	196.839 ± 0.030	5.100 ± 0.027	
KOI-1681	56490.54	Kp	3	4982.2 ± 4.4	251.113 ± 0.050	6.724 ± 0.081	
KOI-1692	56116.61	Kp+C06	2	2110.8 ± 6.2	171.108 ± 0.168	8.612 ± 0.169	
KOI-1692	56116.61	Kp	2	3198.1 ± 3.6	338.437 ± 0.063	6.675 ± 0.064	
KOI-1725	56152.38	Kp+C06	2	4063.8 ± 1.7	99.078 ± 0.023	1.807 ± 0.112	8
KOI-1738	56882.32	Kp	5	2050.7 ± 1.7	154.565 ± 0.046	6.035 ± 0.011	
KOI-1738	56882.32	Kp	5	3901.9 ± 2.4	3.555 ± 0.034	7.451 ± 0.033	
KOI-1738	56882.32	Kp	5	4675.2 ± 2.1	244.903 ± 0.024	6.638 ± 0.022	
KOI-1781	56152.37	Kp	1	3449.3 ± 1.7	332.310 ± 0.027	2.320 ± 0.003	8
KOI-1788	56880.47	Kp	4	4585.5 ± 4.0	19.867 ± 0.049	7.699 ± 0.071	
KOI-1800	56152.45	Kp	3	3935.5 ± 3.3	43.390 ± 0.047	7.578 ± 0.056	
KOI-1833	56867.46	Kp	4	4511.4 ± 3.2	277.843 ± 0.040	7.759 ± 0.053	
KOI-1835	56151.40	Kp	3	1437.7 ± 3.2	136.396 ± 0.126	6.363 ± 0.056	
KOI-1843	56491.56	Kp	3	3115.5 ± 2.3	267.557 ± 0.042	7.190 ± 0.032	
KOI-1879	56490.55	Kp	3	1526.2 ± 4.7	346.755 ± 0.176	7.573 ± 0.089	
KOI-1879	56490.55	Kp	3	5180.0 ± 4.8	253.453 ± 0.052	7.620 ± 0.088	

TABLE 5
KECK/NIRC2 IMAGING CANDIDATE COMPANIONS

KOI-1880	56867.44	Kp	4	1713.5 ± 1.6	100.261 ± 0.052	4.279 ± 0.005	6
KOI-1880	56867.44	Kp	4	4928.9 ± 2.4	188.226 ± 0.028	7.277 ± 0.033	
KOI-1902	56491.48	Kp	3	5007.0 ± 3.5	241.618 ± 0.039	7.167 ± 0.060	
KOI-1902	56491.48	Kp	3	5777.2 ± 2.3	199.769 ± 0.021	6.233 ± 0.025	
KOI-1908	56882.26	Kp	4	1272.8 ± 1.5	259.374 ± 0.069	3.221 ± 0.004	
KOI-1908	56882.26	Kp	4	4829.9 ± 1.8	293.325 ± 0.020	3.677 ± 0.005	
KOI-1934	56501.47	Kp	5	5265.4 ± 3.1	30.276 ± 0.034	6.934 ± 0.051	
KOI-1934	56501.47	Kp	2	6218.5 ± 2.1	51.272 ± 0.018	3.177 ± 0.018	
KOI-1937	56151.47	Kp	3	2311.6 ± 1.6	243.590 ± 0.040	4.702 ± 0.010	
KOI-1967	56151.42	Kp	3	3023.6 ± 4.0	154.303 ± 0.076	6.306 ± 0.074	
KOI-1985	56869.39	Kp	3	2777.4 ± 1.6	155.211 ± 0.032	2.901 ± 0.003	
KOI-1988	56867.56	Kp	4	1580.3 ± 2.1	58.711 ± 0.077	6.735 ± 0.029	
KOI-2001	56151.51	Kp	3	1173.8 ± 1.6	342.871 ± 0.075	4.451 ± 0.006	
KOI-2001	56151.51	Kp	3	6962.4 ± 2.8	202.714 ± 0.022	6.863 ± 0.037	
KOI-2005	56501.51	Kp	4	2057.6 ± 2.6	136.713 ± 0.071	6.524 ± 0.041	
KOI-2029	56152.50	Kp	2	5870.4 ± 4.3	122.846 ± 0.042	7.955 ± 0.077	
KOI-2031	56501.50	Kp	4	3581.3 ± 4.9	45.525 ± 0.078	7.793 ± 0.092	
KOI-2031	56501.50	Kp	2	4268.8 ± 4.3	329.887 ± 0.057	7.099 ± 0.080	
KOI-2031	56501.50	Kp	4	4835.9 ± 1.9	264.482 ± 0.021	4.665 ± 0.011	
KOI-2031	56501.50	Kp	2	6489.4 ± 2.2	219.671 ± 0.018	5.265 ± 0.021	
KOI-2035	56152.50	Kp	3	4020.5 ± 5.7	130.897 ± 0.081	8.081 ± 0.108	
KOI-2036	56491.47	Kp	3	3247.6 ± 5.3	299.121 ± 0.094	8.010 ± 0.102	
KOI-2036	56491.47	Kp	1	6348.4 ± 3.9	203.787 ± 0.034	6.806 ± 0.067	
KOI-2057	56490.47	Kp	3	5817.2 ± 1.9	295.286 ± 0.018	4.263 ± 0.008	
KOI-2067	56869.55	Kp	4	1642.4 ± 1.5	314.863 ± 0.053	0.734 ± 0.002	
KOI-2067	56869.55	Kp	4	2759.5 ± 4.6	55.149 ± 0.094	7.481 ± 0.085	
KOI-2079	56882.38	Kp	4	4660.1 ± 1.8	219.255 ± 0.021	5.361 ± 0.008	
KOI-2079	56882.38	Kp	4	6038.9 ± 1.9	8.262 ± 0.017	3.004 ± 0.003	
KOI-2156	56490.53	Kp	2	3315.6 ± 1.7	305.637 ± 0.029	3.944 ± 0.012	
KOI-2158	56151.52	Kp	3	1646.9 ± 1.9	193.502 ± 0.064	6.446 ± 0.021	
KOI-2158	56151.52	Kp	3	2326.9 ± 1.6	16.218 ± 0.039	4.400 ± 0.006	7
KOI-2158	56151.52	Kp	3	2698.6 ± 3.1	41.279 ± 0.066	7.942 ± 0.054	
KOI-2169	56152.43	Kp	3	3505.7 ± 1.7	67.765 ± 0.026	2.781 ± 0.003	
KOI-2173	56152.41	Kp	3	5150.9 ± 2.9	287.028 ± 0.032	7.728 ± 0.046	
KOI-2181	56501.57	Kp	4	3534.8 ± 2.5	71.213 ± 0.040	6.410 ± 0.038	
KOI-2181	56501.57	Kp	4	3826.7 ± 2.2	27.603 ± 0.032	5.933 ± 0.029	
KOI-2181	56501.57	Kp	2	7557.1 ± 2.7	184.418 ± 0.019	5.781 ± 0.032	
KOI-2191	56491.46	Kp	4	1737.5 ± 1.6	234.266 ± 0.052	5.405 ± 0.009	
KOI-2191	56491.46	Kp	4	5246.7 ± 5.0	311.529 ± 0.054	8.691 ± 0.092	
KOI-2208	56881.46	Kp	4	2813.4 ± 1.7	110.463 ± 0.035	6.598 ± 0.014	
KOI-2208	56881.46	Kp	4	3440.2 ± 3.7	120.470 ± 0.062	8.526 ± 0.067	
KOI-2225	56501.56	Kp	5	2397.7 ± 1.8	188.920 ± 0.042	5.615 ± 0.016	
KOI-2225	56501.56	Kp	5	3486.9 ± 2.2	10.473 ± 0.035	6.494 ± 0.028	
KOI-2287	56152.36	Kp	1	2845.3 ± 1.7	11.232 ± 0.034	5.207 ± 0.014	
KOI-2287	56152.36	Kp+C06	2	5622.0 ± 2.6	144.329 ± 0.026	9.006 ± 0.118	
KOI-2295	56116.59	Kp	2	2179.1 ± 1.6	78.910 ± 0.041	0.921 ± 0.006	
KOI-2311	56152.43	Kp	3	1027.5 ± 1.6	70.177 ± 0.091	5.257 ± 0.012	11
KOI-2332	56115.61	Kp	2	3763.6 ± 3.1	176.913 ± 0.047	7.938 ± 0.052	
KOI-2332	56115.61	Kp	2	4014.6 ± 2.5	121.353 ± 0.035	7.618 ± 0.037	
KOI-2390	56152.47	Kp	3	918.5 ± 1.8	119.379 ± 0.115	6.481 ± 0.021	
KOI-2390	56152.47	Kp	3	4539.4 ± 1.8	119.351 ± 0.022	5.144 ± 0.008	
KOI-2390	56152.47	Kp	3	5832.1 ± 1.9	236.959 ± 0.017	4.035 ± 0.005	
KOI-2418	56868.36	Kp	4	2387.2 ± 4.6	104.419 ± 0.110	7.793 ± 0.086	
KOI-2418	56868.36	Kp	4	3947.8 ± 2.4	328.370 ± 0.035	6.845 ± 0.035	
KOI-2418	56868.36	Kp	4	4173.7 ± 1.8	30.235 ± 0.023	3.713 ± 0.007	
KOI-2453	56490.57	Kp	3	2129.7 ± 3.6	352.377 ± 0.096	7.545 ± 0.065	
KOI-2462	56153.52	Kp	2	2842.7 ± 2.9	303.828 ± 0.058	7.138 ± 0.048	
KOI-2479	56152.49	Kp	3	6032.5 ± 2.3	272.806 ± 0.020	5.889 ± 0.023	
KOI-2479	56152.49	Kp	3	6159.2 ± 4.6	274.129 ± 0.042	7.406 ± 0.084	
KOI-2481	56115.61	Kp	2	1146.8 ± 2.7	183.923 ± 0.137	6.921 ± 0.046	8
KOI-2481	56115.61	Kp	2	4260.7 ± 3.8	0.372 ± 0.051	7.369 ± 0.068	
KOI-2481	56115.61	Kp	2	4499.9 ± 3.4	125.546 ± 0.042	7.215 ± 0.058	
KOI-2486	56868.51	Kp	6	6247.7 ± 2.0	85.351 ± 0.017	4.392 ± 0.008	
KOI-2522	56882.42	Kp	4	5644.9 ± 4.4	261.927 ± 0.044	8.308 ± 0.079	
KOI-2545	56152.35	Kp+C06	2	5716.8 ± 5.0	106.480 ± 0.050	10.264 ± 0.146	
KOI-2593	56510.42	Kp+C06	2	2940.3 ± 4.4	342.120 ± 0.087	9.614 ± 0.140	
KOI-2650	56490.57	Kp	3	3124.7 ± 4.2	125.168 ± 0.077	7.252 ± 0.079	
KOI-2657	56881.48	Kp	4	738.1 ± 1.5	132.045 ± 0.117	0.104 ± 0.002	6
KOI-2672	56511.40	Kp	3	643.4 ± 1.5	307.001 ± 0.135	3.891 ± 0.003	
KOI-2672	56511.40	Kp	3	4667.1 ± 1.8	310.893 ± 0.021	5.967 ± 0.010	7
KOI-2686	56882.34	Kp	3	4479.6 ± 1.8	115.716 ± 0.022	5.011 ± 0.008	
KOI-2693	56511.48	Kp	3	4641.4 ± 1.8	119.364 ± 0.021	5.130 ± 0.007	7
KOI-2704	56490.48	Kp	3	3900.3 ± 3.7	279.597 ± 0.053	7.547 ± 0.065	
KOI-2705	56868.34	Kp	4	1890.3 ± 1.6	304.480 ± 0.046	2.643 ± 0.003	
KOI-2706	56511.34	Kp	3	1664.4 ± 1.6	166.016 ± 0.054	5.231 ± 0.007	7
KOI-2754	56510.47	Kp+C06	2	776.8 ± 1.5	260.948 ± 0.111	1.608 ± 0.113	7
KOI-2754	56510.47	Kp+C06	2	2431.4 ± 4.6	312.994 ± 0.107	9.223 ± 0.142	

TABLE 5
KECK/NIRC2 IMAGING CANDIDATE COMPANIONS

KOI-2755	56511.49	Kp	3	6750.8 ± 2.2	194.800 ± 0.018	5.890 ± 0.019	
KOI-2790	56869.32	Kp	12	2642.1 ± 1.8	198.710 ± 0.038	6.278 ± 0.016	
KOI-2790	56869.32	Kp	12	3270.2 ± 2.0	212.737 ± 0.034	6.631 ± 0.022	
KOI-2790	56869.32	Kp	6	5452.5 ± 1.9	9.472 ± 0.019	4.673 ± 0.008	7
KOI-2790	56869.32	Kp	9	5584.7 ± 2.6	250.679 ± 0.026	7.042 ± 0.036	7
KOI-2790	56869.32	Kp	7	5796.8 ± 2.0	243.634 ± 0.019	5.575 ± 0.013	
KOI-2792	56869.37	Kp+C06	2	3781.4 ± 3.7	273.909 ± 0.056	10.536 ± 0.129	
KOI-2801	56511.38	Kp	3	1473.6 ± 3.1	231.946 ± 0.119	8.376 ± 0.053	
KOI-2803	56511.40	Kp	3	3753.4 ± 1.7	62.252 ± 0.025	2.649 ± 0.003	7
KOI-2803	56511.40	Kp	3	3850.6 ± 2.4	307.631 ± 0.035	7.018 ± 0.035	
KOI-2803	56511.40	Kp	3	4372.9 ± 1.8	64.863 ± 0.023	5.423 ± 0.012	7
KOI-2813	56882.39	Kp	4	1827.5 ± 1.9	187.888 ± 0.059	6.385 ± 0.022	
KOI-2862	56867.41	Kp	4	3411.6 ± 3.3	55.995 ± 0.054	6.475 ± 0.056	
KOI-2862	56867.41	Kp	4	4242.5 ± 1.9	345.945 ± 0.025	4.743 ± 0.018	
KOI-2948	56866.49	Kp+C06	2	2982.3 ± 3.2	108.579 ± 0.061	9.010 ± 0.125	
KOI-2992	56868.37	Kp	4	6024.7 ± 5.7	238.399 ± 0.054	7.700 ± 0.107	
KOI-3075	56511.44	Kp	3	4407.8 ± 2.2	51.908 ± 0.028	6.920 ± 0.027	7
KOI-3119	56868.38	Kp	4	1086.6 ± 1.7	306.198 ± 0.087	3.931 ± 0.014	
KOI-3119	56868.38	Kp	3	3935.8 ± 4.6	285.952 ± 0.067	6.640 ± 0.086	
KOI-3119	56868.38	Kp	4	5862.9 ± 2.0	221.567 ± 0.018	3.676 ± 0.013	
KOI-3119	56868.38	Kp	4	6405.5 ± 2.0	218.380 ± 0.017	3.126 ± 0.011	
KOI-3158	56511.33	Kp	3	1839.9 ± 1.5	253.296 ± 0.048	2.237 ± 0.002	8
KOI-3179	56511.54	Kp	3	5124.5 ± 3.9	141.975 ± 0.043	7.630 ± 0.069	
KOI-3196	56510.43	Kp	4	5501.4 ± 2.7	52.613 ± 0.027	7.447 ± 0.039	
KOI-3208	56868.55	Kp+C06	2	2500.3 ± 2.5	359.389 ± 0.056	8.252 ± 0.119	
KOI-3246	56511.41	Kp	3	3761.0 ± 3.5	130.408 ± 0.053	8.259 ± 0.062	
KOI-3255	56867.55	Kp	4	3037.9 ± 1.7	44.035 ± 0.031	3.846 ± 0.010	
KOI-3284	56867.49	Kp	6	3962.8 ± 1.7	4.304 ± 0.024	2.894 ± 0.002	
KOI-3309	56882.30	Kp	4	3558.1 ± 1.7	43.817 ± 0.026	2.821 ± 0.005	
KOI-3309	56882.30	Kp	4	5285.7 ± 6.3	243.009 ± 0.067	7.521 ± 0.120	
KOI-3414	56867.51	Kp	4	4873.0 ± 3.4	242.952 ± 0.039	7.201 ± 0.058	
KOI-3425	56510.54	Kp	3	4526.1 ± 3.8	222.328 ± 0.048	6.627 ± 0.068	
KOI-3444	56882.29	Kp	2	1087.7 ± 1.5	10.291 ± 0.080	2.452 ± 0.003	8
KOI-3444	56882.29	Kp+C06	2	2043.1 ± 2.6	332.128 ± 0.072	9.247 ± 0.118	
KOI-3444	56882.29	Kp+C06	2	3056.7 ± 2.7	282.131 ± 0.050	9.025 ± 0.119	
KOI-3444	56882.29	Kp+C06	2	3390.1 ± 3.2	192.597 ± 0.053	9.483 ± 0.124	
KOI-3444	56882.29	Kp	2	3569.8 ± 1.7	264.520 ± 0.027	5.090 ± 0.009	8
KOI-3444	56882.29	Kp+C06	2	3710.5 ± 2.0	26.071 ± 0.030	8.185 ± 0.113	
KOI-3444	56882.29	Kp	2	3872.9 ± 4.3	353.598 ± 0.064	8.095 ± 0.079	
KOI-3444	56882.29	Kp+C06	2	6002.6 ± 6.1	248.714 ± 0.057	10.374 ± 0.160	
KOI-3506	56510.55	Kp	3	2380.0 ± 1.9	188.221 ± 0.045	5.711 ± 0.022	
KOI-3681	56881.51	Kp+C06	2	4091.6 ± 2.5	285.489 ± 0.034	8.448 ± 0.118	
KOI-3681	56881.51	Kp+C06	2	5240.6 ± 4.6	96.283 ± 0.049	9.586 ± 0.140	
KOI-3681	56881.51	Kp+C06	2	5285.9 ± 5.2	326.176 ± 0.056	9.720 ± 0.149	
KOI-3891	56882.44	Kp	4	1014.0 ± 1.6	242.163 ± 0.088	5.150 ± 0.008	
KOI-3891	56882.44	Kp	4	1421.1 ± 3.8	187.825 ± 0.151	7.923 ± 0.069	
KOI-3891	56882.44	Kp	4	1988.5 ± 1.6	137.081 ± 0.045	4.503 ± 0.006	
KOI-3891	56882.44	Kp	4	4688.5 ± 2.6	98.316 ± 0.031	7.304 ± 0.038	
KOI-3891	56882.44	Kp	4	6121.9 ± 2.9	78.050 ± 0.026	7.481 ± 0.043	
KOI-3908	56868.56	Kp+C06	2	1695.8 ± 6.8	103.006 ± 0.229	10.099 ± 0.173	
KOI-3908	56868.56	Kp+C06	2	3533.9 ± 5.9	122.690 ± 0.095	10.033 ± 0.159	
KOI-3908	56868.56	Kp+C06	2	4368.1 ± 3.9	93.124 ± 0.050	9.404 ± 0.132	
KOI-3908	56868.56	Kp+C06	2	5444.6 ± 2.6	82.132 ± 0.026	8.474 ± 0.118	
KOI-3925	56880.45	Kp	4	4937.7 ± 2.4	72.048 ± 0.027	6.579 ± 0.032	
KOI-3925	56880.45	Kp	4	5438.8 ± 2.0	53.442 ± 0.020	5.582 ± 0.015	
KOI-4004	56869.45	Kp	4	1940.1 ± 1.6	218.437 ± 0.045	2.385 ± 0.002	
KOI-4016	56510.41	Kp	2	1769.1 ± 3.0	209.958 ± 0.098	7.541 ± 0.053	
KOI-4016	56510.41	Kp	3	3333.9 ± 1.7	186.270 ± 0.029	5.140 ± 0.011	
KOI-4016	56510.41	Kp	1	5553.1 ± 1.9	35.600 ± 0.019	2.711 ± 0.010	8
KOI-4226	56510.54	Kp	3	2450.2 ± 1.6	269.854 ± 0.037	4.117 ± 0.006	
KOI-4269	56510.52	Kp	3	6443.1 ± 2.3	194.054 ± 0.019	6.037 ± 0.022	
KOI-4287	56881.45	Kp	4	4023.8 ± 2.1	271.388 ± 0.029	6.643 ± 0.025	
KOI-4287	56881.45	Kp	4	4431.4 ± 2.1	24.749 ± 0.026	6.518 ± 0.024	
KOI-4288	56511.49	Kp	3	2927.8 ± 2.0	280.931 ± 0.038	6.830 ± 0.023	
KOI-4288	56511.49	Kp	3	5264.1 ± 2.4	224.540 ± 0.025	7.205 ± 0.032	
KOI-4292	56869.50	Kp	13	1937.7 ± 1.6	30.256 ± 0.046	4.663 ± 0.004	
KOI-4399	56510.45	Kp	2	2116.5 ± 1.6	17.534 ± 0.042	3.912 ± 0.005	
KOI-4399	56510.45	Kp	2	2325.3 ± 3.5	358.785 ± 0.087	7.451 ± 0.063	
KOI-4399	56510.45	Kp+C06	2	2682.2 ± 5.4	348.320 ± 0.115	10.107 ± 0.152	
KOI-4407	56511.38	Kp	3	2256.1 ± 3.9	205.345 ± 0.099	8.743 ± 0.071	
KOI-4407	56511.38	Kp	3	2461.1 ± 1.6	299.767 ± 0.036	2.009 ± 0.001	11
KOI-4407	56511.38	Kp	3	2665.8 ± 1.6	311.055 ± 0.034	5.096 ± 0.005	11
KOI-4407	56511.38	Kp	3	4135.3 ± 2.5	188.857 ± 0.034	7.957 ± 0.037	
KOI-4427	56868.39	Kp	4	3200.7 ± 3.0	252.946 ± 0.053	6.991 ± 0.050	
KOI-4427	56868.39	Kp	3	3374.8 ± 6.4	146.356 ± 0.108	7.804 ± 0.123	
KOI-4427	56868.39	Kp	4	5263.9 ± 1.9	272.727 ± 0.019	3.201 ± 0.007	
KOI-4446	56511.41	Kp	3	2054.1 ± 1.6	77.738 ± 0.045	6.254 ± 0.011	

TABLE 5
KECK/NIRC2 IMAGING CANDIDATE COMPANIONS

KOI-4556	56868.52	Kp+C06	2	3904.6 \pm 1.9	359.425 \pm 0.027	7.671 \pm 0.113
KOI-4582	56611.26	Kp	2	2745.4 \pm 2.2	308.227 \pm 0.046	6.090 \pm 0.031
KOI-4582	56611.26	Kp	2	3577.7 \pm 1.7	288.648 \pm 0.026	3.402 \pm 0.006
KOI-4657	56882.34	Kp	4	2129.7 \pm 1.6	233.899 \pm 0.041	1.924 \pm 0.002
KOI-4657	56882.34	Kp	4	3055.0 \pm 3.8	310.643 \pm 0.072	8.350 \pm 0.070
KOI-4657	56882.34	Kp	4	5298.7 \pm 2.3	199.043 \pm 0.024	7.023 \pm 0.028
KOI-4775	56510.52	Kp	2	5270.7 \pm 4.3	51.037 \pm 0.046	7.875 \pm 0.077
KOI-4875	56868.41	Kp	4	1743.7 \pm 1.6	21.693 \pm 0.053	4.230 \pm 0.010
KOI-4875	56868.41	Kp	4	5206.4 \pm 2.2	247.098 \pm 0.023	5.765 \pm 0.024
False Positives						
KOI-0044	56882.53	Kp	4	3391.5 \pm 1.7	124.833 \pm 0.027	3.825 \pm 0.004
KOI-0044	56882.53	Kp	4	4587.2 \pm 3.5	34.451 \pm 0.043	7.812 \pm 0.060
KOI-0044	56882.53	Kp	4	5035.8 \pm 4.5	130.804 \pm 0.051	8.022 \pm 0.084
KOI-0113	56869.27	Kp	12	1324.6 \pm 1.9	123.378 \pm 0.080	6.872 \pm 0.022
KOI-0113	56869.27	Kp	12	3224.7 \pm 2.7	292.789 \pm 0.047	7.703 \pm 0.043
KOI-0113	56869.27	Kp	6	3631.2 \pm 2.6	47.608 \pm 0.041	7.254 \pm 0.040
KOI-0113	56869.27	Kp	9	5223.8 \pm 1.9	264.707 \pm 0.020	5.815 \pm 0.011
KOI-0113	56869.27	Kp	6	5821.2 \pm 2.3	177.634 \pm 0.022	6.592 \pm 0.027
KOI-0113	56869.27	Kp	6	5842.4 \pm 2.1	178.733 \pm 0.019	5.992 \pm 0.016
KOI-0113	56869.27	Kp	3	6478.4 \pm 2.1	164.302 \pm 0.017	5.071 \pm 0.010
KOI-0201	56880.46	Kp	4	2331.1 \pm 3.2	229.140 \pm 0.079	7.428 \pm 0.056
KOI-0201	56880.46	Kp	4	3982.6 \pm 1.9	275.179 \pm 0.026	5.705 \pm 0.017
KOI-0201	56880.46	Kp	4	4038.8 \pm 3.1	272.722 \pm 0.043	7.171 \pm 0.052
KOI-0201	56880.46	Kp	4	4508.9 \pm 4.1	311.415 \pm 0.051	7.645 \pm 0.073
KOI-0201	56880.46	Kp	4	5295.4 \pm 2.2	117.072 \pm 0.023	6.265 \pm 0.025
KOI-0256	56490.47	Kp	3	4502.9 \pm 3.7	300.839 \pm 0.047	7.902 \pm 0.066
KOI-0263	56153.36	Kp	1	3287.8 \pm 1.7	269.653 \pm 0.029	0.635 \pm 0.012
KOI-0302	56116.61	Kp+C06	2	3073.4 \pm 2.3	189.753 \pm 0.043	6.953 \pm 0.122
KOI-0302	56116.61	Kp+C06	2	4500.7 \pm 2.9	184.723 \pm 0.036	7.564 \pm 0.126
KOI-0302	56116.61	Kp+C06	2	5758.3 \pm 2.1	46.187 \pm 0.020	6.203 \pm 0.119
KOI-0371	56114.63	Kp+C06	2	3186.9 \pm 2.5	91.595 \pm 0.044	8.119 \pm 0.119
KOI-0371	56114.63	Kp+C06	2	3972.7 \pm 4.9	60.941 \pm 0.071	9.426 \pm 0.147
KOI-0371	56114.63	Kp+C06	2	5483.9 \pm 4.0	97.040 \pm 0.041	9.134 \pm 0.133
KOI-0371	56114.63	Kp+C06	2	6039.8 \pm 2.4	116.190 \pm 0.021	7.606 \pm 0.117
KOI-0981	56153.37	Kp+C06	2	4508.4 \pm 6.3	139.534 \pm 0.079	11.001 \pm 0.164
KOI-1019	56113.62	Kp+C06	2	2492.1 \pm 1.7	247.723 \pm 0.038	7.971 \pm 0.111
KOI-1019	56113.62	Kp+C06	2	2963.3 \pm 1.8	334.994 \pm 0.035	8.719 \pm 0.112
KOI-1019	56113.62	Kp+C06	2	3216.8 \pm 2.0	109.278 \pm 0.035	9.366 \pm 0.113
KOI-1019	56113.62	Kp+C06	2	3294.0 \pm 1.8	336.290 \pm 0.031	8.583 \pm 0.112
KOI-1054	56152.33	Kp	1	6138.0 \pm 4.3	334.602 \pm 0.040	7.802 \pm 0.076
KOI-1222	56152.32	Kp+C06	2	6286.4 \pm 2.0	124.487 \pm 0.017	5.384 \pm 0.111
KOI-1686	56491.49	Kp	3	3482.7 \pm 4.6	261.453 \pm 0.075	7.298 \pm 0.086
KOI-1686	56491.49	Kp	3	3825.8 \pm 2.5	346.074 \pm 0.037	6.135 \pm 0.037
KOI-1924	56866.41	Kp+C06	6	5162.5 \pm 4.1	38.777 \pm 0.045	13.233 \pm 0.132
KOI-1924	56113.59	Kp+C06	1	5505.9 \pm 6.6	157.313 \pm 0.068	13.512 \pm 0.168
KOI-3782	56881.49	Kp	4	1857.7 \pm 3.0	62.760 \pm 0.092	7.744 \pm 0.051
Duplicate Detections						
KOI-0001	56114.59	Kp+C06	2	1110.9 \pm 1.5	136.606 \pm 0.078	2.006 \pm 0.113
KOI-0002	56153.43	Kp+C06	2	3859.5 \pm 1.8	90.417 \pm 0.025	6.116 \pm 0.113
KOI-0070	56053.60	Kp+C06	2	3786.4 \pm 1.7	53.267 \pm 0.025	4.117 \pm 0.113
KOI-0075	56116.60	Kp+C06	2	3541.1 \pm 1.7	127.313 \pm 0.027	6.445 \pm 0.112
KOI-0122	56510.47	Kp+C06	2	4171.8 \pm 1.9	213.073 \pm 0.025	6.236 \pm 0.114
KOI-0315	56116.62	Kp+C06	2	4104.7 \pm 1.8	213.908 \pm 0.024	4.667 \pm 0.120
KOI-0372	56881.53	Kp+C06	2	5964.6 \pm 1.9	36.601 \pm 0.017	4.209 \pm 0.113
KOI-0663	56151.48	Kp+C06	2	3229.1 \pm 2.0	62.063 \pm 0.034	6.494 \pm 0.119
KOI-0975	56113.60	Kp+C06	2	771.1 \pm 1.5	128.925 \pm 0.113	4.232 \pm 0.111
KOI-1230	56116.62	Kp+C06	2	2774.0 \pm 1.8	108.780 \pm 0.036	6.577 \pm 0.115
KOI-1299	56152.37	Kp+C06	2	880.1 \pm 1.5	21.286 \pm 0.100	5.380 \pm 0.111
KOI-1316	56882.48	Kp+C06	2	2886.8 \pm 1.7	106.655 \pm 0.033	7.034 \pm 0.112
KOI-1316	56882.48	Kp+C06	2	2977.9 \pm 1.8	107.968 \pm 0.033	7.372 \pm 0.112
KOI-1615	56114.61	Kp+C06	2	4769.5 \pm 1.8	267.246 \pm 0.021	6.089 \pm 0.112
KOI-1619	56114.61	Kp+C06	2	2063.1 \pm 1.6	227.078 \pm 0.043	1.955 \pm 0.112
KOI-1621	56611.26	Kp+C06	2	5131.8 \pm 1.9	160.464 \pm 0.020	6.032 \pm 0.113
KOI-1692	56116.61	Kp+C06	2	3193.5 \pm 2.1	338.373 \pm 0.036	6.340 \pm 0.122
KOI-1781	56152.37	Kp+C06	2	3447.8 \pm 1.7	332.355 \pm 0.027	2.509 \pm 0.111
KOI-2287	56152.36	Kp+C06	2	2842.4 \pm 1.6	11.300 \pm 0.032	5.272 \pm 0.112
KOI-3196	56510.44	Kp+C06	2	5503.5 \pm 2.0	52.592 \pm 0.020	7.350 \pm 0.113
KOI-3444	56882.29	Kp+C06	2	1090.0 \pm 1.5	10.352 \pm 0.080	3.013 \pm 0.111
KOI-3444	56882.29	Kp+C06	2	3569.2 \pm 1.7	264.515 \pm 0.026	5.642 \pm 0.111
KOI-3444	56882.29	Kp+C06	2	3865.8 \pm 2.9	353.469 \pm 0.043	9.405 \pm 0.121
KOI-4399	56510.45	Kp+C06	2	2117.7 \pm 1.6	17.572 \pm 0.042	3.832 \pm 0.112
KOI-4399	56510.45	Kp+C06	2	2329.0 \pm 1.8	358.722 \pm 0.043	7.416 \pm 0.113
KOI-4582	56611.26	Kp+C06	2	2750.9 \pm 1.7	308.282 \pm 0.036	6.772 \pm 0.113
KOI-4582	56611.26	Kp+C06	2	3578.6 \pm 1.7	288.705 \pm 0.026	4.008 \pm 0.112

TABLE 5
KECK/NIRC2 IMAGING CANDIDATE COMPANIONS

NOTE. — When candidate companions were detected in both coronagraphic and non-coronagraphic imaging, we list the non-coronagraphic entry first and use it for all analysis; the coronagraphic detections are listed at the end of the table for completeness, but are not used further. References: 1) Howell et al. (2011), 2) Adams et al. (2012), 3) Lillo-Box et al. (2012), 4) Horch et al. (2012), 5) Adams et al. (2013), 6) Law et al. (2013), 7) Dressing et al. (2014), 8) Lillo-Box et al. (2014), 9) Wang et al. (2014), 10) Gilliland et al. (2014), 11) Everett et al. (2015), 12) Borucki et al. (2013), 13) Daemgen et al. (2009), 14) Narita et al. (2010).

TABLE 6
KECK/NIRC2 PSF-FITTING CANDIDATE COMPANIONS

Name	MJD	Filter + Coronagraph	N_{frames} (mas)	ρ (deg)	PA (mag)	Δm	Refs
KOI-0005	56153.45	Kp	2	133.29 \pm 3.21	306.710 \pm 1.195	2.587 \pm 0.138	9
KOI-0098	56866.50	Kp	12	288.90 \pm 1.52	144.925 \pm 0.298	0.424 \pm 0.003	1, 2, 4, 6
KOI-0112	56869.32	Kp	12	101.01 \pm 1.51	115.933 \pm 0.851	1.105 \pm 0.014	2
KOI-0174	56263.21	Kp	4	583.55 \pm 3.63	76.892 \pm 0.149	2.567 \pm 0.020	5, 6
KOI-0177	56869.51	Kp	15	227.96 \pm 1.54	217.915 \pm 0.377	0.185 \pm 0.004	6
KOI-0227	56501.50	Kp	8	301.88 \pm 1.63	69.117 \pm 0.285	0.018 \pm 0.001	1
KOI-0270	56869.27	Kp	12	165.08 \pm 1.51	64.647 \pm 0.521	0.555 \pm 0.003	2
KOI-0284	56869.45	Kp	4	869.62 \pm 2.05	98.162 \pm 0.099	0.257 \pm 0.004	2, 11
KOI-0288	56153.43	Kp	3	346.96 \pm 1.52	319.875 \pm 0.248	3.034 \pm 0.019	
KOI-0356	56882.51	Kp	4	548.94 \pm 1.52	217.064 \pm 0.157	1.693 \pm 0.003	6
KOI-0588	56151.33	Kp	3	279.93 \pm 1.52	277.066 \pm 0.307	0.862 \pm 0.006	
KOI-0640	56882.43	Kp	4	429.09 \pm 1.54	301.618 \pm 0.200	0.053 \pm 0.001	6
KOI-0854	56490.53	Kp	3	154.21 \pm 1.51	181.644 \pm 0.558	3.589 \pm 0.076	
KOI-1174	56151.41	Kp	3	571.39 \pm 1.51	227.399 \pm 0.151	5.279 \pm 0.013	
KOI-1422	56490.48	Kp	3	214.34 \pm 1.54	217.470 \pm 0.401	1.165 \pm 0.006	4, 10
KOI-1589	56053.63	Kp	2	177.68 \pm 1.50	138.188 \pm 0.485	0.635 \pm 0.017	
KOI-1681	56490.54	Kp	3	148.83 \pm 1.59	141.691 \pm 0.578	0.069 \pm 0.016	
KOI-1841	56151.45	Kp	3	306.47 \pm 1.53	74.673 \pm 0.281	2.099 \pm 0.010	
KOI-1890	56882.51	Kp	4	406.47 \pm 1.51	144.798 \pm 0.212	2.039 \pm 0.003	6
KOI-1962	56153.38	Kp	3	116.86 \pm 1.51	114.542 \pm 0.735	0.082 \pm 0.026	6
KOI-1964	56114.60	Kp	3	394.74 \pm 1.52	2.316 \pm 0.218	1.904 \pm 0.014	6, 11
KOI-2059	56152.41	Kp	3	384.90 \pm 1.53	290.237 \pm 0.224	0.142 \pm 0.001	6
KOI-2179	56491.52	Kp	2	133.59 \pm 1.51	356.485 \pm 0.654	0.458 \pm 0.004	
KOI-2486	56868.51	Kp	12	228.73 \pm 1.51	67.729 \pm 0.376	0.143 \pm 0.003	6
KOI-2542	56868.46	Kp	17	764.02 \pm 1.53	29.190 \pm 0.113	0.932 \pm 0.002	
KOI-2593	56510.42	Kp	2	352.88 \pm 1.55	320.547 \pm 0.245	5.559 \pm 0.009	
KOI-2790	56869.32	Kp	12	254.57 \pm 1.51	135.448 \pm 0.338	0.501 \pm 0.002	7
KOI-2862	56867.41	Kp	4	574.06 \pm 1.58	23.997 \pm 0.150	-0.001 \pm 0.001	
KOI-3255	56867.55	Kp	4	180.17 \pm 1.53	336.668 \pm 0.477	0.116 \pm 0.004	11
KOI-3263	56868.33	Kp	4	821.98 \pm 1.55	275.558 \pm 0.105	2.278 \pm 0.003	8
KOI-3284	56867.49	Kp	6	438.75 \pm 1.51	193.283 \pm 0.196	2.037 \pm 0.003	11
KOI-3309	56882.30	Kp	4	594.08 \pm 1.51	205.313 \pm 0.145	1.410 \pm 0.002	
KOI-3681	56881.51	Kp	2	272.06 \pm 1.58	284.703 \pm 0.316	5.962 \pm 0.033	
KOI-3991	56869.55	Kp	6	202.61 \pm 1.51	111.694 \pm 0.425	1.475 \pm 0.006	
KOI-4097	56511.47	Kp	3	174.10 \pm 1.60	14.570 \pm 0.494	3.610 \pm 0.019	
KOI-4184	56511.47	Kp	3	205.90 \pm 1.54	223.842 \pm 0.418	0.050 \pm 0.003	
KOI-4287	56881.45	Kp	4	576.62 \pm 1.53	79.115 \pm 0.149	1.324 \pm 0.004	
KOI-4775	56867.39	Kp	13	439.33 \pm 1.54	35.905 \pm 0.196	5.538 \pm 0.062	
KOI-0387 A-B	56151.49	Kp	3	915.33 \pm 1.50	351.139 \pm 0.095	4.047 \pm 0.006	3
KOI-0387 A-C	56151.49	Kp	3	651.28 \pm 1.63	28.891 \pm 0.158	6.401 \pm 0.155	
KOI-0652 A-B	56265.20	Kp	3	1204.87 \pm 1.74	273.144 \pm 0.079	0.864 \pm 0.015	
KOI-0652 A-C	56265.20	Kp	3	1280.64 \pm 1.51	274.584 \pm 0.093	1.578 \pm 0.056	
KOI-2032 A-B	56152.42	Kp	3	1084.76 \pm 1.51	138.906 \pm 0.082	0.153 \pm 0.002	
KOI-2032 A-C	56152.42	Kp	3	1149.55 \pm 1.55	138.700 \pm 0.076	0.412 \pm 0.007	
KOI-2626 A-B	56491.52	Kp	3	205.34 \pm 1.53	213.302 \pm 0.426	0.477 \pm 0.012	10
KOI-2626 A-C	56491.52	Kp	3	162.97 \pm 1.52	185.083 \pm 0.562	1.038 \pm 0.029	10
KOI-2733 A-B	56867.52	Kp	4	108.80 \pm 1.53	295.083 \pm 0.814	-0.058 \pm 0.030	
KOI-2733 A-C	56867.52	Kp	4	777.20 \pm 2.05	303.916 \pm 0.147	4.989 \pm 0.022	
KOI-2813 A-B	56882.39	Kp	4	1058.38 \pm 1.51	261.209 \pm 0.081	1.816 \pm 0.001	7
KOI-2813 A-C	56882.39	Kp	4	827.33 \pm 1.56	272.302 \pm 0.104	5.034 \pm 0.014	
KOI-3497 A-B	56510.51	Kp	5	840.15 \pm 1.52	176.594 \pm 0.104	1.024 \pm 0.004	
KOI-3497 A-C	56510.51	Kp	5	764.16 \pm 1.52	174.056 \pm 0.115	1.689 \pm 0.006	
False Positives							
KOI-0113	56869.27	Kp	12	174.43 \pm 1.52	168.654 \pm 0.493	1.459 \pm 0.004	1
KOI-0976	56113.61	Kp	3	254.92 \pm 1.51	136.756 \pm 0.337	0.492 \pm 0.012	
Duplicate Detections							
KOI-1613	56153.39	Kp	3	211.76 \pm 1.57	184.840 \pm 0.406	1.032 \pm 0.006	6
KOI-1835	56151.40	Kp	3	53.57 \pm 1.52	353.713 \pm 1.616	0.286 \pm 0.016	
KOI-1977	56151.39	Kp	3	84.89 \pm 1.50	78.161 \pm 1.012	0.103 \pm 0.033	
KOI-2418	56868.36	Kp	4	106.12 \pm 1.59	3.498 \pm 0.810	2.579 \pm 0.023	
KOI-4032	56511.43	Kp	3	126.08 \pm 1.53	29.990 \pm 0.682	2.840 \pm 0.016	

NOTE. — When candidate companions were detected in both NRM observations and imaging observations, we use the NRM detection for all analysis; the imaging measurements are listed at the end of this table for completeness, but are not used further. The exceptions are KOI-0005 and KOI-0854, where the imaging and NRM detections represent separate companions in compact triple systems. References: 1) Howell et al. (2011), 2) Adams et al. (2012), 3) Lillo-Box et al. (2012), 4) Horch et al. (2012), 5) Adams et al. (2013), 6) Law et al. (2013), 7) Dressing et al. (2014), 8) Lillo-Box et al. (2014), 9) Wang et al. (2014), 10) Gilliland et al. (2014), 11) Everett et al. (2015), 12) Borucki et al. (2013)

TABLE 7
 SYSTEM PROPERTIES FOR CANDIDATE BINARY SYSTEMS

Name	M_{sec} (M_\odot)	q (M_s/M_p)	Sep (AU)
KOI-0005	1.055	0.968	15.7
KOI-0214	0.275	0.302	42.5
KOI-0289	0.924	0.983	10.7
KOI-0291	0.727	0.742	36.1
KOI-0854	0.493	0.948	5.3
KOI-1316	0.249	0.215	17.9
KOI-1397	0.508	1.016	9.0
KOI-1613	0.797	0.813	78.5
KOI-1615	0.665	0.599	8.6
KOI-1833	0.381	0.668	4.7
KOI-1835	0.821	1.001	24.8
KOI-1961	0.869	0.955	14.2
KOI-1977	0.671	0.972	28.4
KOI-2005	0.498	0.859	9.3
KOI-2031	0.319	0.469	20.9
KOI-2036	<0.099	<0.174	14.9
KOI-2124	0.589	0.998	16.6
KOI-2418	0.141	0.294	21.6
KOI-3892	0.226	0.213	46.2
KOI-3908	0.974	0.994	18.5
KOI-4032	0.408	0.434	43.0
KOI-4252	0.459	0.883	6.4
KOI-0005	0.653	0.599	73.3
KOI-0098	1.352	0.939	284.0
KOI-0112	0.715	0.737	47.6
KOI-0174	0.319	0.449	166.8
KOI-0177	0.919	0.978	138.1
KOI-0227	0.582	1.021	82.6
KOI-0270	0.889	0.966	55.9
KOI-0284	0.892	0.959	309.3
KOI-0288	0.706	0.480	145.4
KOI-0356	0.472	0.647	213.9
KOI-0588	0.439	0.813	81.0
KOI-0640	0.902	0.991	218.0
KOI-0854	0.104	0.200	50.9
KOI-1174	<0.099	<0.136	113.0
KOI-1422	0.249	0.579	47.0
KOI-1589	0.855	0.864	213.6
KOI-1681	0.401	0.978	37.4
KOI-1841	0.457	0.557	97.8
KOI-1890	0.737	0.652	175.5
KOI-1962	1.027	1.017	39.5
KOI-1964	0.535	0.601	49.9
KOI-2059	0.760	0.962	108.2
KOI-2179	0.411	0.874	35.1
KOI-2486	1.044	1.014	182.0
KOI-2542	0.182	0.628	85.7
KOI-2593	0.169	0.137	127.9
KOI-2790	0.668	0.868	98.1
KOI-2862	0.522	1.004	219.3
KOI-3255	0.686	0.980	74.8
KOI-3263	0.180	0.367	216.3
KOI-3284	0.202	0.412	59.9
KOI-3309	0.572	0.681	384.3
KOI-3681	0.132	0.109	104.1
KOI-3991	0.458	0.674	60.5
KOI-4097	0.155	0.242	29.9
KOI-4184	0.804	0.993	83.8
KOI-4287	0.919	0.806	217.4
KOI-4775	0.110	0.117	140.4
KOI-0387	0.139	0.211	189.7
KOI-0387	<0.099	<0.150	135.0
KOI-0652	0.664	0.781	550.3
KOI-0652	0.550	0.647	584.9
KOI-2032	0.884	0.982	468.4
KOI-2032	0.835	0.928	496.4
KOI-2626	0.316	0.832	47.9
KOI-2626	0.226	0.595	38.0
KOI-2733	0.828	1.010	53.7
KOI-2733	0.111	0.135	383.5
KOI-2813	0.373	0.592	281.6
KOI-2813	<0.099	<0.157	220.2
KOI-3497	0.544	0.756	187.9
KOI-3497	0.455	0.632	170.9
KOI-0001	0.494	0.520	227.8

TABLE 7 — *Continued*

Name	M_{sec} (M_\odot)	q (M_s/M_p)	Sep (AU)
KOI-0001	<0.099	<0.104	1230.3
KOI-0002	0.102	0.069	1025.7
KOI-0002	0.227	0.154	1284.0
KOI-0012	0.410	0.336	206.0
KOI-0012	<0.099	<0.081	649.8
KOI-0013	1.597	0.974	560.4
KOI-0041	<0.099	<0.095	979.4
KOI-0042	0.728	0.622	235.6
KOI-0069	<0.099	<0.112	213.3
KOI-0069	<0.099	<0.112	476.2
KOI-0070	0.214	0.240	1069.2
KOI-0072	<0.099	<0.115	360.4
KOI-0075	0.197	0.158	1400.1
KOI-0082	<0.099	<0.125	590.6
KOI-0082	<0.099	<0.125	627.2
KOI-0084	<0.099	<0.115	634.0
KOI-0085	<0.099	<0.082	844.1
KOI-0087	0.101	0.120	1129.0
KOI-0089	0.114	0.091	2294.2
KOI-0089	<0.099	<0.079	2889.2
KOI-0092	<0.099	<0.100	1669.3
KOI-0099	0.100	0.133	813.1
KOI-0103	<0.099	<0.108	1228.3
KOI-0104	<0.099	<0.124	1224.8
KOI-0105	0.241	0.294	289.2
KOI-0105	<0.099	<0.121	1297.9
KOI-0105	<0.099	<0.121	1829.9
KOI-0116	<0.099	<0.103	699.0
KOI-0116	<0.099	<0.103	1248.6
KOI-0116	<0.099	<0.103	1935.6
KOI-0118	0.381	0.381	594.1
KOI-0119	1.492	1.015	1102.9
KOI-0122	0.122	0.113	1826.3
KOI-0137	<0.099	<0.109	2453.2
KOI-0141	0.636	0.677	598.8
KOI-0144	<0.099	<0.118	1030.1
KOI-0144	<0.099	<0.118	1111.7
KOI-0144	<0.099	<0.118	1484.4
KOI-0144	<0.099	<0.118	1808.2
KOI-0148	0.134	0.154	772.2
KOI-0148	0.304	0.349	1348.5
KOI-0152	0.163	0.148	2290.7
KOI-0152	0.108	0.098	3845.2
KOI-0152	0.100	0.091	3869.3
KOI-0152	0.234	0.213	4237.5
KOI-0152	0.194	0.176	4541.0
KOI-0157	0.205	0.223	781.1
KOI-0157	<0.099	<0.108	2382.5
KOI-0157	0.232	0.252	2491.1
KOI-0157	0.143	0.155	2894.2
KOI-0157	<0.099	<0.108	3131.6
KOI-0157	<0.099	<0.108	3715.0
KOI-0161	0.112	0.132	764.5
KOI-0161	<0.099	<0.116	910.2
KOI-0177	0.102	0.109	1385.0
KOI-0177	<0.099	<0.105	1739.6
KOI-0177	<0.099	<0.105	2558.9
KOI-0177	<0.099	<0.105	3472.7
KOI-0177	0.383	0.407	3965.2
KOI-0177	<0.099	<0.105	4566.3
KOI-0177	<0.099	<0.105	4817.3
KOI-0205	<0.099	<0.124	1204.7
KOI-0214	0.117	0.129	2279.2
KOI-0216	0.180	0.200	1134.7
KOI-0216	<0.099	<0.110	3145.1
KOI-0216	0.409	0.454	3626.4
KOI-0227	<0.099	<0.174	917.2
KOI-0227	0.204	0.358	1792.3
KOI-0232	<0.099	<0.100	4519.8
KOI-0242	0.298	0.310	3710.4
KOI-0249	0.232	0.663	342.2
KOI-0251	<0.099	<0.187	607.4
KOI-0252	<0.099	<0.183	1412.3
KOI-0252	<0.099	<0.183	1444.8
KOI-0253	0.392	0.632	1309.9
KOI-0253	<0.099	<0.160	1350.0

TABLE 7 — *Continued*

Name	M_{sec} (M_\odot)	q (M_s/M_p)	Sep (AU)
KOI-0254	<0.099	<0.177	880.3
KOI-0254	<0.099	<0.177	1065.6
KOI-0254	<0.099	<0.177	1966.6
KOI-0255	0.109	0.210	730.9
KOI-0257	<0.099	<0.085	417.4
KOI-0257	<0.099	<0.085	983.9
KOI-0261	<0.099	<0.103	409.7
KOI-0261	<0.099	<0.103	663.9
KOI-0268	0.603	0.507	476.5
KOI-0268	0.430	0.361	682.6
KOI-0269	<0.099	<0.077	792.2
KOI-0282	0.211	0.229	1286.2
KOI-0283	<0.099	<0.101	1351.9
KOI-0285	0.425	0.370	670.0
KOI-0285	<0.099	<0.086	1045.3
KOI-0289	<0.099	<0.105	2051.3
KOI-0298	0.756	0.945	651.6
KOI-0299	<0.099	<0.104	954.3
KOI-0303	0.260	0.292	1711.3
KOI-0305	<0.099	<0.127	1167.6
KOI-0306	0.502	0.564	568.3
KOI-0306	<0.099	<0.111	1486.9
KOI-0314	<0.099	<0.183	277.9
KOI-0314	<0.099	<0.183	403.0
KOI-0315	0.117	0.165	810.0
KOI-0315	<0.099	<0.139	1066.9
KOI-0316	<0.099	<0.097	1953.1
KOI-0346	<0.099	<0.122	523.7
KOI-0348	<0.099	<0.137	663.3
KOI-0348	<0.099	<0.137	1431.3
KOI-0356	<0.099	<0.136	1590.2
KOI-0366	0.203	0.115	888.4
KOI-0370	<0.099	<0.073	796.4
KOI-0372	<0.099	<0.105	814.9
KOI-0372	<0.099	<0.105	1099.1
KOI-0372	0.246	0.262	1848.3
KOI-0387	<0.099	<0.150	394.0
KOI-0421	<0.099	<0.114	1685.4
KOI-0421	<0.099	<0.114	2136.8
KOI-0421	<0.099	<0.114	2666.8
KOI-0421	<0.099	<0.114	2832.5
KOI-0438	0.244	0.444	709.6
KOI-0490	0.201	0.268	732.6
KOI-0500	<0.099	<0.171	464.8
KOI-0500	<0.099	<0.171	1058.4
KOI-0505	<0.099	<0.125	815.1
KOI-0554	<0.099	<0.099	3720.9
KOI-0554	0.568	0.568	5100.5
KOI-0554	0.425	0.425	5257.5
KOI-0571	<0.099	<0.202	389.5
KOI-0571	<0.099	<0.202	587.3
KOI-0623	0.576	0.633	1747.8
KOI-0640	<0.099	<0.109	593.4
KOI-0650	0.658	0.685	2024.6
KOI-0657	<0.099	<0.136	346.3
KOI-0663	<0.099	<0.177	252.2
KOI-0663	<0.099	<0.177	460.6
KOI-0663	<0.099	<0.177	710.3
KOI-0676	<0.099	<0.180	1134.9
KOI-0678	<0.099	<0.111	2028.7
KOI-0701	<0.099	<0.143	607.3
KOI-0701	0.141	0.204	847.6
KOI-0701	<0.099	<0.143	1002.9
KOI-0701	<0.099	<0.143	1860.6
KOI-0852	0.109	0.115	4617.1
KOI-0852	0.671	0.706	6175.4
KOI-0868	<0.099	<0.148	1637.0
KOI-0886	<0.099	<0.202	898.4
KOI-0899	<0.099	<0.236	408.3
KOI-0908	0.266	0.280	968.8
KOI-0908	0.241	0.254	1313.3
KOI-0908	<0.099	<0.104	2358.1
KOI-0908	0.123	0.129	2714.4
KOI-0908	<0.099	<0.104	2721.8
KOI-0908	<0.099	<0.104	5241.7
KOI-0947	<0.099	<0.198	767.5

TABLE 7 — *Continued*

Name	M_{sec} (M_\odot)	q (M_s/M_p)	Sep (AU)
KOI-0947	<0.099	<0.198	1011.2
KOI-0961	<0.099	<0.825	223.1
KOI-0975	0.437	0.387	73.9
KOI-0975	<0.099	<0.088	104.7
KOI-0975	<0.099	<0.088	601.1
KOI-0984	0.851	0.967	420.2
KOI-0984	<0.099	<0.112	1154.2
KOI-0987	0.490	0.527	571.1
KOI-0987	<0.099	<0.106	631.7
KOI-0987	<0.099	<0.106	1547.2
KOI-0987	<0.099	<0.106	1748.4
KOI-1146	<0.099	<0.220	840.9
KOI-1174	<0.099	<0.136	612.0
KOI-1174	<0.099	<0.136	688.4
KOI-1174	<0.099	<0.136	981.6
KOI-1201	<0.099	<0.254	491.0
KOI-1201	<0.099	<0.254	674.4
KOI-1201	<0.099	<0.254	926.6
KOI-1221	<0.099	<0.085	858.5
KOI-1230	0.368	0.297	3049.9
KOI-1241	<0.099	<0.088	2837.2
KOI-1241	<0.099	<0.088	5977.3
KOI-1298	0.208	0.353	317.9
KOI-1299	0.495	0.467	718.0
KOI-1300	0.388	0.732	200.2
KOI-1316	0.106	0.091	1066.1
KOI-1316	<0.099	<0.085	1107.6
KOI-1361	0.200	0.333	259.4
KOI-1361	<0.099	<0.165	324.4
KOI-1361	<0.099	<0.165	1862.6
KOI-1393	<0.099	<0.180	1627.3
KOI-1397	<0.099	<0.198	569.0
KOI-1397	<0.099	<0.198	736.3
KOI-1397	<0.099	<0.198	1156.0
KOI-1397	<0.099	<0.198	1201.1
KOI-1408	<0.099	<0.165	578.4
KOI-1408	<0.099	<0.165	811.6
KOI-1408	<0.099	<0.165	1013.7
KOI-1428	0.205	0.256	1278.1
KOI-1431	<0.099	<0.099	2421.0
KOI-1436	0.288	0.320	3989.4
KOI-1442	0.299	0.308	660.3
KOI-1515	<0.099	<0.198	185.3
KOI-1588	<0.099	<0.177	346.5
KOI-1588	<0.099	<0.177	1103.0
KOI-1588	<0.099	<0.177	1126.5
KOI-1589	<0.099	<0.100	4747.6
KOI-1589	0.186	0.188	6912.9
KOI-1589	0.230	0.232	6944.2
KOI-1589	0.127	0.128	7518.1
KOI-1615	<0.099	<0.089	796.7
KOI-1615	<0.099	<0.089	829.4
KOI-1615	0.123	0.111	1286.6
KOI-1615	<0.099	<0.089	1494.1
KOI-1618	<0.099	<0.078	1268.2
KOI-1619	<0.099	<0.146	111.3
KOI-1619	0.378	0.556	242.7
KOI-1621	0.232	0.193	2702.7
KOI-1621	<0.099	<0.082	3154.1
KOI-1681	<0.099	<0.241	1024.0
KOI-1681	<0.099	<0.241	1253.0
KOI-1692	<0.099	<0.105	571.4
KOI-1692	<0.099	<0.105	865.7
KOI-1725	0.182	0.444	210.9
KOI-1738	<0.099	<0.124	660.3
KOI-1738	<0.099	<0.124	1256.4
KOI-1738	<0.099	<0.124	1505.4
KOI-1781	0.401	0.508	557.4
KOI-1788	<0.099	<0.122	1972.2
KOI-1800	<0.099	<0.109	1081.5
KOI-1833	<0.099	<0.174	1235.7
KOI-1835	<0.099	<0.121	696.1
KOI-1843	<0.099	<0.194	351.7
KOI-1879	<0.099	<0.174	451.0
KOI-1879	<0.099	<0.174	1530.7
KOI-1880	<0.099	<0.183	286.7

TABLE 7 — *Continued*

Name	M_{sec} (M_\odot)	q (M_s/M_p)	Sep (AU)
KOI-1880	<0.099	<0.183	824.6
KOI-1908	0.175	0.292	363.0
KOI-1908	0.140	0.233	1377.5
KOI-1934	<0.099	<0.165	1672.8
KOI-1934	0.188	0.313	1975.6
KOI-1937	<0.099	<0.160	418.4
KOI-1967	<0.099	<0.134	1142.9
KOI-1985	0.302	0.387	879.6
KOI-1988	<0.099	<0.124	531.5
KOI-2001	0.142	0.182	301.7
KOI-2001	<0.099	<0.127	1789.3
KOI-2005	<0.099	<0.171	845.5
KOI-2029	<0.099	<0.125	1580.9
KOI-2031	<0.099	<0.146	1342.6
KOI-2031	<0.099	<0.146	1600.4
KOI-2031	0.100	0.147	1813.0
KOI-2031	<0.099	<0.146	2432.9
KOI-2035	<0.099	<0.115	1348.1
KOI-2036	<0.099	<0.174	1070.1
KOI-2036	<0.099	<0.174	2091.8
KOI-2057	<0.099	<0.171	1422.3
KOI-2067	0.866	0.893	873.9
KOI-2067	<0.099	<0.102	1468.3
KOI-2079	0.128	0.132	1660.4
KOI-2079	0.424	0.437	2151.7
KOI-2156	<0.099	<0.261	612.1
KOI-2158	<0.099	<0.111	537.9
KOI-2158	0.172	0.193	760.0
KOI-2158	<0.099	<0.111	881.4
KOI-2169	0.406	0.441	927.6
KOI-2173	<0.099	<0.132	1000.3
KOI-2181	<0.099	<0.116	1672.0
KOI-2181	<0.099	<0.116	1810.0
KOI-2181	<0.099	<0.116	3574.5
KOI-2191	<0.099	<0.183	325.1
KOI-2191	<0.099	<0.183	981.7
KOI-2208	<0.099	<0.099	1007.2
KOI-2208	<0.099	<0.099	1231.6
KOI-2225	<0.099	<0.121	984.0
KOI-2225	<0.099	<0.121	1431.0
KOI-2287	<0.099	<0.136	428.8
KOI-2287	<0.099	<0.136	847.2
KOI-2295	0.626	0.773	383.5
KOI-2311	0.126	0.134	318.4
KOI-2332	<0.099	<0.110	1251.4
KOI-2332	<0.099	<0.110	1334.9
KOI-2390	0.163	0.138	624.6
KOI-2390	0.331	0.281	3086.8
KOI-2390	0.530	0.449	3965.8
KOI-2418	<0.099	<0.206	488.2
KOI-2418	<0.099	<0.206	807.3
KOI-2418	<0.099	<0.206	853.5
KOI-2453	<0.099	<0.275	315.8
KOI-2462	<0.099	<0.092	1132.8
KOI-2479	0.163	0.175	3396.3
KOI-2479	<0.099	<0.106	3467.6
KOI-2481	0.545	0.395	3170.1
KOI-2481	0.478	0.346	11777.9
KOI-2481	0.499	0.362	12439.1
KOI-2486	0.250	0.243	4972.5
KOI-2522	<0.099	<0.130	1622.9
KOI-2545	<0.099	<0.068	3414.1
KOI-2593	<0.099	<0.080	1065.9
KOI-2650	<0.099	<0.177	1062.7
KOI-2657	0.821	0.977	314.7
KOI-2672	0.253	0.272	146.4
KOI-2672	<0.099	<0.106	1061.8
KOI-2686	<0.099	<0.136	1226.5
KOI-2693	<0.099	<0.146	834.5
KOI-2704	<0.099	<0.619	316.7
KOI-2705	0.119	0.290	147.4
KOI-2706	0.302	0.224	453.7
KOI-2754	0.601	0.646	235.0
KOI-2754	<0.099	<0.106	735.5
KOI-2755	<0.099	<0.106	1859.2
KOI-2790	<0.099	<0.129	1018.5

TABLE 7 — *Continued*

Name	M_{sec} (M_\odot)	q (M_s/M_p)	Sep (AU)
KOI-2790	<0.099	<0.129	1260.7
KOI-2790	0.130	0.169	2101.9
KOI-2790	<0.099	<0.129	2152.9
KOI-2790	<0.099	<0.129	2234.7
KOI-2792	<0.099	<0.106	916.2
KOI-2801	<0.099	<0.094	331.7
KOI-2803	0.478	0.483	1112.1
KOI-2803	<0.099	<0.100	1140.9
KOI-2803	0.126	0.127	1295.7
KOI-2813	<0.099	<0.157	486.3
KOI-2862	<0.099	<0.190	1303.6
KOI-2862	<0.099	<0.190	1621.1
KOI-2948	<0.099	<0.108	792.7
KOI-2992	<0.099	<0.168	2338.2
KOI-3075	<0.099	<0.115	1668.8
KOI-3119	<0.099	<0.309	248.5
KOI-3119	<0.099	<0.309	900.1
KOI-3119	<0.099	<0.309	1340.8
KOI-3119	<0.099	<0.309	1464.9
KOI-3158	0.386	0.551	69.7
KOI-3179	<0.099	<0.105	1403.6
KOI-3196	<0.099	<0.093	1646.0
KOI-3208	<0.099	<0.103	729.6
KOI-3246	<0.099	<0.125	614.5
KOI-3255	0.163	0.233	1261.9
KOI-3284	0.132	0.269	540.9
KOI-3309	0.329	0.392	2301.7
KOI-3309	<0.099	<0.118	3419.3
KOI-3414	<0.099	<0.187	1254.8
KOI-3425	<0.099	<0.091	2402.9
KOI-3444	0.145	0.315	82.2
KOI-3444	<0.099	<0.215	154.5
KOI-3444	<0.099	<0.215	231.1
KOI-3444	<0.099	<0.215	256.3
KOI-3444	<0.099	<0.215	269.9
KOI-3444	<0.099	<0.215	280.5
KOI-3444	<0.099	<0.215	292.8
KOI-3444	<0.099	<0.215	453.8
KOI-3506	0.150	0.135	1565.8
KOI-3681	<0.099	<0.082	1565.0
KOI-3681	<0.099	<0.082	2004.5
KOI-3681	<0.099	<0.082	2021.9
KOI-3891	0.103	0.116	337.3
KOI-3891	<0.099	<0.111	472.7
KOI-3891	0.138	0.155	661.4
KOI-3891	<0.099	<0.111	1559.4
KOI-3891	<0.099	<0.111	2036.1
KOI-3908	<0.099	<0.101	808.0
KOI-3908	<0.099	<0.101	1683.9
KOI-3908	<0.099	<0.101	2081.4
KOI-3908	<0.099	<0.101	2594.4
KOI-3925	<0.099	<0.101	3036.7
KOI-3925	0.121	0.123	3344.9
KOI-4004	0.425	0.512	588.8
KOI-4016	<0.099	<0.155	416.1
KOI-4016	<0.099	<0.155	784.1
KOI-4016	0.250	0.391	1306.1
KOI-4226	0.321	0.272	1211.9
KOI-4269	<0.099	<0.112	1777.7
KOI-4287	0.116	0.102	1517.4
KOI-4287	0.123	0.108	1671.1
KOI-4288	<0.099	<0.098	1139.5
KOI-4288	<0.099	<0.098	2048.8
KOI-4292	0.177	0.190	737.9
KOI-4399	0.228	0.259	454.4
KOI-4399	<0.099	<0.112	499.2
KOI-4399	<0.099	<0.112	575.9
KOI-4407	<0.099	<0.079	657.4
KOI-4407	0.734	0.583	717.2
KOI-4407	0.220	0.175	776.8
KOI-4407	<0.099	<0.079	1205.0
KOI-4427	<0.099	<0.194	730.4
KOI-4427	<0.099	<0.194	770.1
KOI-4427	0.121	0.237	1201.2
KOI-4446	<0.099	<0.108	492.8
KOI-4556	<0.099	<0.108	1078.8

TABLE 7 — *Continued*

Name	M_{sec} (M_\odot)	q (M_s/M_p)	Sep (AU)
KOI-4582	<0.099	<0.112	606.5
KOI-4582	0.315	0.358	790.3
KOI-4657	0.486	0.586	744.8
KOI-4657	<0.099	<0.119	1068.3
KOI-4657	<0.099	<0.119	1853.0
KOI-4775	<0.099	<0.105	1684.0
KOI-4875	<0.099	<0.194	428.3
KOI-4875	<0.099	<0.194	1278.7